Anno 2011_Numero 09

Miscellanea INGV

Riassunti estesi

Conferenza A. Rittmann
"PER GIOVANI RICERCATORI"

Nicolosi (Catania) 7 | 9 giugno 2011

09

Istituto Nazionale di
Geofisica e Vulcanologia

Anno 2011_Numero 09

Miscellanea INGV

RIASSUNTI ESTESI

CONFERENZA A. RITTMANN "PER GIOVANI RICERCATORI"

NICOLOSI (CATANIA) 7 | 9 GIUGNO 2011

a cura del Comitato Organizzatore

Comitato Organizzatore

Bruno Capaccioni	Università di Bologna
Raffaello Cioni	Università di Cagliari
Mauro Coltelli	INGV Sezione di Catania - Osservatorio Etneo
Rosa Anna Corsaro	INGV Sezione di Catania - Osservatorio Etneo
Susanna Falsaperla	INGV Sezione di Catania - Osservatorio Etneo
Carmelo Ferlito	Università di Catania
Domenico Patanè	INGV Sezione di Catania - Osservatorio Etneo
Marco Viccaro	Università di Catania

Editor

Massimo Pompilio	INGV - Sezione di Pisa

Revisione e normazione ortoeditoriale

Francesca Di Stefano	Centro Editoriale Nazionale INGV
Rossella Celi	Centro Editoriale Nazionale INGV

Sponsor

Indice

Rock-Magnetic Investigation of the Kizilkaya Ignimbrite (Central Anatolian Volcanic Province)

Alessandro Agrò[1], Jean L. Le Pennec[2], Abidin Temel[3], Elena Zanella[1]

[1]*Università di Torino, Dipartimento di Scienze della Terra, Turin, Italy*
[2]*Laboratoire Magmas et Volcans, IRD, Blaise Pascal University, Clermont-Ferrand, France*
[3]*Department of Geological Engineering, Hacettepe University, Ankara, Turkey*

The convergence of the Afro-Arabian and the Eurasian Plates in the Eastern Mediterranean led to the closure of the Neotethys Ocean and to continent-continent collision by the Miocene. As a consequence of it, Anatolia experienced an extensive volcanism which has developed along several provinces from Neogene to Quaternary. In the Central Anatolian Volcanic Province (CAVP), a widespread calc-alkaline volcanism occurred within the Nevşehir Plateau; the main phase of this volcanic activity is the emplacement of a high-K calc-alkaline rhyolitic ignimbrite sequence, occurred between 11–2.8 My [Innocenti et al., 1975], that comprises at least nine major and two minor ignimbrite sheets emplaced at 1-2 My intervals, interbedded with continental sedimentary deposits.

The Pliocene Kızılkaya ignimbrite (4.5–5.5 My old from K-Ar data [Innocenti et al., 1975; Besang et al., 1977]) is the youngest large-volume unit of the ignimbrite sequence in the CAVP. It erupted from a large silicic complex within the Nevşehir plateau and consists of a simple flow- and cooling-unit [Le Pennec et al., 1998]. Many paleomagnetic studies have been carried out on this ignimbrite unit in order to investigate its areal distribution, age, source location, magnetic mineralogy and paleomagnetic directions [Le Pennec et al., 1998; Le Pennec, 2000; Le Pennec et al., 2005; Piper et al., 2002]. However, there are still many problems in reconciling these data: some are in contrast each other (especially those concerning paleomagnetism), while anisotropy of magnetic susceptibility (AMS) data used to infer source area are not enough to accurately constrain it.

In this study a rock magnetic investigation was carried out in order to evaluate the homogeneity of the ignimbrite through the entire deposit unit, by means of anisotropy of magnetic susceptibility (AMS), magnetic mineralogy and magnetic remanence determinations. Our data show that even if Kızılkaya ignimbrite is a single cooling unit, its magnetic properties suffer substantial variations through the deposit. Six areal distributed localities were sampled at different stratigraphic height within the devitrified portion of the ignimbrite. A total of 33 sites were sampled and 444 oriented specimens recovered and analyzed.

Both the isothermal remanent magnetization (IRM) acquisition curves and the Lowrie method point to a low-Ti magnetite as the main magnetic carrier; locally, the occurrence of a minor high-coercivity mineral (oxidized magnetite and/or hematite) is suggested by the high field value (B > 0.8 T) needed to reach IRM saturation.

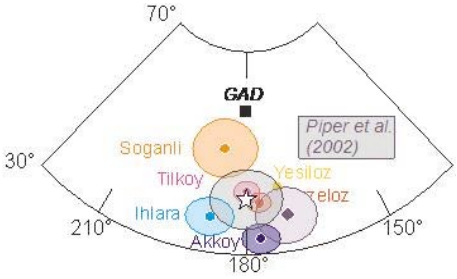

Figure 1. Paleomagnetic direction of Kizilkaya Ignimbrite: Equal-area projections of mean locality directions (colored dots) and 95% confidence limits (ellipses). Symbols: star = mean paleomagnetic direction and confidence ellipse; diamond = paleomagnetic direction from Piper et al., 2002; square: local GAD direction.

At some sites, Characteristic Remanent Magnetization (ChRM) directions were clearly isolated by both stepwise thermal and AF demagnetizations, and the ChRM was calculated by the Principal Component Analysis in the Zijderveld diagrams (Figure 1). Here, the mean value for 20 sites (D = 175°, I = -42°) is fully consistent with previously published paleomagnetic data [Piper et al., 2002]. In other sites, remanence appears more complex: its direction moves along a great circle and no stable end-point direction is found, revealing the occurrence of two remanent components with overlapping coercivity and blocking temperature spectra. In this case the mean site ChRM was estimated combining best-fit great circles and lines [McFadden and McElhinny, 1998]. Here, paleomagnetic directions vary significantly along the stratigraphic section; the

magnetic declination ranges from 170° to 210°, the inclination from -34° to -55°. Large deflections from the mean direction occur at sites characterized by the occurrence of oxidized magnetite and/or hematite. Besides, at these sites the magnetic susceptibility is one order of magnitude lower than usual. These results suggest that at some sites the Kizilkaya ignimbrite acquired first a thermal remanent magnetization and then, during the final cooling or a short time after, a chemical remanent magnetization component.

AMS measurements detected a well developed magnetic fabric. Magnetic foliation is gently dipping at most sites and its plunge is regarded as a proxy of the flow direction (Figure 2). At four of the six studied localities, the mean flow direction agrees pointing to a vent location in an area between Derinkuyu Basin and Göllü Dağ rhyolitic massif (as proposed in the literature by Le Pennec, 2000). However, the magnetic fabric changes along the stratigraphic section: the magnetic foliation is nearly horizontal in the central part of the deposit, regardless of its thickness.

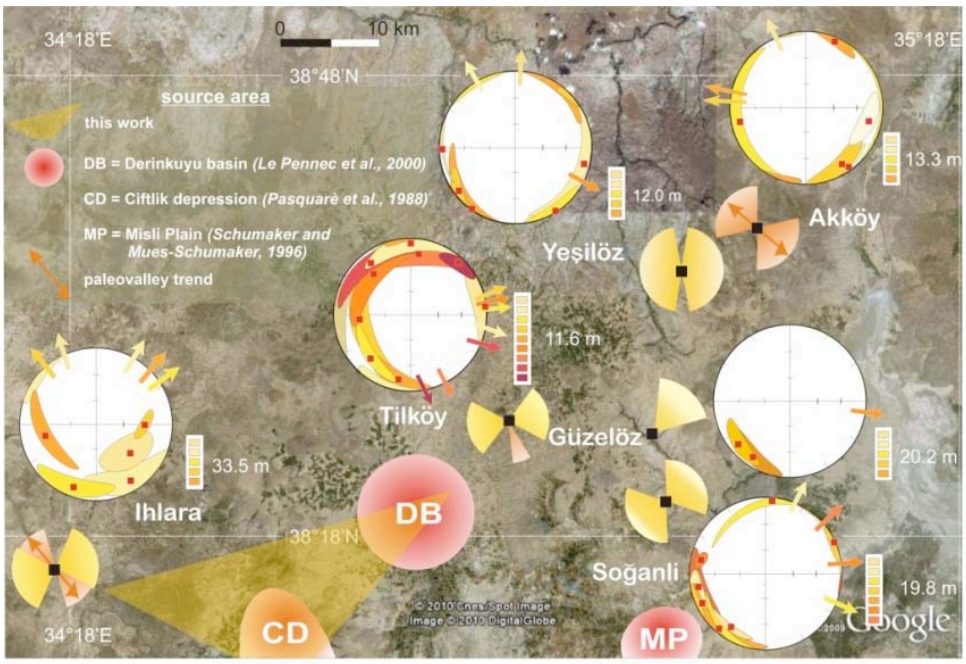

Figure 2. Magnetic fabric: Equal-area projections of the AMS data at sampling localities. Different colors indicate sites sampled in different stratigraphic position within each locality. For each site, the magnetic lineation (red square) and the 95% confidence ellipse are shown together with the flow direction (colored arrow) inferred from the magnetic foliation imbrication. Colored fans show the dominant flow direction: undisturbed directions are in yellow, while orange fan are interpreted as controlled by paleotopography. Intersection of yellow fans corresponds to the inferred source area (orange area). Literature data (red areas) are shown for comparison.

Though Kızılkaya ignimbrite is a single cooling unit, its magnetic properties suffer substantial variations through the deposit and the remanent magnetization characteristics show that the acquisition of remanence results from the overlapping of thermal and chemical processes. The Kızılkaya case shows that thick pyroclastic deposits should be sampled following a stratigraphic approach, sampling different sites at different stratigraphic heights at each individual location. Otherwise, undersampling may severely affect the paleomagnetic results.

References

Besang, C., Eckhart, F.J., Harre, W., Kreuzer, H., Müller, P., (1977). *Radiometrische altersbestimmungen an neogenen eruptigesteinen der Turkei*. Geol. Jahrb. B25, 3-36.

Innocenti, F., Mazzuoli, R., Pasquaré, G., Redicati de Brozolo, F., Villari, L., (1975). *The Neogene calk-alkaline volcanism of central Anatolia: Geochronological data from the Kayseri-Niğde area*. Geol.

Mag. 112, 349-360.

Le Pennec, J.L., (2000). *Identifying ash flow sources with directional data: An application to the Kızılkaya ignimbrite, central Anatolia*. Journal Of Geophysical Research, Vol 105, No. B12, 28,427-28,441.

Le Pennec, J.L., Chen, Y., Diot, H., Froger, J.L., Gourgaud, A., (1998). *Interpretation of anisotropy of magnetic susceptibility fabric of ignimbrites in termo f kinematic and sedimentological mechanism: An Anatolian case-study*. Earth and Planetary Science Letters 157, 105-127.

Le Pennec, J.L., Temel, A., Froger, J.L, Sen, S., Gourgaud, A., Bourdier, J.L., (2005). *Stratigraphy and age of the Cappadocia ignimbrites, Turkey: reconciling field constraints with paleontologic, radiochronologic, geochemical and paleomagnetic data*. J. of Volcan. And Geother. Res 141, 45-64.

McFadden, P.L. and McElhinny, M.W., (1998). The *combined analysis of remagnetization circles and direct observations in palaeomagnetism*. Earth Planet. Sci. Lett. 87, 161-172.

Piper, J.D.A., Gürsoy, H., Tatar, O., (2002). *Paleomagnetism and magnetic properties of the Cappadocian ignimbrite succession, central Turkey and neogene tectonics of the Anatolian collage*. J. Volcanol. Geotherm. Res. 117, 237-262.

Do Volcanic Eruptions Solve Global Atmospheric Mercury Pollution?

Emanuela Bagnato[1], Sergio Calabrese[1], Alessandro Aiuppa[1,2], Francesco Parello[1]

[1]*Università di Palermo, Dipartimento Scienze della Terra e del Mare, Palermo, Italy*
[2]*Istituto Nazionale di Geofisica e Vulcanologia, Sezione di Palermo, Italy*

Besides human activities, volcanoes also introduce significant quantities of potentially harmful chemical compounds into the environment, mainly in the forms of gases and particles. High-temperature emissions from persistently degassing volcanoes are a known source of trace metal emissions to the atmosphere which may have important environmental consequences. Among these metals, mercury (Hg) is of particular interest since it is a toxic volatile metal found at elevated concentrations in remote regions of the world. The anthropogenic contribution to the global atmospheric Hg budget is now well constrained, with most recent estimates ranging from 1484 [AMAP/UNEP, 2008] to 1894 t yr^{-1} [2005/2006 inventory; Streets et al 2009]. Hg emissions from natural sources are, on the other hand, still poorly characterized, though being likely in the same range [estimates from 500 to 3000 t yr^{-1}; Nriagu 1989] of those reported for anthropogenic release.

The poorly constrained Hg speciation in volcanic emissions, and the limited number of studies so far, have hampered accurate estimation of the global Hg flux, with previous estimates ranging from as low as ~1 t yr^{-1} [Ferrara et al. 2000] to >800 t yr^{-1} [Varekamp and Buseck 1986]. Besides, historical archives such as ice-cores documented that large eruptions can release quantities of Hg similar to the present anthropogenic burden. The effects, or potential effects, of active volcanoes on the environment and on public health is an important issue, given the large number of communities and populated cities that exist and keep growing around and upon active and dormant volcanoes. Poisonous gases, and in the specific mercury, are also released continuously or semi-continuously into the environment by non-erupting volcanoes causing however regional environmental effects equally severe to the volcanic events of massive proportions.

A major uncertainty regarding the impacts of volcanic Hg is the extent to which Hg emitted from a volcano is deposited locally or transported globally. Actually, volcanogenic mercury fluxes are poorly constrained and there is an almost complete absence of data on the factors (magma composition, eruptive temperature, or volcanic gas composition) that influence its degassing rates at different volcanoes.

In order to better understand the role of volcanoes in the global mercury budget and to extend the currently limited dataset on volcanogenic Hg emissions, a number of field campaigns were carried out to evaluate Hg flux in volcanic gases by the simultaneously-determined Hg/SO_2 ratios and SO_2 flux. Measurements were made at the crater edge of a number of quiescently degassing volcanoes (Etna, Stromboli, Asama, Miyakejima, Montserrat, Ambrym, Yasur, Nyiragongo, Masaya). Emissions from open vents were investigated and concentrations of Hg elevated above usual background levels (rural areas far from emitting source, 1-2 ng m^{-3}) were detected. We found that in volcanic plume, mercury is mainly found as the relatively inert form of the gaseous elemental mercury (GEM) with concentrations ranging from 18 to 373 ng Hg m^{-3}. GEM has a long atmospheric lifetime estimated as 0.5-2 years due to its low solubility and gaseous nature, promoting long-range global transport [Nriagu 1989; Pyle and Mather, 2003]. High variability found in plume Hg concentrations depends on both volcanic (gas flux) and non-volcanic factors (extent of mixing and dilution in the vent; wind speed and direction), hence comparing the concentrations of Hg species between different volcanoes is not necessarily meaningful and it is more useful to compare Hg/SO_2 ratios. Using our determined Hg/SO_2 mass ratios in tandem with the simultaneously-determined SO_2 emission rates, we estimated that the investigated volcanoes have Hg emission rates ranging from 0.2 to 18 $t \cdot yr^{-1}$ (corresponding to a total Hg flux of ~54 $t \cdot yr^{-1}$).

The broad correlation found between GEM and $SO_{2(g)}$ concentrations suggests the rather similar degassing behaviour of the open-conduit volcanoes studied. Based on our dataset and previous works, we propose that a Hg/SO_2 plume ratio $\sim 10^{-5}$ is best-representative of gas emissions from quiescent degassing volcanoes. Using this ratio, we infer a global volcanic Hg flux from persistent degassing of ~95 $t \cdot yr^{-1}$. If representative of other volcanoes, these results suggest degassing of basaltic magma plays an important part of the global atmospheric Hg budget.

According to both these data and recent observations [Bagnato et al., 2010], volcanism thus would contribute from as little as 12 to as much as 78% of the estimated global natural Hg budget. Volcanic Hg

therefore has a greater potential for local and global environmental impact than Hg from the more prodigious but diffuse natural and anthropogenic sources. In particular, Hg released from Mt Etna degassing, the largest active volcano in Europe, represents approximately 5% of the total industrial Hg emissions in the Mediterranean area [~105 $t \cdot yr^{-}1$, Pirrone et al., 2009] and about 2% of the anthropogenic Hg supplies throughout Europe [~239 $t \cdot yr^{-1}$, EMEP 2002].

With these new estimates we critically revisit the idea that volcanic activity is a trivial contribution to the atmospheric Hg supply in the Mediterranean area. We shall re-examine the status of the global volcanic mercury emissions budget and its uncertainties, even when only considering quiescent phases of volcanic activity. Besides, large sectors of the planet (SW Pacific) are still un-explored, and thus our global Hg flux value estimated from passive degassing may constitutes a lower limit. However, Hg flux measurements in eruptive gases is a priority for future mercury research at volcanoes.

References

Bagnato, E., Aiuppa, A., Parello, F., Allard, P., Liuzzo, M., Giudice, G. and Shinohara, H., (2011). *New clues on mercury contribution from Earth volcanism.* Bulletin of Volcanology (in press.; available on-line DOI: 10.1007/s00445-010-0419-y).

Ferrara, R., Mazzolai, B., Lanzillotta, E., Nucaro, E. and Pirrone, N., (2000). *Volcanoes as emission sources of atmospheric mercury in the Mediterranean basin*. Sci Total Environ 259, pp 115-121.

Nriagu, J.O., (1989). *A global assessment of natural sources of atmospheric trace metals*. Nature 338, pp 47-49.

Pirrone, N., Cinnirella, S., Feng, X., Finkelman, R.B., Friedli, H.R., Leaner, J., Mason, R., Mukherjee, A.B., Stracher, G., Streets, D.G. and Telmer, K., (2009). *Global mercury emissions to the atmosphere from natural and anthropogenic sources*. In: Pirrone, N., and Mason, R (eds), Mercury fate and transport in the global atmosphere, Springer, New York, pp 3-59.

Pyle, D.M., Mather, T.A., (2003). *The importance of volcanic emissions for the global atmospheric mercury cycle*. Atmos Environ 3, pp 5115-5124.

Streets, D. G., Hao, J., Wang, S. and Wu, Y., (2009). *Mercury emissions from coal combustion in China*, Springer, New York, USA, 2, pp 51–65.

Varekamp, J.C., Buseck, P.R., (1986). *Global mercury flux from volcanic and geothermal sources*. Appl Geochem 1, pp 65-73.

Static Stress Interaction between Magmatic and Seismic Activity at Mt. Etna Volcano

Amalia Bonanno

Università degli Studi di Catania, Dipartimento di Elettrica, Elettronica e dei Sistemi, Catania, Italy

Magma movement through the shallow crust commonly affects the seismic pattern in volcanic areas. Changes in stress state have been observed at several volcanoes occurring as a consequence of the deformation produced by the pressurization of a magmatic body or due to the propagation of a magma filled fracture. Several studies investigated earthquake triggering and occurrence of seismic swarms within or close to volcanic edifices [Cayol et al., 2000; Hill et al., 2002; Walter and Amelung, 2004]. Spatial and temporal relationships between stress changes and earthquakes are explained through the Coulomb failure stress (CFS) change defined as:

$$\Delta CFS = \Delta\tau + \mu'\Delta\sigma_n \qquad (1)$$

Where $\Delta\tau$ is the shear stress change computed in the direction of slip on the fault, $\Delta\sigma_n$ is the normal stress change and μ' is the effective friction. For simplicity, a constant effective friction model is considered [Cocco and Rice 2002], assuming pore pressure ΔP proportional to the normal stress changes. It is demonstrated that small positive static stress changes ($\geq$ 0.1 bars) produced by a magmatic source may trigger seismicity within a rock volume close to the critical state of failure [Stein, 1999; Toda et al., 2002].

On Mt. Etna volcano numerous eruptions and associated deformation episodes occurred. In the last four hundred years, about half of the eruptions occurred along the rift zones through fissures opened on the volcano flanks [Behncke et al., 2005]. These fissures are usually related to the lateral intrusion of dikes radiating from a shallow magma conduit system. In order to investigate the relationships between eruptions and earthquakes I compute the CFS patterns induced by deformation sources on the seismogenic faults located on the eastern and southwestern flank of volcano. At first I simulate stress changes due to typical intrusions occurred on March 1981 and on July 2001, respectively. Static stress analysis performed using Coulomb software indicates that the opening of 1981 NNW fissure on the NW side of the volcano rises ΔCFS on both the Timpe and Pernicana faults. In contrast, 2001 N-S intrusion on the south flank increases ΔCFS only on Timpe Fault System. These results are compatible with the observed pattern of seismicity, but emphasize an extremely heterogeneous state of stress on the east flank of the volcano [Gresta et al., 2005].

Furthermore by integrating seismological and geodetic data I investigate the 1997-1998 seismic swarms occurring beneath the western flank of Mt. Etna. On the basis of stress tensor inversion and SH_{MAX} analyses I infer an inflating pressure source located at 5.5 km b.s.l. beneath the western flank of the volcano. Evaluation of Coulomb failure stress related to the proposed model, shows how a large part of the seismogenic fault experienced Coulomb failure stress increases (> 5 bars) (Figure 1). I suppose the presence of a sub-vertical weakness-strength region N50°E oriented beneath the western sector of Mt. Etna. This structure could be brought closer to failure thereby generating seismic swarms as the effect of elastic stress transfer induced by movement and/or overpressure of magmatic masses within the upper crust under the volcano. A deep stress changes analysis may help to forecast the behavior during future volcanic crisis at Mount Etna, which is important in minimizing volcanic and seismic hazards on the highly populate volcanic area.

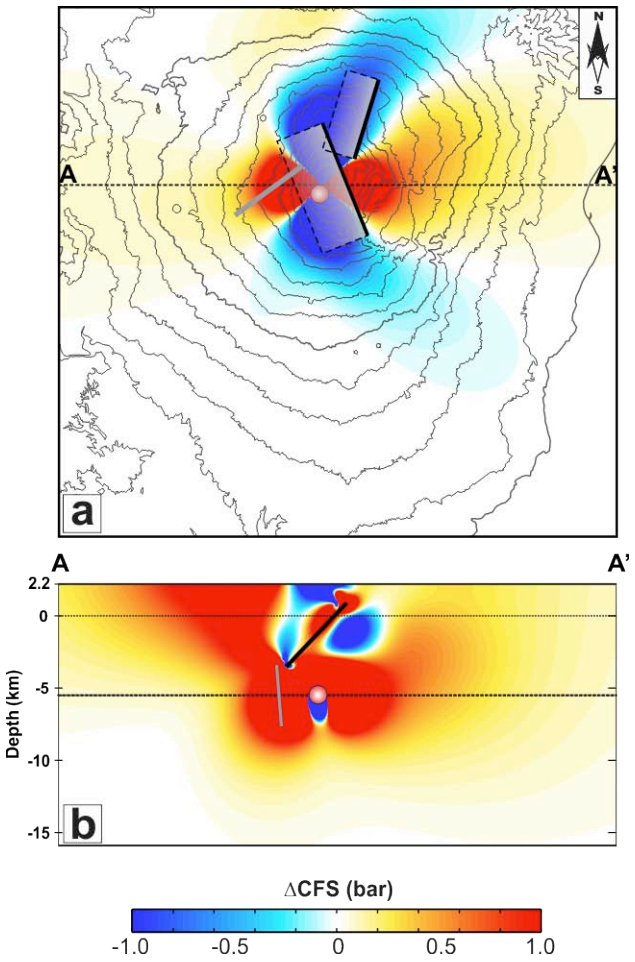

Figure 1. ΔCFS computation due to three modeled sources (black lines and red circle) inferred by integrating of seismic and deformation data collected during 1997-1998 period at Etna volcano. (a) Map and (b) cross section show how a large part of the seismogenic fault (grey line) experienced Coulomb failure stress increases (> 5 bars).

References

Behncke, B. Neri, M., Nagay A. (2005). *Lava flow hazard at Mount Etna (Italy): new data from a GIS-based study*. In: Manga M, Ventura G (eds.) Kinematics and dynamics of lava flows. Geological Society of America Special Papers, 396, 189–209.

Cayol, V., Dieterich, J. H., Okamura, A. and Miklius, A., (2000). *High magma storage rates before the 1983 eruption of Kilauea, Hawaii*. Science, 288, 2343-2346.

Cocco, M. and Rice, J.R., (2002). *Pore pressure and poroelasticity effects in Coulomb stress analysis of earthquake interactions*. Journal of Geophysical Research, 107 (B2), 2030, doi:10.1029/2000JB000138.

Gresta, S., F. Ghisetti, E. Privitera, and A. Bonanno (2005). *Coupling of eruptions and earthquakes at Mt. Etna (Sicily, Italy): A case study from the 1981 and 2001 events*. Geophysical Research Letters, 32, L05306, doi:10.1029/ 2004GL021479.

Hill, D.P., Pollitz, F. and Newhall C., (2002). *Earthquake-volcano interactions*. Phys. Today, 55, 41- 47.

Stein, R.S., (1999). *The role of stress transfer in earthquake occurrence*. Nature, 402, 605-609.

Toda, S., Stein, R. S., and Sagiya, T., (2002). *Evidence from the AD 2000 Izu islands earthquake swarm that stressing rate governs seismicity*. Nature, 49, 58-61.

Walter, T. R., and Amelung, F., (2004). *Influence of volcanic activity at Mauna Loa, Hawaii, on earthquake occurrence in the Kaoiki Seismic Zone*. Geophysical Research Letters, 31, L07622, doi:10.1029/2003GL019131.

Estimating Probabilities of Eruption at Mt. Etna volcano (Sicily, Italy)

Alfonso Brancato and Stefano Gresta

Università di Catania, Dipartimento di Scienze Geologiche, Catania, Italy

Advances in volcano monitoring and forecasting need of a multidisciplinary collaborative framework. In light of this, a Bayesian Event Tree approach was performed, for the first time, at the active open-conduit Mt. Etna volcano. The code named BET_EF (Bayesian Event Tree_Eruption Forecasting; Marzocchi et al., 2004, 2008) is applied to analyze the space-time distribution of the volcanic activity of Mt. Etna during 2001-2005.

The algorithm is composed by a *non monitoring* component and a *monitoring* one. The aim of the application consists of tying the historical volcanic background with the modern monitoring capacity. Therefore, the procedure is set to estimate an a priori probability distribution based upon theoretical knowledge, to accommodate it by using past data, and to modify it further by using current monitoring data. The output of the code is based on the estimation of the probabilities along a selected path of five nodes (unrest/no unrest, magma/no magma, eruption/no eruption, vent location and size/type of eruption, respectively).

The experimentation in estimating probabilities at Mt. Etna volcano started three years ago, when the code was applied to analyze the July-August 2001 flank eruption [Brancato et al., in print]. Considering a reliable forecasting time window of a week, anomalies in the monitoring dataset were able to predict the flank activity more than a month in advance of the effective onset of the eruption. Then, the code was extensively applied to a longer period (2001-2005), where two more flank eruptions occurred (October 2002-January 2003 and September 2004-March 2005, respectively) with the aim of a retrospective analysis [Brancato et al., submitted].

For the pioneer test, an a priori model that deals with the present tectonic and volcanic structure of the Mt. Etna, mainly based on past vent locations and fracture location datasets (last 100 years of eruptive history of the volcano) was considered [Brancato et al., in print]. A subdivision in five sectors (central crater area, and east, north, west and north sectors) was adopted for the vent location.

For the subsequent retrospective analysis, the historical background was back extended to the last 400 years of flank volcanic activity, and a grid of 22x22 1 km squared cell was used to better define the first outbreak of the eruptive scenario [Brancato et al., submitted]. In both cases, the variation of the information through time, and their relationship with the structural setting of the volcano, were able to define an a posteriori probability map for next vent opening.

For short-term forecasting vent opening hazard assessment, the monitoring has a leading role, primarily based on seismological and volcanological data, integrated with strain, geochemical, gravimetric and magnetic data. As a consequence, an expert team was elicited.

A reliable monitoring dataset has been defined after some elicitation sessions, during which the involved parameters were set in terms of inertia and thresholds, as well as the relative Boolean or fuzzy perspective.

Being the monitoring an expression of the state of the volcano, the parameters must be expressive of a certain level of anomaly. Considering a single threshold for each monitoring parameter, distinguished among two possible states ("anomalous" or "not anomalous"), seems a coarse decision. In fact, a system can evolve to an anomalous state gradually, rather than overcoming one specific value of a monitoring measure. Moreover, the definition of a threshold is strongly subjective and, thus, can strongly affects the outcomes. A more appropriate solution is provided when the monitoring measure is considered by a fuzzy approach, with a membership function. Through this approach we were able to associate a certain degree of anomaly of the considered measure. By the way, if the monitoring variable has a binary value, then a more conservative Boolean case will be considered.

Constant unrest probability of 100%, with magma involvement usually higher than 95.0% has been computed along the analyzed time period. Eruption probability values higher than 90% have been estimated few days before the onsets of the July-August 2001 and October 2002-January 2003 flank eruptions. Values slightly higher than 75% have been observed during the lava fountaining June-July 2001 period. On the contrary, the probability values flattened around 30% for the September 2004-March 2005 flank eruption.

With suitable data, a well depiction of the real location of the eruptive scenario for the 2001 and 2002-2003 events was given.

The fifth node (size/type of eruption) deserves more attention. Theoretical approaches have been proved that no monitoring parameter is able to provide insights into the style and size of an incoming eruptive activity. In the pioneer test, the aim was to analyze the type of an eruption, being distinguished among subplinian, lava fountaining, strombolian, and effusive. In the longer retrospective analysis, the size was analyzed in terms of volume and duration of an eruption. In the former, the quality of the elicited parameters was not able to discriminate among the considered different volcanic activities, whereas, in the latter, the estimated probabilities did not show any significant variation with time.

The different approaches in both analysis have clearly shown how at Mt. Etna such a application is needed to assure the primary role of the monitoring in the short term eruptive hazard of the volcano. Therefore, anomalies in the dataset were able to track the probabilities pattern with a good matching with the real occurred scenario.

In any case, the methodology allowed a clear identification of assumptions and monitoring parameter thresholds and provided rational means for their revision if new data or information are incoming.

References

Marzocchi, W., Sandri, L., Gasparini, P., Newhall, C. and Boschi, E., (2004). *Quantifying probabilities of volcanic events: The example of volcanic hazard at Mount Vesuvius*. Journal of Geophysical Research, 109, B11201, doi:10.1029/2004JB00315U.

Marzocchi, W., Sandri, L. and Selva, J., (2008). *BET_EF: a probabilistic tool for long- and short-term eruption forecasting*. Bulletin of Volcanology, 70, doi: 10.1007/s00445-007-0157-y.

Brancato, A., Gresta, S., Sandri, L., Selva, J., Marzocchi, W., Alparone, S., Andronico, D., Bonforte, A., Caltabiano, T., Cocina, O., Corsaro, R.A., Cristofolini, R., Di Grazia, G., Distefano, G., Ferlito, C., Gambino, S., Giammanco, S., Greco, F., Napoli, R., Tusa, G. and Viccaro, M., (in print). *Quantifying probabilities of eruption at a well-monitored active volcano: an application at Mount Etna (Sicily, Italy)*. Bollettino Geofisica Teorica e Applicata.

Brancato, A., Gresta, S., Alparone, S., Andronico, D., Bonforte, A., Caltabiano, T., Cocina, O., Corsaro, R.A., Cristofolini, R., Di Grazia, G., Distefano, G., Ferlito, C., Gambino, S., Giammanco, S., Greco, F., Napoli, R., Sandri, L., Selva, J., Tusa, G. and Viccaro, M., (in print). *Application of BET_EF at Mount Etna: a retrospective analysis (years 2001-2005)*. Submitted to Annals of Geophysics.

Impact of Volcanic Emissions on Trace Elements Contents Measured in Endemic Plants at Mt. Etna (Italy)

Sergio Calabrese[1], Emanuela Bagnato[1], Sergio Bellomo[2], Marcello Bitetto[1], Lorenzo Brusca[2], Walter D'Alessandro[2], Francesco Parello[1], Filippo Saiano[3]

[1]*Università di Palermo, Dipartimento Scienze della Terra e del Mare, Palermo, Italy*
[2]*Istituto Nazionale di Geofisica e Vulcanologia, Sezione di Palermo, Italy*
[3]*Università di Palermo, Dipartimento ITAF, sez. Chimica, Palermo, Italy*

Land use on Mount Etna has been well described as a series of concentric zones changing with altitude [Chester et al., 1985]. The area below 1000 m is extensively cultivated with orchard plantations, vineyards, cereals, pistachio and hazel shrubbery. The zone between 1000 and 2000 m is covered by woods (pines, chestnuts, oaks, beeches and birches). Above 2000 m, the desert zone, the ground is usually characterized by volcanic ash and lava flows where only few pioneer plants resist to the extreme environment.

Biomonitoring may be defined as the use of organisms and biomaterials (biomonitors) to obtain informations on certain characteristics of a particular medium (atmosphere, hydrosphere etc.). In particular the accumulation of trace metal in mosses, lichens and plant leaves has long been used in studies on the impact and spatial distribution of pollution. Recently such biomonitoring techniques have been applied also to ascertain the impact of contaminants naturally released by volcanic activity [Le Guern et al., 1988; Bellomo et al., 2007; Watt et al., 2007; Martin et al., 2009; Quayle et al., 2010; Martin et al., 2011].

In the present study a biomonitoring survey, using leaves of trees (*Betulla aethnensis, Pinus nigra and Populus tremula*) and two endemic species (*Senecio aethnensis* and *Rumex aethnensis*) above treeline level, was performed on Mt. Etna, in order to evaluate the dispersion and the impact of volcanic emissions. Samples of leaves were collected in summer 2007-2008 from 30 sites in the upper part of the volcano (800-3000 m a.s.l). Acid digestion of samples was carried out with a microwave oven (HNO_3 + H_2O_2), and 44 elements were analyzed by using plasma spectrometry (ICP-MS and ICP-OES).

Major constituents in Senecio and Rumex leaves are K, Ca, Mg, Na, Si, Al and Fe ranging from about 10^3 to 10^5 ppm. Manganesium, Sr, Rb, Ba, Zn, B, Cu show also relatively high concentrations (10^1-10^3 ppm) while the remaining elements (As, Bi, Cd, Ce, Co, Cr, Cs, Ga, Li, Mo, Ni, Pb, Sb, Sc, Se, Th, Tl, U, V, Y and lanthanide series) display much lower values (10^1-10^{-3} ppm). Nearly all investigated elements show their highest concentrations in the samples collected closest to the degassing craters. Increased concentrations are also found in the samples collected on the eastern flank of Mt. Etna, which, being in the downwind direction with respect to the summit vents, is most impacted by volcanic emissions (fig.1). The high concentrations of many toxic elements in the leaves allow us to consider these plants as highly tolerant species to the volcanic emissions, and suitable for biomonitoring researches.

Leaves collected along two radial transects from the active vents on the eastern flank, highlight that the levels of metals decrease from one to two orders of magnitude with the distance from the source. Figure 1 shows for example the measured concentrations of Thallium. The decrease is stronger for volatile elements, which are highly enriched in the Etnean volcanic emissions, (As, Bi, Cd, Cs, Pb, Sb, Tl) than for more refractory elements (Al, Ba, Sc, Si, Sr, Th, U). The different species of plants show significant differences in the bioaccumulation processes for most of the analyzed elements, in particular lanthanides, which are systematically enriched in Rumex leaves. Needles of pine (non-deciduous tree) represents a good tool for biomonitoring investigation because they are important tracers of accumulation with time as showed in figure 1.

The present study further confirms that biomonitoring has a strong potential in tracing the impact and geographic distribution of volcanic emissions.

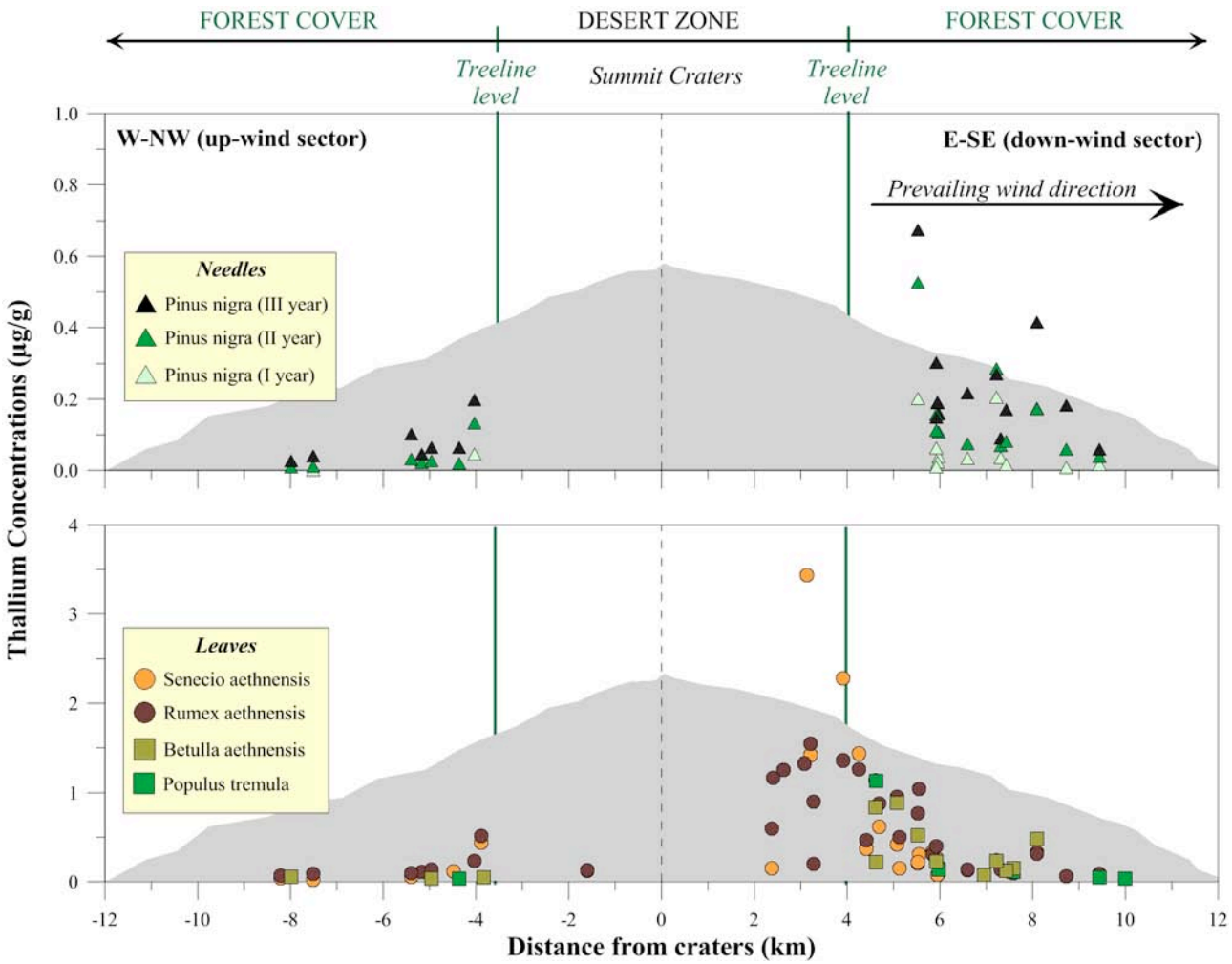

Figure 1. Spatial and time distribution of Thallium concentrations in the five studied plants species.

References

Bellomo, S., Aiuppa, A., D'Alessandro, W. and Parello, F., (2007). *Environmental impact of magmatic fluorine emission in the Mt. Etna area*. Journal of Volcanology and Geothermal Research, 165, 1-2, 87-101.

Chester, D.K., Duncan, A.M., Guest, J.E. and Kilbum, C.R.J., (1985). In: *"Mount Etna: The Anatomy of a Volcano"*. Chapman & Hall, London.

Le Guern F., Faivre-Pierret R.X. and Garrec, P. (1988). *Atmospheric contribution of volcanic sulphur vapor and its influence on the surrounding vegetation.* Journal of Volcanology and Geothermal Research, 35, 173-178.

Martin, R.S., Mather, T.A., Pyle, D.M., Watt, S.F.L., Day, J., Collins, S.J., Wright, T.E., Aiuppa, A. and Calabrese, S., (2009). *Sweet chestnut (Castanea sativa) leaves as a bio-indicator of volcanic gas, aerosol and ash deposition onto the flanks of Mt Etna in 2005-2007.* Journal of Volcanology and Geothermal Research, 179, 107–119.

Martin, R.S., Witt, M.L.I., Pyle, D.M., Mather, T.A., Watt, S.F.L., Bagnato, E. and Calabrese, S. (2011). *Rapid oxidation of mercury (Hg) at volcanic vents: insights from high temperature thermodynamic models of Mt Etna's emissions.* Chemical Geology, 283, 279-286, doi:10.1016/j.chemgeo.2011.01.027.

Quayle, B.M., Mather, T.A., Witt, M., Maher, B.A., Mitchell, R. and Martin, R.S. (2010). *Application and evaluation of biomagnetic and biochemical monitoring of the dispersion and deposition of volcanically-derived particles at Mt. Etna.* Journal of Volcanology and Geothermal Research, 191/1-2, 107-116.

Watt, S.F.L., Pyle D.M., Mather T.A., Day J.A. and Aiuppa A. (2007). *The use of tree-rings and foliage as an archive of volcanogenic cation deposition.* Environmental Pollution, 148, 48–61, doi:10.1016/j. envpol.2006.11.007

Dynamic Stress Transfer from Distant Earthquakes at Mt. Etna: January 2006 and May 2008 Cases of Study

Andrea Cannata[1], Giuseppe Di Grazia[1], Placido Montalto[1], Marco Aliotta[1,2], Domenico Patanè[1] and Enzo Boschi[3,4]

[1]*Istituto Nazionale di Geofisica e Vulcanologia, Sezione di Catania - Osservatorio Etneo, Italy*
[2]*Università degli Studi di Catania, Dipartimento di Informatica, Catania, Italy*
[3]*Istituto Nazionale di Geofisica e Vulcanologia, Rome, Italy*
[4]*Università degli Studi di Bologna (Dipartimento di Fisica, Settore Geofisica)*

Influences of distant earthquakes on volcanic systems by dynamic stress transfer are well documented [Manga and Brodsky, 2006]. In this work we analyzed seismic signals and volcanic activity at Mt. Etna during two periods, January 2006 and May 2008, that clearly showed variations coincident with distant earthquakes. During the first period, characterized at Mt. Etna by mild volcano activity, an earthquake in Greece with magnitude 6.8 took place, during the second, that showed an intense explosive activity, an earthquake with magnitude 7.9 occurred in Sichuan province (China). The values of peak dynamic stress at Mt. Etna, on which at first approximation the ability of an earthquake to trigger seismicity and/or affect the state of geothermal and volcanic systems depend [Hill and Prejean, 2007], were equal to 13 ± 3 and 4 ± 0.7 kPa for the earthquakes in Greece and Sichuan, respectively. Similar values of peak dynamic stress in geothermal and volcanic areas were able to trigger earthquakes [Brodsky and Prejean, 2005], tremor [Miyazawa et al., 2005], or more generally modify the state of geothermal and volcanic systems [e.g., Walter et al., 2009].

Different analyses were performed on the recorded seismic signals: calculation of seismic root-mean-square (RMS) and percentile envelopes over RMS moving windows, short time Fourier transform, β-statistic maps. The use of percentiles enables us to separately consider the contributions of continuous signal (volcanic tremor) and seismic transients (mainly earthquakes and LP events). On the other hand, the β-statistic maps are drawn to investigate prospective changes in the seismo-volcanic activity before and after the passage of large earthquake seismic waves, and then to show the spatial distribution of likely instances of dynamic triggering.

In the first period, January 2006, the effect of the dynamic stress transfer was twofold: (1) banded tremor activity changed its features and almost disappeared; (2) a swarm of volcano-tectonic (VT) earthquakes took place. Banded tremor is a particular kind of seismic tremor observed at volcanoes and geysers, and its source has been modeled as a two-phase hydrothermal instability flow model [Fujita, 2008]. Since the behavior of banded tremor may be considered chaotic [Cannata et al., 2010], and then very sensitive to the initial conditions, the changes of the banded tremor can be due to slight variations in rock permeability caused by fluid flows driven by dynamic strain. In the same way, the occurrence of the swarm of VT earthquakes 2 h after the wave arrival of the Greek earthquake (Figure 1a) probably developed as a secondary process, promoted by the dynamically triggered activation of magmatic fluids.

During the second period, May 2008, the dynamic stress transfer, associated with the arrival of the seismic waves of the Sichuan earthquake, affected the character of the seismo-volcanic signals and on the following day triggered an eruption. In particular, we observed a gradual decrease of the volcanic tremor amplitude, starting just after the teleseismic wave arrival, mainly related to a deepening and northward shift of the source. Further, an increase of number and energy of LP events took place roughly 9 h later (Figure 1b). According to the widely accepted model of Chouet [1996], LP events are the result of the acoustic resonance of fluid-filled cracks triggered by pressure transients. On the basis of this model, the observed enhanced LP activity seems to suggest an increasing overpressure, likely triggered by dynamic stress transfer, that led on the following day to an eruption. Indeed, according to Manga and Brodsky [2006], under proper conditions, small pressure changes, associated with dynamic stresses, in a crystallizing magma close to critical supersaturation, should be capable of triggering a significant increase in bubble nucleation leading to a marked pressure increase.

In conclusion, we have presented evidence that phenomena of dynamic stress transfer took place at Mt. Etna and, if the system is in a critical state, are able to modify the state of the volcano, and even lead to eruptions.

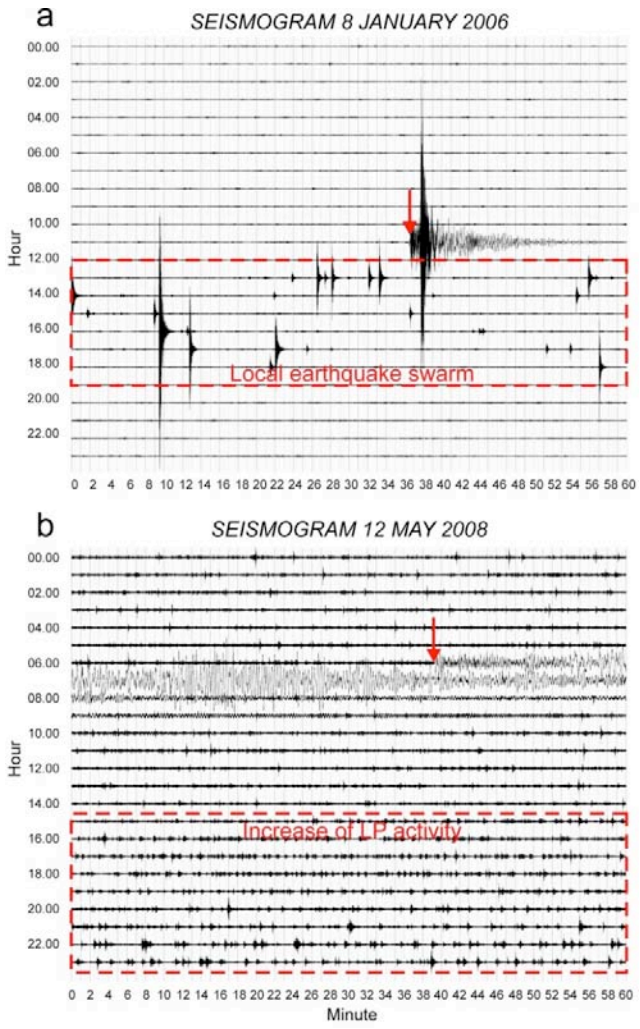

Figure 1. 24-h helicorder plots from the vertical component of EMPL and EPDN stations (located on Mt. Etna volcano) for 8 January 2006 (a) and 12 May 2008 (b), respectively. The red arrows indicate the arrival time of seismic waves of the Greek and Sichuan earthquakes in (a) and (b), respectively.

References

Brodsky, E. E. and Prejean, S. G., (2005). *New constraints on mechanisms of remotely triggered seismicity at Long Valley Caldera*. J. Geophys. Res., 110, B04302, doi:10.1029/2004JB003211.

Cannata, A., Di Grazia, G., Montalto, P., Ferrari, F., Nunnari, G., Patane, D. and Privitera, E., (2010). *New insights into banded tremor from the 2008–2009 Mt. Etna eruption*. J. Geophys. Res., doi:10.1029/2009JB007120.

Chouet, B., (1996). *Long-period volcano seismicity: Its source and use in eruption forecasting*. Nature, 380, 309-316.

Fujita, E., (2008). *Banded tremor at Miyakejima volcano, Japan: Implication for two-phase flow instability*. J. Geophys. Res., 113, B04207, doi:10.1029/2006JB004829.

Hill, D. P., and Prejean, S., (2007). *Dynamic triggering*. In: Treatise on Geophysics, vol. 4 (H. Kanamori ed.), pp. 257–291. Elsevier, Amsterdam.

Manga, M., and Brodsky, E., (2006). *Seismic triggering of eruptions in the far field: Volcanoes and geysers*. Annu. Rev. Earth Planet. Sci., 34, 263–291.

Miyazawa, M., Nakanishi, I., Sudo, Y. and Ohkura, T., (2005). *Dynamic response of frequent tremors at Aso volcano to teleseismic waves from the 1999 Chi-Chi, Taiwan earthquake*. J. Volcanol. Geotherm. Res., 147, 173–186.

Walter, T. R., Wang, R., Acocella, V., Neri, M., Grosser, H. and Zschau, J., (2009). *Simultaneous magma and gas eruptions at three volcanoes in southern Italy: An earthquake trigger?* Geology, 37, 251–254.

Pele's Hairs: Case Studies from Kilauea Volcano

Chiara B. Cannata[1], Rosanna De Rosa[1], Bruce Houghton[2], Paola Donato[1], Andrea Nudo[1]

[1]*Università della Calabria, Dipartimento di Scienze della Terra, Arcavacata di Rende, Italy*
[2]*Department of Geology and Geophysics, University of Hawai'i at Manoa, Honolulu, USA*

Pele's hairs are long, thin strands of basaltic volcanic glass formed when small drops of magma are spun or drawn out by the wind or streams of volcanic gas into long hair-like strands. Named for Pele, the Hawaiian goddess of fire, they are basically found in Hawaiian eruption deposits. Pele's hairs are deep yellow or gold and are commonly found downwind from active vents concentrated in hollows or other low energy 'traps'. In literature the origin of these thin strands of glass have been linked to fountains from Hawaiian eruptions. Beside the high fountaining, Pele's hairs are actually found in other environments. In this work we investigated in detail the dimensions, surface textures and inner structure of Pele's hairs, from three typical environment of formation at Hawaiian volcanoes: high fountaining, weak explosive activity, lava ocean entry (magma-water interaction). Samples have been characterized in terms of textural and morphological features in 3D and thin section under the optical microscopy and SEM images. Pele's hairs consist of long strands of gold sideromelane, showing variable length, from an half to tens of mm, sometimes including Pele's tears inside or at the end. They are often found incomplete, since they get easily broken on landing or even during transport. Their surfaces are mostly rough, with 'ploughs' of different sizes and large cavities. Vesicles are visible in the cross sections of Pele's hairs. There are two mostly size population of bubbles: one elongated, arranged central and parallel to the axis of elongation of the hair and the other one smaller and rounded, dispersed across it's cross section. Pele's hairs often show, in thin section, a single inner elongate vesicle in the middle of the fragment, linked to bubbles coalescence phenomena, along the entire length of the hair. In this preliminary work we show that samples from the three volcanic environments have different features in terms of their shape, surface textures and micro-textures. We show also preliminary data on the bubble size distribution (BSD) of the products of the three volcanic environments.

Future work will be focused on the bubble size distribution (BSD) of the two recognized main population of vesicles to understand the role played by cooling, degassing and shear effects on the texture and shape of Pele's hairs, as well as their formation.

Dynamics of Strombolian Eruptions: Parameterizing through High-Speed Video Analysis

Antonio Capponi

Università degli Studi La Sapienza, Dipartimento di Scienze della Terra, Rome, Italy

Strombolian explosive activity is generally characterized by a series of short mild explosions caused by the bursting of large individual gas bubbles at the magma free surface; however this activity shows a wide range of styles.

Stromboli volcano offers an excellent location to study this activity, due to its persistent explosive activity with a broad range of styles - from normal Strombolian activity up to violent and sustained explosions - and its ease to access. Our high-speed video analysis study of several explosions at Stromboli - so far focused on two of three active craters - has shown how this events can be complex and heterogeneous with gas release, pressure and temperature values and explosion depth linked to unclear conduit dynamics and magma behavior.

Our data acquisition system includes a NAC HotShot 512 SC high-speed camera (all videos were acquired at 500 frame per seconds), a GPS unit for time-synchronization, a customized commercial microphone (linear response in the 1-20000 Hz freq. range) and a laptop; all powered by 12V batteries. The C-MOS sensor of the camera is monochromatic and sensitive to the near-infrared spectral region, so we can distinguish hot zones (brighter tones) from the cold ones.

Application of high speed imaging to Strombolian activity at Stromboli volcano revealed previously unreported or poorly reported processes, including pre- and post- explosion crater floor deformation, multiple jet pulses within a single explosion, deformation and fragmentation of in-flight scoria, different explosive styles within the same vent. Frame analysis (Fig. 1A) allow us to precisely determine pyroclasts exit velocities, trajectories, granulometry and mass flux.

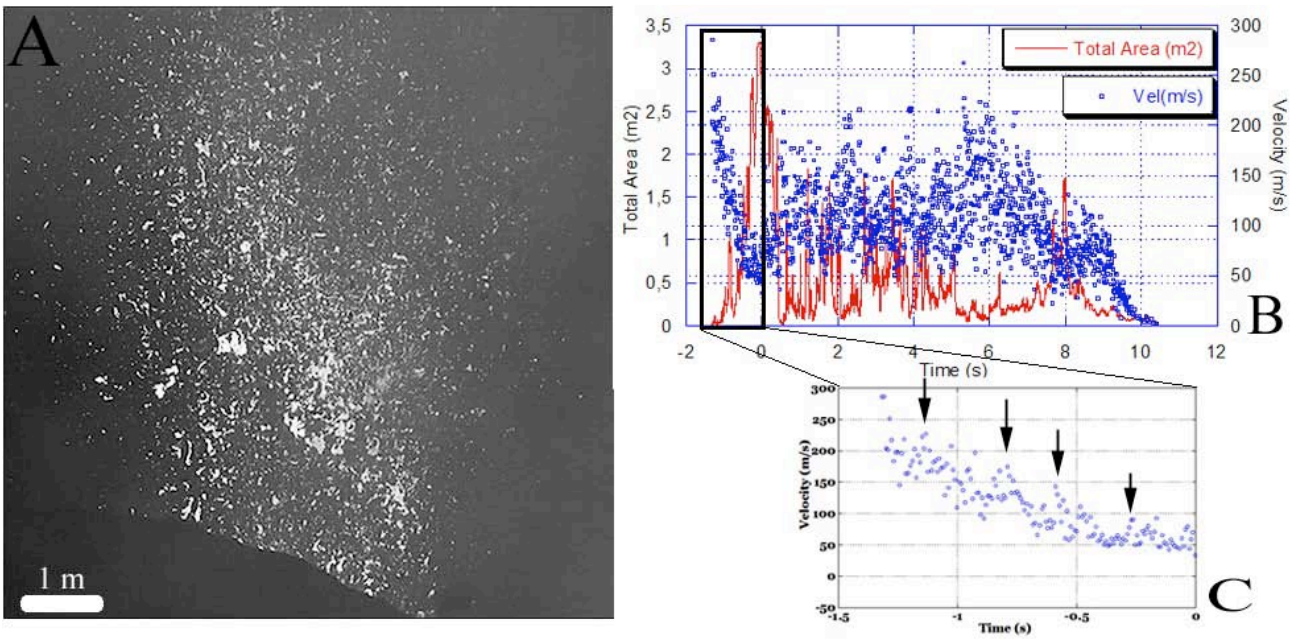

Figure 1. A) Example of a frame extracted from a high-speed video; B) Example of the resulting data: correlation between mass flow and velocities of the ejecta C) Detail of particle velocity of a single pulse, also made up of different sub-pulses (indicated by black arrows).

In particular, our manually measured velocity values are far higher than those reported in previous studies [Chouet et al. 1974; Blackburn et al. 1976; Weill et al. 1992; Ripepe et al. 1993; Patrick et al. 2007], revealing peak velocities >300 m/s - unprecedented for Strombolian activity - and showing not only repeated oscillations, but also a clear reversed correlation with the mass flux (Fig. 1B).

The complex fluctuations of these two parameters within every single impulse seem to be caused by multiple bubble bursting (and/or variable gas-particle coupling in the flow), while the inverse correlation is probably due to the constancy of momentum.

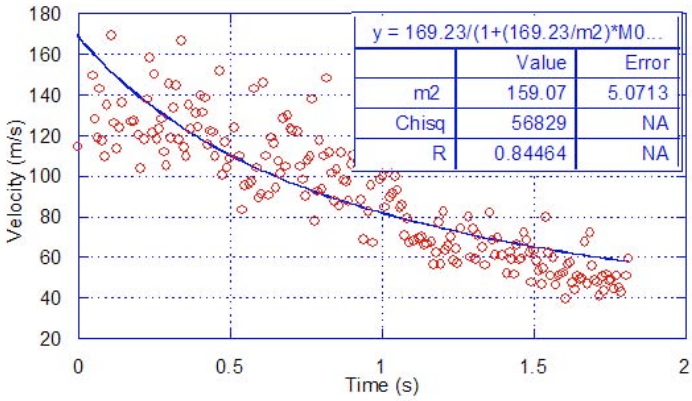

Figure 2. Exit velocities of pyroclasts during a pulse in an explosion and curve fit based on the model.

Furthermore, video analysis pointed out how every explosion is featuring multiple pulses, also made up of different sub-pulses: these pulses consist of the fast release (from a few milliseconds to a few seconds) of well-collimated pyroclasts jets and are characterized by exponentially decreasing velocity of progressively erupted pyroclasts (Fig. 1C).

By comparing the experimental data of jets reproduced through Shock-Tube experiments [Alatorre et al. 2010] with the data obtained from the video, it was possible to characterize each of these sub-pulses. Such confrontation allowed us to create a model that describes the decay rate (deceleration of the particles) and maximum velocity as a function of pressure, volume and the depth of explosion (Fig. 2).

Another aspect to be further developed is the relationship between the synchronized acoustic signals associated with an explosion (recorded during high-speed videos acquisition) and the mass flux: in our preliminary analysis, frequency and amplitude of acoustic signals seem to be inversely correlated with flux and velocity of ejecta.

Finally, a possible application of the model could be the study of ballistics aimed at the creation of related impact's probability hazard maps.

References

Chouet, B., Hamisevicz, N. and McGetchin, T., (1974). *Photoballistics of Volcanic Jet Activity at Stromboli, Italy*. Journal of Geophysical Research, 79(32), 4961-4976.

Blackburn, E.A., Wilson, L. and Sparks, R.S.J., (1976). *Mechanism and Dynamics of Strombolian Activity*. Journal of the Geological Society, 132, 429-440.

Weill, A., Brandeis, G., Vergniolle, S., Baudin, F., Bilbille, J., Fèvre, J.F., Piron, B. and Hill, X., (1992). *Acoustic Sounder Measurements of the Vertical Velocity of Volcanic Jets at Stromboli Volcano*. Geophysical Research Letters, 23, 2357-2360.

Ripepe, M., Rossi, M. and Saccorotti, G., (1993). *Image processing of explosive activity at Stromboli.* Journal of Volcanology and Geothermal Research, 54, 3-4, 335-351, DOI: 10.1016/0377-0273(93)90071-X.

Patrick, M.R., Harris, J.L.A., Ripepe, M., Dehn, J., Rothery, A. and Calvari, S., (2007). *Strombolian Explosive Styles and Source Conditions: Insights from Thermal (FLIR) Video*. Bulletin of Volcanology, 69, 769-784.

Alatorre, M., Scheu, B., Dingwell, D.B., Delgado-Granados, H. and Taddeucci, J., (2010). *Energy Consuption by Magmatic Fragmentation and Pyroclast Ejection During Vulcanian Eruptions*. Earth and Planetary Sciences Letters 291, 60-69.

Numerical Modelling of Explosive Eruptions and Pyroclastic Density Currents

Susanna Carcano

Politecnico di Milano, MOX – Dipartimento di Matematica, Milan, Italy

The purpose of the work is the development of accurate and efficient numerical methods for the simulation of explosive eruptions and pyroclastic density currents. The starting point is the numerical model PDAC developed over the last 15 years at INGV-Pisa (see e.g. [Neri et al. (2003)]). This model is based on a set of equations of motion for a mixture of gas and solid particles, described as interpenetrating continua. The equations for gaseous and particle species are coupled through drag and heat transfer terms. The gas phase is compressible and obeys the ideal gas law, while the solid phase is incompressible at the microscopic level.

The first objective of the project is to carry out a dimensional analysis of the equations, in order to get some insight into the fundamental properties of the mathematical model. Through this analysis we introduce non dimensional parameters in order to identify the relevant scales for the physical phenomena that we are considering. We consider two essentially different regimes. In the first case (A), we analyse the flow dynamics above the volcano's vent during the eruption, supposing to have a continuous ejection of the gas-particles mixture. In the second case (B), we suppose that the volcano has stopped ejecting the mixture and we analyse the properties of the pyroclastic density current along the volcano side. We refer to [Neri et al. (1996); Todesco et al. (2002); Neri et al. (2003); Esposti Ongaro et al. (2008)] for the values of the physical coefficients.

In case (A), we obtain that, concerning the momentum equations, the viscous momentum transfer is negligible with respect to the inertial forces, because of the high velocity of the flow coming out from the vent. The most relevant physical phenomena are advection and the gas-particle drag. The effect of the pressure gradient cannot be neglected in the gas momentum balance, but its coefficient becomes small in the solid momentum balance whereas the solid density is much larger than the gas density. If we estimate the Mach number using an appropriate definition of the speed of sound in a mixture [Pelanti et al. (2006)], we obtain a value larger than one, thus suggesting that the compressibility of the gas phase can not be neglected and the flow regime is supersonic. Concerning the gravitational force, its effect is quite small if we consider the phenomenon near the vent, where the kinetic energy of the gas-particle mixture is large.

In the non-dimensional form of the energy balance equations, conductive heat transfer is negligible because of the high velocity of the flow. Advection and the heat transfer between different phases are the dominant phenomena, but also the gas expansion can not be neglected either.

In case (B), after the ejection of the mixture is ended, the dynamics of the flow starts changing significantly. The flow looses part of its kinetic energy, it slows down until the gravitational force becomes dominant and causes the heaviest particles to fall down, forming the pyroclastic density current. This change can be seen in the increase of the coefficient related to the gravitational force, that becomes quite relevant. Also the effect of the pressure gradient and the viscous term are no more negligible for the gas phase. If we estimate the Mach number, we observe that it becomes smaller than before. Also in this case, the phenomenon is dominated by the drag force. Concerning the energy balance, the diffusive terms are not negligible for the gas phase only and the lower velocities allow for a larger heat exchange between the solid and the gas phase.

In conclusion, the dimensional analysis seems to suggest that the mathematical model, as well as the numerical methods applied to solve it, could be adapted in time in order to capture the most relevant phenomena as the process changes.

From the dimensional analysis we have seen that advection is one of the dominating phenomena in the process in both the case (A) and (B), so we expect that a proper numerical treatment of the advection terms should be necessary in order to obtain an accurate numerical solution. Therefore, a first possible modification of the numerical method that is currently being implemented is the introduction in the upwind discretization of the convective fluxes the so-called transverse fluxes [Saltzman J. (1993); LeVeque R.J. (1996)]. In the standard *donor cell* upwind method, the convective flux through one single cell boundary is split into independent fluxes along the x-, y- and z-directions by using the velocities u, v and w in the directions normal to each interface. A better method can be obtained by considering the flux with the proper speed (u,v,w), without splitting it on the three space directions. The unsplit upwind is both more accurate and more stable

that the original version and we expect that this scheme should introduce a lower numerical dissipation than the unsplit upwind method. A similar improvement in the accuracy of the solution should be achieved by the introduction of a second order implicit Crank-Nicholson time discretization to replace the current first order implicit Euler method.

The purpose of the future work is to take further advantage of the results of the dimensional analysis in order to develop improved implicit numerical schemes to reduce significantly the computational cost of the eruption simulation and enhance its accuracy.

References

Esposti Ongaro, T., Neri, A., Menconi, G., de' Michieli Vitturi, M., Marianelli, P., Cavazzoni, C., Erbacci, G., Baxter, P.J., (2008). *Transient 3D numerical simulations of column collapse and pyroclastic density current scenarios at Vesuvius*. Journal of Volcanology and Geothermal Research, 178: 378-396.

LeVeque, R.J., (1996). *High-resolution conservative algorithms for advection in incompressible flow*. SIAM Journal of Numerical Analysis, 33: 627-665.

Neri, A., Esposti Ongaro T., Macedonio G. and D. Gidaspow, (2003). *Multiparticle simulation of collapsing volcanic columns and pyroclastic flow*. Journal of Geophysical Research, 108(B4), 2202, doi: 10.1029/2001JB000508.

Neri, A. and Macedonio, G., (1996). *Physical modeling of collapsing volcanic columns and pyroclastic flows*. In: Monitoring and mitigation of volcano hazards (R. Scarpa and R.I. Tilling ed.), Springer-Verlag Berlin Heidelberg.

Pelanti, M. and LeVeque R.J., (2006). *High-resolution finite volume methods for dusty gas jets and plumes*. SIAM Journal on Scientific Computing, 28: 1335-1360.

Saltzman, J., (1993). *An unsplit 3D method for hyperbolic conservation laws*. Journal of Computational Physics, 115: 153-168.

Todesco, M., Neri, A., Esposti Ongaro, T., Papale, P., Macedonio, G., Santacroce, R., Longo, A., (2002). *Pyroclastic flow hazard assessment at Vesuvius (Italy) by using numerical modeling. I. Large-scale dynamics*. Bulletin of Volcanology, 64: 155-177.

The Submerged Portion of Etna Volcano

Danilo Cavallaro[1], Mauro Coltelli[1], Francesco L. Chiocci[2], Alessandro Bosman[2,3]

[1]*Istituto Nazionale di Geofisica e Vulcanologia, Sezione di Catania - Osservatorio Etneo, Italy*
[2]*Università degli Studi La Sapienza, Rome, Italy*
[3]*CNR-IGAG, Istituto di Geologia Ambientale e Geoingegneria, Italy*

Etna volcano is located on the Ionian coast of Sicily and a significant portion of its eastern flank lies underwater. The submerged portions of Etna are known only in small part, but it appears of fundamental importance in order to understand the dynamic evolution of the volcano.

Between 2005-2009 several marine geophysical surveys have been carried out along the Etna offshore to investigate the main submarine features of the seabottom. The dataset includes more than 2000 km^2 high-resolution bathymetry data (sonar multibeam data), mono-channel seismic reflection data (Sub Bottom Chirp and Sparker data), Side Scan Sonar data, seafloor samples (mostly dredged and grabbed samples) and Rov dives. This dataset is expanded by some photos took during scuba dives in the shallower offshore.

The morphobathymetric analysis of Etna's offshore allows to reveal a very complex setting of the Ionian continental margin just in front of the volcano area because of the presence all together of depositional processes, erosive phenomena, small and large scale gravitational instability and a very active tectonics.

We identify several morphostructural domain that are hereinafter described in details from north to south:

The Fiumefreddo Valley (FV in fig. 1) is a E-W trending huge submarine valley that develops on the continental margin in the offshore the homonymous village for an overall length of 38 km. The thalweg is extremely flat and large up to 4 km and presents some steps inside. The channel-head is located in very shallow water at 15 m of depth only 100 m from the shore line.

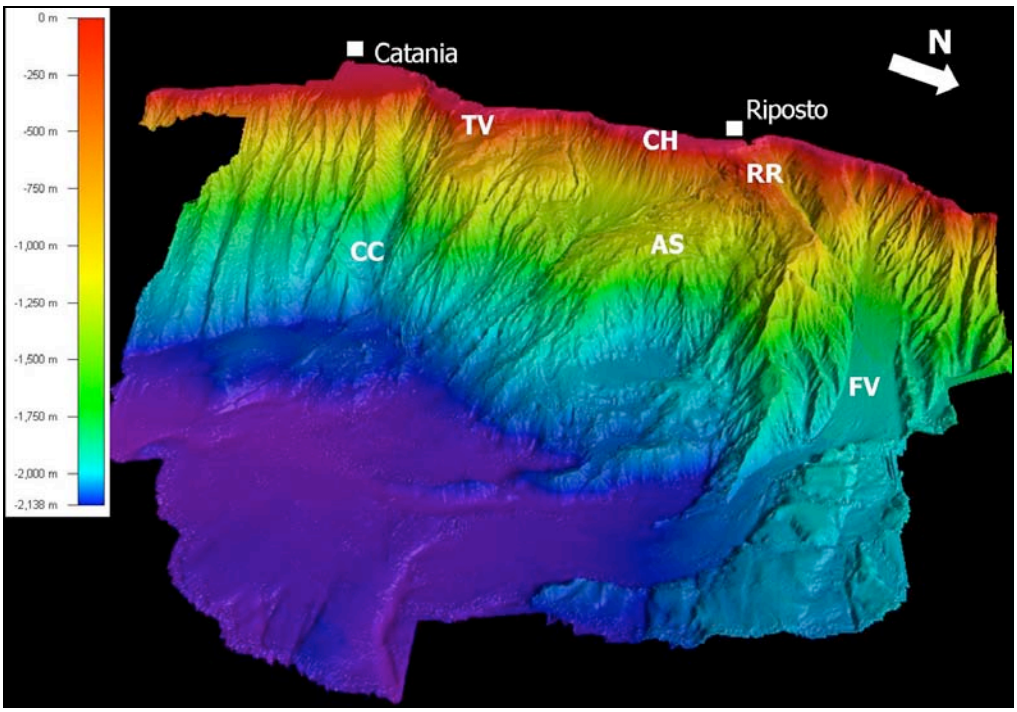

Figure 1 Morphobathymetric 3D view (vertical exaggeration 2x) offshore Etna volcano. CC: Catania Canyon; TV: Timpe Volcano; CH: Chiancone fanglomerate; AS: amphitheatre-shaped structure; RR: Riposto Ridge; FV: Fiumefreddo Valley.

The Riposto Ridge (RR) represents a E-W trending wide morphostructure located offshore the coast between Fiumefreddo and Torre Archirafi. According with Gabbianelli et al. [1995] it represents the underwater prosecution of the Appennino-Maghrebide chain that develops inland with the same trend. The shallow portion of the ridge is divided into two sectors by a deep canyon, called Riposto Canyon; it develops for more than 10 km with a NE-SW trend. The northern sector, called Fondachello Ridge, is characterized by several morphological heights with a conic shape interpret as mud volcanoes. They are arranged in linear and circular clustering and associated with some small scarps interpreted as fault that permitted the up rise of the fluids. The southern one is the Riposto Shoal; it is rimmed by several deep scarps. On the shallow portion of the shoal elongated flat-topped morphologies occur; they are located near the scarps that offset the ridge. According with Patanè et al., [2009] we interpreted these structures as volcanic features emplaced in an age older the last low stand.

The central portion of the surveyed area is characterized by the presence of a huge depositional lobe-shaped body; this deposit is interpreted as the underwater prosecution of the 7,5 ka old Chiancone fanglomerate (CH). It covers an area of about 35 km^2 from Riposto offshore to S. Tecla one and from the coastline to around 650 m of depth. The entire south-central portion is deeply cut by several NE-SW trending faults with scarps high up to 20 m connected to the Riposto Ridge structures and arranged in an en-echelon geometry.

The morphobathymetric analysis of the Etna's offshore highlights the presence of a wide flat-topped morphological high situated between the offshores S. Tecla and Acitrezza, called Timpe Plateau. The overall area of this structure is around 45 km^2 developing for 6,5 km of width (from the coast line to a depth of 600 m) and 8 km of length (from the S. Tecla offshore to Acitrezza-Acicastello one). The Timpe Plateau is characterized by a steep-morphology because of the presence of several deep fault scarps both linear (with an almost N-S trend) and curved (from NNW-SSE to NO-SE). Seismic profiles carried across the plateau show large wedged-shaped sedimentary basins located between morphological highs acoustically blind and rimmed by scarps. This plateau could be interpreted as the remnants of an ancient volcanic edifice (Timpe Volcano, TV) linked with the volcanism occurred between 225 Ka and 130 Ka B.P., according with Branca et al. [2008] and Corsaro et al., [2002] on the base of coastal outcroppings.

The Catania Canyon (CC) is by far the greater erosive structure of the surveyed area. It develops in the offshore the homonymous city for 15 km from the coastline to the bathyal plain at around 1800 of depth with an overall E-W trending. Its canyon-head is located at around 100 m to the shoreline eroding copiously the continental shelf and a portion of the coast (testified by an embayment sited in the Cannizzaro area); this fact is an evidence of the present-day activity of the canyon.

From a structural point of view all the area is characterized by a huge semicircular shaped fault system that cut both the Etna offshore and the coast [Chiocci et al., 2011]. It is formed by several from linear to curved fault systems that join all together up to form some concentric lineaments; these last cut the continental slope with a steps arrangement forming high scarps. This fact allow us to reinterpret the Timpe fault system like the most western portion of the semicircular system instead of the direct subaerial prosecution of the Ibleo Maltese Escarpment [Chiocci et al., 2011], us interpreted until now by all the literature. All these fault systems show offsetting consistent with the deformation rate registered of the subaerial eastern flank.

Inside the semicircular system the morpho-batymetric and seismo-stratigraphic analysis offshore Etna allow us to identify a huge amphitheatre-shaped structure (AS). It is characterized by the presence of two large and deep landslide scarp crowns rimmed by several from arcuate to linear ridges characterized often by a reversed setting; at the base of the crowns chaotic morphologies interpreted as the landslide deposits occur.

All this setting represents an evidence of old and recent gravitational instability occurring on the continental slope offshore Etna.

References

Branca, S., Coltelli, M., De Beni, E., Wijbrans, J., (2008). *Geological evolution of Mount Etna volcano (Italy) from earliest products until the first central volcanism (between 500 and 100 ka ago) inferred from geochronological and stratigraphic data*. Int. J. Earth Sci., Geol. Rundsch. 97, 135–152.

Chiocci, F.L., Coltelli, M., Bosman, A., Cavallaro, D., (2011). *Continental margin large-scale instability controlling the flank sliding of Etna volcano*. Earth and Planetary Science Letters 305, 57–64.

Corsaro, R.A., Neri, M., Pompilio, M., (2002). *Paleo-environmental and volcano-tectonic evolution of the southern flank of Mt. Etna during the last 225 ka inferred from the volcanic succession of the "Timpe", Acireale, Sicily*. J. Volcanol. Geotherm. Res. 113, 289–306.

Gabbianelli, G., Lanzafame, G., Lucchini, F., Pompilio, M., Rossi, L.P., Sartori, R., (1995). *Indagini di geologia marina alla base orientale dell'Etna*. In: Ferrucci, F., Innocenti, F. (Eds.), Progetto Etna 1993–95: Giardini, Pisa, Italy, pp. 79–84.

Patanè, G., Agostino, I., La Delfa, S., Leonardi, R., (2009). *Evolution of volcanism around the eastern sector of Mt. Etna, inland and offshore, in the structural framework of eastern Sicily.* Phys. Earth Planet. Inter. 173, 306–316.

PhD Research Project
The Theory of Turbulent Dispersed Multiphase Flow Applied to Explosive Volcanic Eruptions via Large-Eddy Simulation Methods

Matteo Cerminara[1], Tomaso Esposti Ongaro[2], Augusto Neri[2], Luigi Carlo Berselli[3]

[1]*Scuola Normale Superiore di Pisa, Italy*
[2]*Istituto Nazionale di Geofisica e Vulcanologia, Sezione di Pisa, Italy*
[3]*Università di Pisa, Dipartimento di Matematica Applicata "U. Dini", Pisa, Italy*

We are planning to apply the theory of Turbulent Dispersed Multiphase Flow to the dynamics of gas and solid pyroclasts ejected from the volcanic vent during explosive eruptions. In order to do numerical simulations of the turbulence we want to use Large Eddy Simulations (LES) methods.

This work naturally follows and aims to improve the present PDAC Eulerian model [Neri et al., 2003; Ongaro et al. 2007; Neri et al. 2007] where the turbulence is modelled using the mean field theory of J. Smagorinski [Smagorinski, 1963].

Recently [Balachandar and Eaton, 2009] new fast methods were discovered to deal with such complex problems. The historical example is the "Dusty Gas" model [Marble, 1970], a zero-order approximation where pyroclastic particles are perfectly coupled to the fluid flow. Here we want to use a first-order approximation [Ferry and Balachandar, 2001] to model the dynamics of particle concentration. In this way it will be possible to accurately represent and compute efficiently important phenomena such as preferential concentration and turbophoresis avoiding to fully resolve the standard Eulerian method. "In particular, the approximate method accurately captures preferential concentration in regions of high strain and low vorticity" [Ferry and Balachandar, 2001].

In order to capture the key phenomenon of turbulence while preserving the numerical model efficiency, we want to use new mathematical techniques developed in advanced LES modelling [Berselli et al. 2006; Berselli, 2010; Berselli et al. 2011] and to compare them with classical eddy viscosity models as the Smagorinski one. Moreover we want to apply LES theory to stratified flows of incompressible and quasi-incompressible fluids [Garnier et al., 2009]. LES techniques are aimed of finding the mean turbulent flow field by filtering the smallest eddies in the Navier-Stokes equations thus avoiding the Direct Numerical Simulation of the turbulent flow that would be computationally unfeasible for volcanic turbulent flows.

References

Balachandar, S. and Eaton, J.K., (2009). *Turbulent Dispersed Multiphase Flow.* Annual Review of Fluid Mechanics, 2010, 42, 111-133.

Berselli, L.C., Iliescu, T. and Layton, W.J., (2006). *Mathematics of Large Eddy Simulation of Turbulent Flows.* Scientific Computation. Springer, Berlin, 348 pp.

Berselli, L.C., 2010. *Some Results on the Navier-Stokes Equations with Navier boundary conditions.* Riv. Mat. Univ. Parma, vol.1 1-75.

Berselli, L.C., Fisher P.F., Iliescu T. and Özgökmen, T.M., (2011). *Horizontal Large Eddy Simulation of Stratified Mixing in a Lock-Exchange System.* Journal of Scientific Computing, DOI 10.1007/s10915-011-9464-8.

Ferry, J. and Balachandar, S., (2001). *A Fast Eulerian Method for Disperse Two-Phase Flow.* International Journal of Multiphase Flow, 27, 1199-1226.

Garnier, E., Adams, N. and Sagaut, P., (2009). *Large Eddy Simulation for Compressible Flows.* Scientific Computation. Springer Science + Business Media B.V., Berlin, 276 pp.

Marble, F.E., (1970). *Dynamics of Dusty Gases.* Annual Review of Fluid Mechanics, 1970, 2, 397-446.

Neri, A., Ongaro, T.E., Macedonio, G. and Gidaspow, G., (2003). *Multiparticle Simulation of Collapsing Volcanic Columns and Pyroclastic Flow.* Journal of Geophysical Research, 108, 2202, 24 pp.

Neri, A., Ongaro, T.E., Menconi, G., Vitturi, M.M., Cavazzoni, C., Erbacci, G. and Baxter B.J., (2007). *4D Simulation of Explosive Eruption Dynamics at Vesuvius.* Geophysical Research Letters, Vol. 34.

Ongaro, T.E., Cavazzoni, C., Erbacci, G., Neri, A. and Salvetti, M.V., (2007). *A Parallel Multiphase Flow Code for the 3D Simulation of Explosive Volcanic Eruptions*. Parallel Computing, 33 pp. 541–560.

Smagorinski, J., (1963). *General Circulation Experiments with the Primitive Equations*. Monthly Weather Rev. 91, 3, 99-164.

Bubble Size Distribution of Ash Samples: a Novel 3D Technique Applied to Italian Quaternary Study cases

Simone Colucci[1], Gopala K. Mulukutla[2], Alexander A. Proussevitch[2], Dork L. Sahagian[3]

[1]*Università degli Studi La Sapienza, Dipartimento di Scienze Geologiche, Rome, Italy*
[2]*Complex Systems Research Center, University of New Hampshire, Durham, New Hampshire 03824, USA*
[3]*Department of Earth & Environmental Sciences, and the Environmental Initiative, Lehigh University, Bethlehem, Pennsylvania 18015, USA*

Determination of pre-fragmentation Bubble Size Distributions (BSD) from ash samples has several applications on eruption dynamics. The morphology of the ash fragments retains a record of bubble size at the time of fragmentation in terms of the curvature of the bubbles surfaces. I applied a novel method to determine the Bubble Size Distributions (BSD) using an application of the Stereo-Scanning Electron Microscopy Technique [Proussevitch et al., 2011]. An accurate statistical analysis of the data is discussed in order to avoid the ambiguity in the Bubble Number Density (BND) definition. The inferred BSDs, so obtained, provide valuable insights regarding eruption styles, magma dynamics and vesiculation processes that led to the ash-rich explosive eruptions.

Here I report two examples from the Quaternary Vulsini Volcanic District, Sovana and Grotte di Castro eruptions, in which the fine-grained nature of deposits even in near-vent settings indicates negligible sorting by transport, implying the eruption of highly fragmented magmas. These units are dated respectively 0.18 My and 0.19 My. The Sovana eruption records the emplacement of a widely dispersed ash-rich pyroclastic current, followed abruptly by "conventional", coarse pumice- and lithic-rich pyroclastic flows, both with a phonolitic bulk composition. The Grotte di Castro example includes early strombolian and subplinian phases, respectively, fed by shoshonitic and phonolitic magma batches, followed by widespread ash-rich surges with a shoshonitic composition. In both cases, the absence of hydromagmatic features rules out magma-aquifer explosive interaction.

The curvature of ash surface features are measured using Stereo Scanning Electron Microscopy (SSEM), with the aid of morphology represented using a Digital Elevation Model (DEM) of ash particle surfaces. The DEMs allows the identification of surface features and measurement of vertical cross-sectional profiles of individual bubble remnants. This method allows measurement of vesicles within a size range from one to over million cubic microns.

References

Proussevitch, A.A., Mulukutla, G.K., Sahagian D.L., (2011). *A New 3d Method of Measuring Bubble Size Distributions From Vesicle Fragments Preserved On Surfaces Of Volcanic Ash Particles.* GSA Geosphere.

Developing a fast and reliable procedure for mapping new lava flows and morphological variations at Mt Etna by means of geodatabase GIS: the application to the evolution of a new pit crater of SE Crater cone, and the 12-13 January 2011 paroxysmal eruption

Emanuela De Beni, Boris Behncke, Stefano Branca, Mauro Coltelli
Cristina Proietti, Letizia Spampinato

Istituto Nazionale di Geofisica e Vulcanologia, Sezione di Catania - Osservatorio Etneo, Italy

During an eruptive crisis different monitoring activities can be carried out for observing, in real time, the dynamics and evolution of the ongoing event [Calvari et al., 2004; Andronico et al.; 2005; Burton et al., 2005]. Accurate daily mapping of a new and expanding lava flow is of remarkable support to the Civil Protection and thus to the management of the eruptive crisis, particularly on a densely populated volcano such as Mount Etna in Sicily. The cartography laboratory of the Istituto Nazionale di Geofisica e Vulcanologia, Osservatorio Etneo, Sezione di Catania has recently developed a standard procedure for facing an eruptive crisis, defining the kinds of data useful to characterise and map new volcanic features and how acquire them. A geodatabase GIS (Geographic Information System) was implemented with the ESRI ArcInfo software [http://www.esri.com] to store and catalogue the data recorded during the monitoring activities [De Beni & Proietti, 2010]. The GIS contains the layers of polygons, lines and points useful for characterizing an effusive events. An attribute table is associated with each layer and includes the fields necessary for storing all the information and physical parameters that can be gathered during the surveys. In order to map newly formed volcanic features, record the data to be inserted in the geodatabase, and update existing maps and geographic databases, we apply a methodology that combines GPS (Global Positioning System) and laser rangefinder measurements, as well as thermal and visible imaging from both ground- and air-based surveys. The GPS measurements are acquired using two GNSS/GIS (Global Navigation Satellite System/GIS) Leica Zeno CS10 model receivers, (http://www.leica-geosystems.com) which combine a rugged handheld system for acquiring reliable data with sub-metre accuracy. The GNSS sensor is integrated with a laser rangefinder, Leica Vector 1500 model for absolute positioning of inaccessible or dangerous targets by measuring the distance and attitude with respect to the operator.

The evolution of the 6 November 2009 pit crater, on the eastern slope of Etna's Southeast Crater, and its 12-13 January 2011 paroxysmal eruptive episode allowed us to test such methodology and to verify the suitability of the instrumentation for acquiring georeferenced quantitative data. The combinations of different techniques shows that the diameter of the pit crater has rapidly increased from 5 x 8 m measured in mid-November 2009 to 190 x 240 m in January 2011. The fast enlargement was mainly due to several collapse episodes that occurred in about a year, allowing the original pit crater to reach dimensions comparable to those of Etna's summit craters. During the 12/13 January 2011 paroxysm, vigorous lava output produced a 4.3 km-long flow field with a total lava volume between 1.3 and 2.3 x 10^6 m^3 consistent with eruption rates of about 114 and 201 m^3/s.

References

Andronico, D., Branca, S., Calvari, S., Burton, M.B., Caltabiano, T., Corsaro, R.A., Del Carlo, P., Garfì, G., Lodato, L., Miraglia, L., Murè, F., Neri, M., Pecora, E., Pompilio, M., Salerno, G. and Spampinato, L., (2005). *A multi-disciplinary study of the 2002–03 Etna eruption: insights into a complex plumbing system.* Bull. Volcanol., 67, 314–330.

Burton, M.R., Neri, M., Andronico, D., Branca, S., Caltabiano, T., Calvari, S., Corsaro, R.A., Del Carlo, P., Lanzafame, G., Lodato, L., Miraglia, L., Salerno, G. and Spampinato, L., (2005). *Etna 2004–2005: An archetype for geodynamically-controlled effusive eruptions.* Geophys. Res. Lett., 32, L09303, doi:10.1029/2005GL022527.

Calvari, S., Del Carlo, P., Branca, S., Andronico, D., Bruno, N., Burton, M.R., Caltabiano, T., Cascone, M., Coltelli, M., Condarelli, D., Corsaro, R.A., Cristaldi, A., De Beni, E., Garfì, G., Lanzafame, G.,

Lodato, L., Longo, V., Mangiagli, S., Messina, L., Miraglia, L., Morabito, F., Muré, F., Neri, M., Pecora, E., Pompilio, M., Salerno, G., Sawyer, G., Scollo, S. and Spampinato, L., (2004). *The first period of the 2002 Etna eruption (27 October-5 November): preliminary results*. Quaderni di Geofisica, 32, 8 pp.

De Beni, E. and Proietti, C., (2010). *Un geodatabase a supporto della mappatura sineruttiva di colate laviche al monte Etna.* Rapporti Tecnici INGV, 165, 16 pp.

Magma Drainage around Rising Gas Slugs and Burst Overpressure in Strombolian Eruptions

Elisabetta Del Bello[1], Edward W. Llewellin[2], Jacopo Taddeucci[1], Piergiorgio Scarlato[1], Steve J. Lane[3]

[1]*Istituto Nazionale di Geofisica e Vulcanologia, Sezione Sismologia e Tettonofisica, Rome, Italy*
[2]*Department of Earth Sciences, Durham University, Durham, United Kingdom*
[3]*Lancaster Environmental Science, Lancaster University, Lancaster, United Kingdom*

Strombolian activity is characterized by the recurrence of mildly-explosive eruptions that are driven by the rise and burst of discrete gas slugs which ascend rapidly through a more-or-less stagnant column of low-viscosity magma. Explosion dynamics and vigour, as observed at the surface, are mainly controlled by the slug's overpressure with respect to the ambient pressure. Depth of gas slug formation and the amount of gas in the slug are, in turn, known to influence the slug overpressure at burst.

We present a physical model for the development of overpressure within a rising gas slug, which allows the overpressure at burst to be calculated. The model neglects inertial and viscous effects and demonstrates that significant overpressure may develop even in their absence. Results show that the thickness of the magma film draining around the rising slug exerts a primary control on the development of overpressure: a thicker liquid film (i.e. a more viscous magma) results in a greater burst overpressure. Film thickness is represented dimensionlessly through the geometrical parameter A', which is the fraction of the conduit section occupied by draining magma in the slug region. A number of models exist which relate A' to conduit diameter and liquid viscosity. We test these models by performing scaled laboratory experiments on air slugs ascending in cylindrical pipes filled with liquids with a range of viscosities. The best-fit model is used to calculate A' for the range of non-dimensional flow conditions expected in volcanic conduits. We apply our model to calculate burst overpressure of Strombolian eruptions using appropriate volcano-scale parameters. Model outputs are compared with previously published estimates of bursting overpressure derived from a broad dataset of eruptions at Stromboli; our results show that magma-static load and geometrical factors alone can account for the observed range of measured overpressures, suggesting that both 'ordinary' activity and 'paroxysmal' eruptions are to be regarded as part of a spectrum of slug-driven eruptions, where eruption intensity is related to the depth of the gas source.

Hydrothermal Circulation on Ischia Island (Southern Italy) Revealed by an Integrated Geochemical, Geophysical and Geological Approach

Rossella Di Napoli[1], Alessandro Aiuppa[1,2], Raffaele Martorana[1], Giovanni Orsi[3], Marco Camarda[2], Sofia De Gregorio[2], Esterina Gagliano Candela[2], Dario Luzio[1], Giovannella Pecoraino[2], Sandro de Vita[3], Mariano Valenza[1]

[1]*Università degli Studi di Palermo, Dipartimento di Scienze della Terra e del Mare (DiSTeM), Palermo, Italy*
[2]*Istituto Nazionale di Geofisica e Vulcanologia, Sezione di Palermo, Italy*
[3]*Istituto Nazionale di Geofisica e Vulcanologia, Sezione di Napoli - Osservatorio Vesuviano, Italy*

Volcano-hosted hydrothermal systems are complex geological objects, whose thorough characterisation requires extensive and interdisciplinary work. Indeed, even thought geological, geochemical and geophysical observations offer highly significant but independent information, only an integrated multidisciplinary approach can yield a comprehensive characterisation of the chemical/physical structure of hydrothermal systems. Notwithstanding the extensive application of geological, geochemical and geophysical techniques in geothermal research, there are only a few examples in the literature of concurrent use of the three techniques [Finizola et al., 2002; Zlotnicki et al., 2009]; these studies overall demonstrate that only an integrated multidisciplinary approach can yield a comprehensive characterisation of the chemical/physical structure of hydrothermal systems.

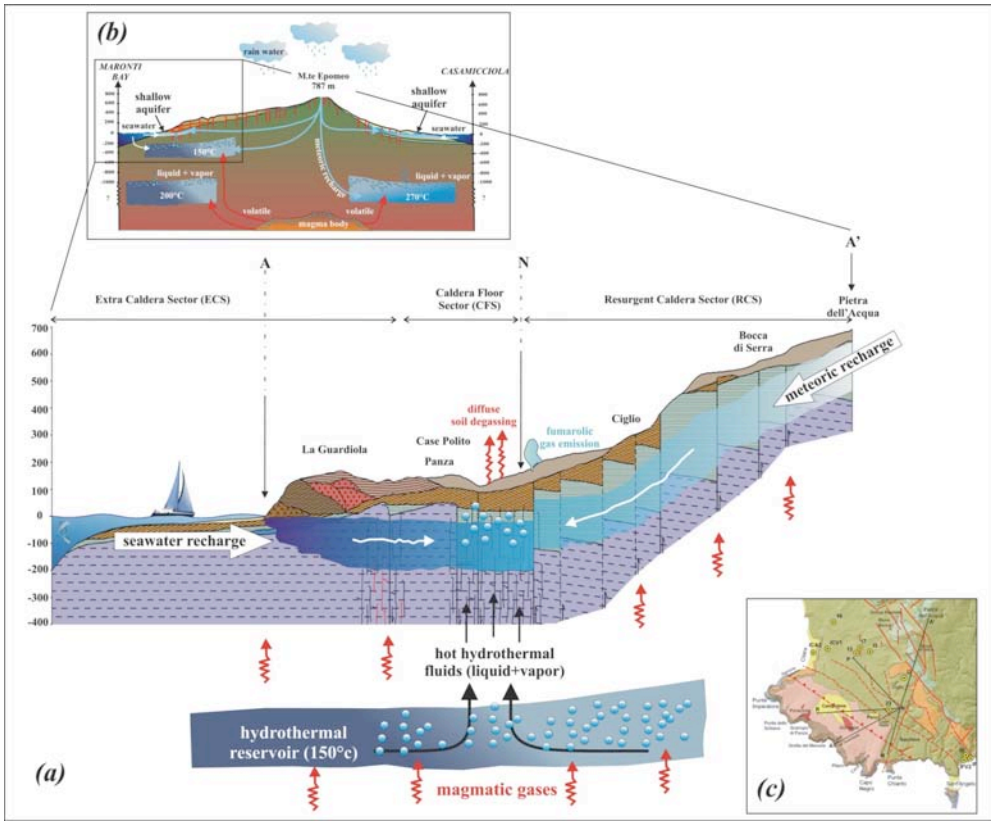

Figure 1. (a) An interpretative circulation model for the shallow hydrothermal groundwater system of SW Ischia along a AA' profile (see Figure1c). (b) General scheme of the structure of Ischia's hydrothermal system, modified from Di Napoli et al., [2009].

Ischia Island, in Southern Italy, is an active resurgent caldera [Orsi et al., 1991] that has produced intense volcanism over the past 10 ka, with the last eruption in 1302 A.D. The island is a very good example of an active volcano hosting a large hydrothermal system [Penta and Conforto, 1951]. In particular, its south-

western sector has long been known for pervasive hydrothermal circulation, as part of the larger hydrothermal system. Thus, this sector of the island is an ideal test site for multidisciplinary geothermal prospecting, since the complex geological and structural setting, the peculiar hydrothermal conditions favouring the formation of remarkably different water types in a relatively small area (~20 km^2) [Di Napoli et al., 2009], and the poorly-known but highly contrasted resistivity structure, all contribute to make interpretation of hydrothermal processes challenging.

Here, we present the results of a multidisciplinary research performed in the south-western sector of Ischia Island by using geological, geochemical (groundwater composition and soil diffuse CO_2 fluxes) and geophysical (Electrical Resistivity Tomography – ERT - and Transient Electromagnetic Method – TEM - soundings) methods. The acquired data are discussed in order to build up a hypothesis for fluid circulation in the shallowest (< 0.5 km) part of the hydrothermal system.

The combined investigations highlight that the deep hydrothermal fluid circulation is strongly dependent on the structural setting of the SW Ischia sector, composed by three distinct sectors: *Extra Caldera Sector* (*ECS*), *Caldera Floor sector* (*CFS*), and *Resurgent Caldera Sector* (*RCS*) (Figure 1a).

This peculiar tectonic/structural setting of the SW portion of Ischia Island force infiltrating waters to flow and accumulate into the structural and topographic low of the *Caldera Floor Sector (CFS* in Figure 1a), in which the shallow thermal aquifer has been identified by resistivity measurements at 100-200 m of depth. This aquifer, hosted into the Mt. Epomeo Green Tuff (MEGT) deposits, is characterized by very low resistivity values (< 1 Ω·m), and has a mixed marine-meteoric derivation. Seawater mostly infiltrates in the SW portion of the area (close to A in Figure 1a), whilst a prevalent contribution from cold diluted waters is evidenced in the NE portion of the study area (close to A' in Figure 1a), along the flanks of Mt. Epomeo relief.

Geochemical investigations have evidenced that meteoric (Total Dissolved Solid content ~ 1.5 g/l and $\delta^{18}O$ ~ -7‰) and marine (Total Dissolved Solid content ~ 33 g/l and $\delta^{18}O$ ~ 0‰) waters accumulate into the aquifer hosted in the *CFS* and form mixed solutions. However, the collected groundwaters only partially overlap the meteoric-sea water mixing trend, claiming for the existence of additional processes. A number of samples are characterized by Mg poor (Mg down to the detection limit) and CO_2-rich (up to 229 cm^3/l at STP) compositions, which are indicative for a deep derivation of these fluids. Indeed, Mg-depletion is a typical features of waters produced in hydrothermal environments [Giggenbach, 1988], as a results of extended water-gas-rock interactions at high temperature, during which Mg was removed from the solution by precipitation of secondary mineral phases. As represented in the interpretative model of Figure 1, the intense network of faults and fractures in the *Caldera Floor Sector*, represents the preferential pathway for the ascent of both thermal waters and deep gases as CO_2, which is also extensively degassed from soil. Finally, the pervasive hydrothermal circulation determine presence of numerous surface thermal manifestations in this sector of Ischia Island.

References

Di Napoli, R., Aiuppa, A., Bellomo, S., Brusca, L., D'Alessandro, W., Gagliano Candela, E., Longo, M., Pecoraino, G. and Valenza, M., (2009). *A model for Ischia hydrothermal system: Evidences from the chemistry of thermal groundwaters*. Journal of Volcanology and Geothermal Research, 86, 133-159.

Finizola, A., Sortino, F., Lénat, J.F. and Valenza, M., (2002). *Fluid circulation at Stromboli volcano (Aeolian Islands, Italy) from self-potential and CO_2 surveys*. Journal of Volcanology and Geothermal Research, 116, 1-18.

Giggenbach, W.F., (1988). *Geothermal solute equilibria. Derivation of Na–K–Mg–Ca geoindicators*. Geochimica Cosmochimica Acta, 52, 2749-2765.

Orsi, G., Gallo, G. and Zanchi, A., (1991). *Simple shearing block-resurgence in caldera depressions. A model from Pantelleria and Ischia*. Journal of Volcanology and Geothermal Research, 47, 1-11.

Penta, F. and Conforto, B., (1951). *Risultati di sondaggi e di ricerche geominerarie nell'isola d'Ischia dal 1939 al 1943, nel campo del vapore, delle acque termali e delle 'forze endogene' in generale*. Annals of Geophysics, 4, 159-191.

Zlotnicki, J., Sasai, Y., Toutain, J.P., Villacorte, E.U., Bernard, A., Sabit, J.P., Gordon Jr, J.M., Corpuz, E.G., Harada, M., Punongbayan, J.T., Hase, H. and Nagao, T., (2009). *Combined Electromagnetic, geochemical and thermal surveys of Taal volcano (Philippines) during the period 2005-2006*. Bulletin of Volcanology, 71, 29-47.

Specific Kinetic Energy (SKE) Released to Pyroclastic Particles During Magmatic Fragmentation: Theory and Experiments

Fabio Dioguardi[1], Tobias Dürig[2], Ralf Büttner[2], Pierfrancesco Dellino[1], Bernd Zimanowski[2]

[1]*Università di Bari, Centro Interdipartimentale di Ricerca sul Rischio Sismico e Vulcanico (CIRISIVU), c/o Dipartimento Geomineralogico, Bari, Italy*
[2]*Physikalisch Vulkanologisches Labor, Universität Würzburg, Pleicherwall Würzburg, Germany*

Explosive volcanic eruptions are mainly driven by the production of volcanic ash particles caused by the brittle fragmentation of magma [Büttner et al., 2006]. This process is the result of a stress field that imposes a strain rate to the magma which is greater than its critical value. Magma fragmentation causes also the release of a certain amount of energy that is coupled to the particles in the form of kinetic energy [Alidibirov and Dingwell, 1996a; Zimanowski et al., 2003]. Consequently the particles accelerate and a gas-particles flow is established. From this brief description it is clear that the process of magma fragmentation plays a crucial role in determining the rate and style of an explosive eruption [Dellino et al., 2010; Woods, 1988].

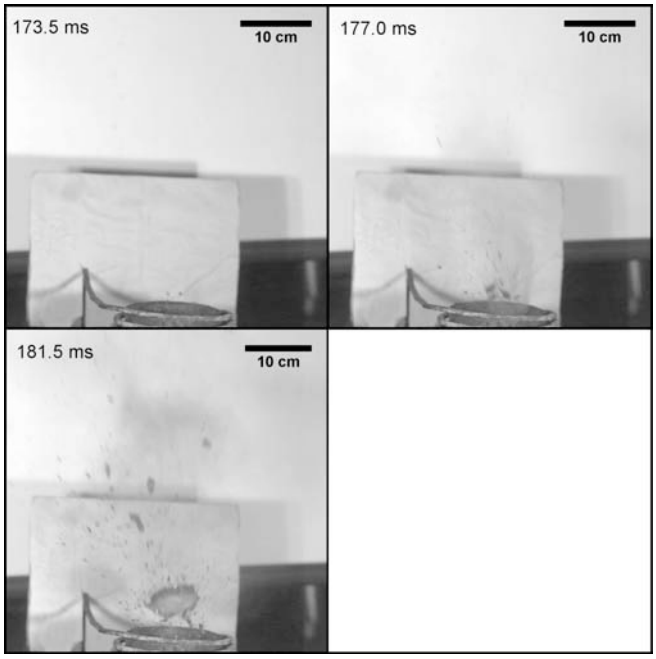

Figure 1. High-speed video recording of an experiment ended with successful fragmentation.

The redistribution of energy during the fragmentation of magmatic melts is a subject of extensive experimental research in the last years [Alatorre-Ibargüengoitia et al. 2010; Alidibirov and Dingwell, 1996b; Büttner et al., 2002, 2006]. A number of experiments has been performed in order to reproduce the proces itself and to measure the energy balances, the velocity of particles shortly after the fragmentation and their physical properties. Here we present a new method for measuring the portion of the involved total energy that is converted into kinetic energy of the generated fragments. The method relies on the experimental determinations of energy balance during brittle fragmentation experiments, the so-called "blowout" experiments developed by the Physikalisch Vulkanologisches Labor, Universität Würzburg [Büttner et al., 2006]. In these investigations pyroclastic particles are melted via an induction coil generating a melt plug that is deformed, fragmented and ejected by a pressurized gas volume (Fig. 1).

The different portions in which the total expansion energy is converted, e.g. deformation, fragmentation, seismic energy, etc., are recognized by identifying the time scales of the related processes and measuring them using the signals recorded by force transducers and pressure sensor placed in the setup [Fig. 2].

The kinetic energy released to fragments is then defined knowing all the other terms in the energy balance equation. By normalizing it to the mass of generated particles one obtains a physical quantity that is closely related to the properties of the melt, as it is verified by calculating it with different kinds of magmatic melts. This quantity is named Specific Kinetic Energy [SKE]. It is worth to note that SKE is by definition a direct measure of the velocity of the particles shortly after fragmentation and therefore it is a useful tool to model the gas-particle conduit flow and eruptive column regime.

References

Alatorre-Ibargüengoitia M. A., Scheu B., and Dingwell D. B., (2010). *Influence of the fragmentation process on the dynamics of Vulcanian eruptions: An experimental approach*. Earth Planetary Science Letters, doi:10.1016/j.epsl.2010.11.045.

Alidibirov M., Dingwell D. B., (1996a). *Magma fragmentation by rapid decompression*. Nature, 380,146-148.

Alidibirov M., Dingwell D. B., (1996b). *An experimental facility for the investigation of magma fragmentation by rapid decompression*. Bulletin of Volcanology, 58, 411-416.

Büttner R., Dellino P., La Volpe L., Lorenz V., and Zimanowski B., (2002). *Thermohydraulic explosions in phreatomagmatic eruptions as evidenced by the comparison between pyroclasts and products from Molten Fuel Coolant Interactions experiments*. Journal of Geophysical Research, doi:10.1029/2001JB000511.

Büttner R., Dellino P., Raue H., Sonder I., and Zimanowski B., (2006). *Stress-induced brittle fragmentation of magmatic melts: Theory and experiments*. Journal of Geophysical Research, doi:10.1029/2005JB003958.

Dellino P., Dioguardi F., Zimanowski B., Büttner R., Mele D., La Volpe L., Sulpizio R., Doronzo D. M., Sonder I., Bonasia R., Calvari S., and Marotta E., (2010). *Conduit flow experiments help constraining the regime of explosive eruptions*. Journal of Geophysical Research, doi:10.1029/2009JB006781.

Woods A. W., (1988). *The fluid dynamics and thermodynamics of eruption columns*. Bulletin of Volcanology, 50, 169–193.

Zimanowski B., Wohletz K., Dellino P., and Büttner R., (2003). *The volcanic ash problem*. Journal of Volcanology and Geothermal Research, 122, 1-5.

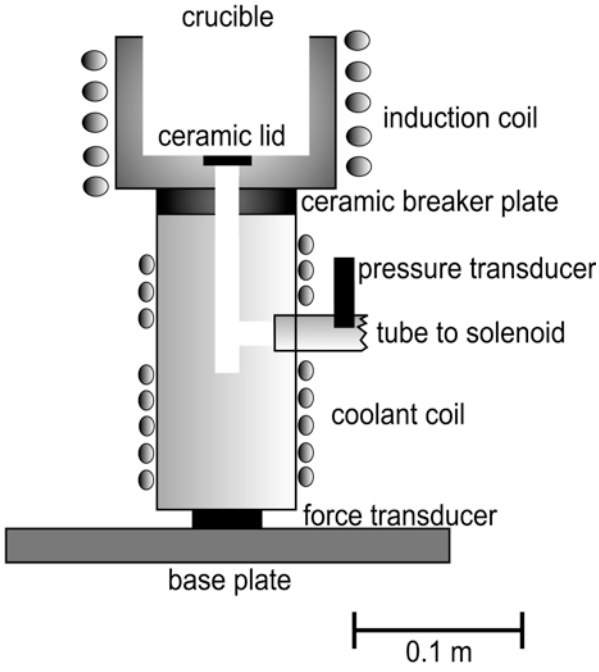

Figure 2. Experimental setup as shown in Büttner et al. [2006].

Petrology of Products Erupted from Mt. Etna from 1995 to 2001: a Study of Magmatic Processes in Pre-Eruptive Conditions

Salvatore Distefano

Istituto Nazionale di Geofisica e Vulcanologia, Sezione di Catania - Osservatorio Etneo, Italy

Mt. Etna is one of the most active volcanoes worldwide and is characterized by explosive and effusive activity. The petrologic study of the erupted products is very important in order to understand the temporal evolution of magmatic processes occurring in the plumbing system of the volcano. In particular, I focused on a period ranging from 1995 to 2001, when an intense activity from the four summit craters, preceded the large flank eruptions of 2001 and 2002-03.

Scientific papers and reports of volcanic activities allowed reconstructing the daily activity of the four summit craters of the volcano: South-East Crater (SEC), North-East Crater (NEC), Voragine (VOR) and Bocca Nuova (BN). The various types of activity (effusive, Strombolian explosions, fire fountains, ash emissions, degassing) were coded and represented as a function of time.

The products erupted from the summit craters from 1995 to 2001, sampled by the staff of IIV and INGV-Sezione di Catania, were subjected to petrographic and compositional study. The content of major, trace elements and Sr-isotopes of the whole rock (carried out by L. Civetta and V. Di Renzo), and the melt inclusions composition in olivine crystals (in collaboration with N. Métrich) have been measured. The acquired data were compared with those already known in the literature [Corsaro and Pompilio, 2004; La Delfa et al., 2001; Armienti et al 1996; Schiavi et al 2006].

PELE, a program that calculates stable silicate liquid-crystal-water assemblages based on free energy minimization techniques [Boudreau, 1999], was used to model the magmatic processes causing the variability of major and trace elements in the analyzed products. The main magmatic processes recognized were: i) mixing between two end members, represented respectively by the 6 June 1996 fire fountain at NEC and the 17 May 2000 fire fountain at SEC, and ii) fractional crystallization of magma residing in the SEC in the period 1996–1998.

Moreover, the variation of SEC, NEC, BN and VOR compositional data from 1995 to 2001 allowed making inferences about the complex geometry (shape and size) of Mt. Etna shallow plumbing system in this period.

Magma feeding the SEC reservoir shows the sharpest fluctuations of compositional patterns. In particular, between 1997 and 1998, the products of SEC are fairly evolved and compatible with a process of fractional crystallization in a temporarily isolated reservoir. Furthermore, at least two main magma recharges affected the CSE reservoir, probably before the 1999 sub-terminal eruption and the 64 lava fountains in 2000. The simple geometry and small volume of SEC reservoir, coupled with a sustained recharge from depth, may likely explain the strong compositional variation observed throughout the investigated period.

Instead, the products erupted by the NEC, showed fairly homogeneous petrographic and compositional features. This suggested that, from 1995 to 2001, the NEC reservoir probably had a simple geometry and a large volume, enabling an efficient mixing between residing and recharging magmas, so to maintain a buffered composition.

Well-defined compositional patterns were not recognized for the products erupted from the BN and VOR; this suggests that the geometry and the magmatic processes occurring in the reservoir/s feeding the two craters were more complex.

Through compositional analysis of olivine, the melt inclusions and their content in CO_2 and H_2O, it was possible to constrain the depths of pre-eruptive magma storage in the investigated period. This proves rather variable in time, resulting between 3.5 and 4 km (about 150 MPa) in 1995 and at about 2 km (80-100 MPa) in 1996.

Finally, the data acquired concurred to implement the 1995-2005 datasets of the Project INGV_DPC FLANK, with the aim of understanding if magmatic processes taking place in the plumbing system of the volcano could somehow have affected the dislocation of the eastern flank of the volcano.

References

Armienti, P., D'Orazio, M., Innocenti, F.,Tonarini, S. and Villari, L., (1996). *October 1995-February 1996 Mt. Etna explosive activity: Trace element and isotopic constraints on the feeding system*. Acta Vulcanol., 8(1), 1±6.

Schiavi, F., Tiepolo, M., Pompilio, M., Vannucci, R, (2006). *Tracking magma dynamics by Laser Ablation (LA)-ICPMS trace element analysis of glass in volcanic ash: the 1995 activity of Mt. Etna*. Geophysical Research Letters, Vol. 33.

Boudreau, A. E., (1999). *PELE version of the MELTS software program for the PC platform.* Computers & Geosciences 25, pp. 201-203.

Corsaro, R. A., and Pompilio, M., (2004). *Magma dynamics in the shallow plumbing system of Mt. Etna as recorded by compositional variations in volcanics of recent summit activity (1995-1999).* Journal of Volcanology and Geothermal Research, 137, pp. 55-71.

La Delfa, S., Patanè, G., Clocchiatti, R., Loron, J. L., Tanguy, J. C., (2001). *Activity of Mount Etna preceding the February 1999 fissure eruption: inferred mechanism from seismological and geochemical data.* Journal of Volcanology and Geothermal Research, 105, pp. 121-139.

A New Sperimental Continuous Monitoring of Geochemical Fumaroles Composition: Application to Phlegrean Fields (Pisciarelli Area)

Alessandro Fedele

Istituto Nazionale di Geofisica e Vulcanologia, Sezione di Napoli - Osservatorio Vesuviano, Italy

Although there were some analytical data of gas composition fumaroles in Phlegrean Fields (South-Italy), only since 1983 a systematic monitoring of the Bocca Grande and Bocca Nuova fumaroles in Solfatara volcano started. Similarly only since 1999, started the sampling of the Pisciarelli's fumaroles, an area located about 1 km southeast of the Solfatara volcano. This sampling provided a series of discontinuous geochemical data (about 2-3 measurements a month) which are not sufficient for an integrated analysis of risk eruption evaluation.

To fill this gap, it was introduced a new method for the continuous sampling of fumaroles and gas in Pisciarelli area. It allows us to obtain a sampling rate of 60 records per hour (1440 detections/day), which make possible the estimation of short-time variation of geochemical data.

Volcanic gas is continuously pumped from fumaroles through 200m Teflon tube, by using a membrane pump located in a small laboratory, close to the fumaroles. Along the Teflon tube volcanic gas is condensed through two small coolers and the gas phase is analyzed minutely by a quadrupole mass spectrometer for H_2S, CO_2, He, CH_4, Ar, N_2, O_2. This sperimental approach provides new data with economic and health operator benefits.

The 2001-2006 Eruptive Period at Mount Etna as Recorded in Plagioclase Phenocrysts: Implications for Magma Ascent Dynamics and Pre-Eruptive Conditions

Pier P. Giacomoni[1], Massimo Coltorti[1] and Carmelo Ferlito[2]

[1]*Università degli Studi di Ferrara, Dipartimento di Scienze della Terra, Ferrara, Italy*
[2]*Università degli Studi di Catania, Dipartimento di Scienze Geologiche, Catania, Italy*

In the last decade Mount Etna activity was characterized by different eruptive styles, from effusive to highly explosive, involving both central open conduit (2004-2006) and lateral feeding systems (2001-2002/2003), not accompanied by significant variation in lava compositions. These features represent a good opportunity for studying the Mount Etna feeding system.

Plagioclase is the most common phenocrysts in all terms of the etnean magmatic suite (~50% in volume). Its stability field depends on chemical-physical variations of the melt and it can be used as a tool to record the processes occurring during the magma uprising. Textural and compositional study of plagioclases has thus been performed on the products emitted during the 2001-2006 eruptive period. Results are compared with theoretical models that constrain its stability field and with the eruptive mechanisms put forward by various authors [Viccaro et al. 2006; Ferlito et al. 2009; Corsaro et al. 2009; Ferlito et al. 2010].

During 2001-2006 eruptions plagioclases present i) An-rich (An_{90-85}) clear crystals (about 800mm in size), with oscillatory zoning or ii) An-poor (An_{85-75}) phenocrysts (4-500mm in size) with clean or dusty cores and complex dissolution textures: when simple dissolution occurs cores are rounded and clear, while if partial dissolution occurs cores are dusty due to numerous glassy inclusions (coarsely sieved cores) [Tsuchiyama 1985]. Plagioclase dissolved cores are surrounded by a lower An overgrowth ranging in size from 100 to 400 mm (based on an average crystal size of 1mm). Finally two types of rims (max 100mm) can be also recognized: i) partially dissolved dusty rims, with An-rich composition and ii) a more albitic rims characterized by alignments of melt inclusions along crystallographic planes.

This detailed textural and petrological study of plagioclase applied to the 2002/2003 bilateral eruption allowed us to put forward the idea that chemical-physical conditions of the deepest part of the feeding system were analogous and that lavas evolve differently on the North East and the South Rift systems only at shallow levels (6-3 km below summit craters). Beside the presence of quartzarenitic xenoliths in lavas from both the NE and S rifts, this hypothesis was also confirmed by major and trace element mass balance and Rayleigh fractionation modelling which suggest that magmas emitted on both the S and NE Rifts depict a common fractionation trend. These new geochemical and mineralogical data support the idea that the main magma feeding the eruption is common on both sides of the volcano even though magma ascent probably occur through the S Rift fractures or trough the central conduits, and is intercepted from the NE Rift system only at relatively shallow depth [Ferlito et al. 2009].

Analogously mixing processes, which have been considered as responsible for the 2001, 2004 and 2006 events were recognized using plagioclase textural and compositional features. In 2001 products, plagioclase characterized by partially dissolution textures at the rim and rounded crystal shape, indicate a mixing process involving an amphibole-bearing shallow magma batch and an incoming most primitive, hotter and volatile-rich magma as proposed by Viccaro et al. [2006]. According to the model proposed by Corsaro et al. [2009], plagioclase from 2004 eruptive event are characterized by the progressively appearance of coarsely sieved cores and resorption dusty rims which testify a mixing occurring between a residual magma batch probably intruded during the 2002/2003 eruption and an incoming more basic but undegassed, melt. Resorption dusty rims testify a mixing process also during the 2006 eruptive event as also proposed by Ferlito et al. [2010].

Furthermore, MELTS calculations have been performed to constrain the crystallization conditions, starting from the most primitive magma (2004/2005 eruption) under different pressure (2500-0 bars) and water contents (3.5-0 wt%). Based on whole-rock composition the program estimates the liquidus temperature, which were decreased by step of 20°C down to 1030°C, that is the lowest T recorded by etnean erupted products. These simulations indicate that An-poor (An_{75-85}) plagioclases crystallized at about P=2500 bars and 1 wt% H_2O, An-rich (An_{85}) plagioclases is stable only at P=800 bars and 2.5 wt% H_2O and clear An-rich (>An_{85}) crystals can be obtained only at very shallow pressure (<1000 bars) with water content of

about 2.5-3.3 wt%.

Clean or dusty dissolved cores An_{85-75} in composition cannot be in equilibrium with high water content at depth greater than 3km. Dissolution processes suggest disequilibrium conditions within the deep magma reservoir which can be related to an input of new undegassed magma or decompression during magma ascent which rise the water pressure. The more albitic overgrowth probably develops at shallower level where the magma can rest, followed by water oversaturation and degassing. The outermost narrow rims can be explained by i) input of new basic magma when dusty texture occur associated with An increase or ii) rapid growth due to degassing just prior to the eruption, recognized by melt inclusions alignments with an abrupt An decrease.

References

Corsaro RA., Civetta L., Di Renzo V., Miraglia L. (2009). *Petrology of lavas from the 2004-2005 flank eruption of Mt. Etna, Italy: inferences on the dynamics of magma in the shallow plumbing system*. Bulletin of Volcanology, 71: 781-793;

Ferlito C., Coltorti M., Cristofolini R., Giacomoni P. P. (2009). *The contemporaneous emission of low-K and high-K trachybasalts and the role of the NE rift during the 2002 eruptive event, Mt. Etna, Italy*. Bulletin of Volcanology, Vol. 67, 4: 314-330;

Ferlito C., Viccaro M., Nicotra E., Cristofolini R. (2010). *Relationship between the flank sliding of the South East Crater (Mt. Etna, Italy) and the paroxysmal event of November 16, 2006*. Bulletin of Volcanology 72, 1179-1190;

Tsuchiyama, A., (1985b). *Dissolution kinetics of plagioclase in the melt of the system diopside–albite–anorthite, and the origin of dusty plagioclase in andesites*. Contribution to Mineralogy and Petrology 89, 1–16;

Viccaro, M., Ferlito, C., Cortesogno, L., Cristofolini, R., Gaggero, L., (2006). *Magma mixing during the 2001 event at Mt. Etna (Italy): effects on the eruptive dynamics*. Journal of Volcanology and Geothermal Research, 149, 139–159;

Calcite-Bearing Foiditic Lava Flows from Colli Albani Volcanic District

Fernando Gozzi[1], Mario Gaeta[1,2], Carmela Freda[2], Tommaso Di Rocco[1*], Luigi Dallai[2,3], Andreas Pack[4]

[1]*Università degli Studi La Sapienza, Dipartimento di Scienze della Terra, Rome, Italy*
[2]*Istituto Nazionale di Geofisica e Vulcanologia, Sezione Sismologia e Tettonofisica, Italy*
[3]*CNR-Istituto di Geoscienze e Georisorse, Pisa, Italy*
[4]*Georg-August-Universität, Geowissenschaftliches Zentrum,Göttingen, Germany*

[*]*Now at Dipartimento di Geoscienze, Università degli Studi di Padova, Italy*

The Colli Albani (hereafter CA) ultrapotassic volcanic district (near the city of Rome, Central Italy) belongs to the Roman Province whose magmatism is thought to result from the combined effects of crystal fractionation and crustal assimilation on a parental magma derived from a metasomatized mantle source. The CA district represents one of the most peculiar volcanic districts on the Earth because of its liquid line of descent characterized by differentiated, low silica ($SiO_2 \leq 45$ wt. %), K-foiditic magmas. Field, geochemical, and experimental studies have demonstrated that such a differentiation trend, starting from trachybasaltic parental magma, is mainly due to magma-carbonate interaction [Gaeta et al., 2009 and references therein]. Despite many studies have investigated petrological and geochemical features of the Colli Albani magmas, several questions remain unanswered. One of these concerns the occurrence of calcite crystals in the groundmass of some lava flows. In general all CA lava flows are made up of leucite and clinopyroxene phenocrysts; some deposits (corresponding to less evolved products) also contain forsteritic olivine. The groundmass, is generally made up of leucite, clinopyroxene, and Ti-magnetite; more evolved products may also contain amphibole or, and these are the object of our study, calcite, usually associated with nepheline.

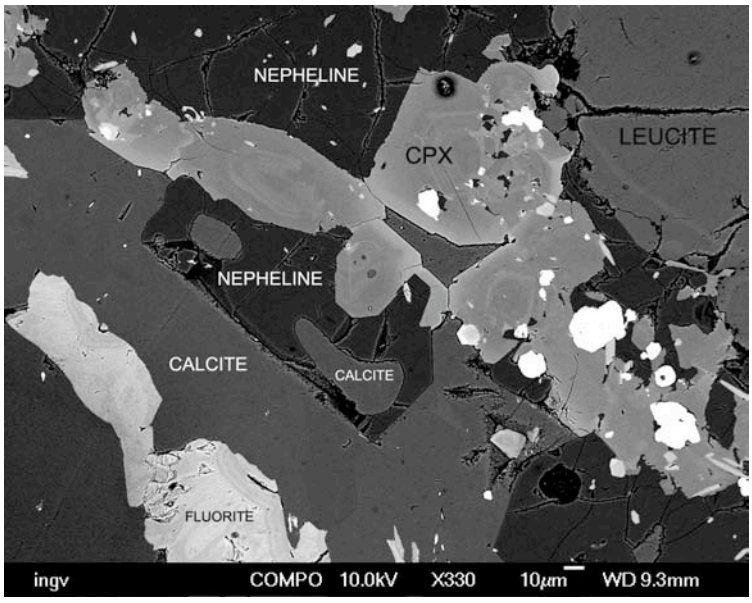

Figure 1. Nepheline - calcite intergrowth. Calcite also shows inclusion of fluorite.

The textural study of calcite-bearing lava flows, by means of Field Emission SEM, revealed that calcite usually occurs as interstitial phase, intergrows with nepheline and, in some cases, contains inclusions of oxide (e.g. hematite) or fluorite (Fig. 1). Calcite is also present in spherical "ocelli" with tangentially arranged crystals of clinopyroxene (Fig. 2) and, rarely, around coronitic texture of leucite produced at the expense of K-feldspar xenocrysts. All these textural features indicate that calcite occurring in the lava flows groundmass crystallize above the solidus temperature. The high activity of calcium in the lava flow groundmass is also supported by the mineral chemistry of silicate phases. For example, olivine crystals in groundmass are enriched in FeO and CaO (up to 4 wt.%) and a positive correlation between CaO in olivine and melt differentiation (i.e. Mg#) was observed.

Carbon and oxygen isotopic composition, as well as trace elements abundance, have been determined on calcite and phenocrysts occurring in the CA lava flows. The oxygen isotopic composition of calcite ($\delta^{18}O$=25-26 ‰ SMOW) results higher than that of phenocrysts (6–8‰ SMOW) and, interestingly, coupled with a very low carbon isotopic composition ($\delta^{13}C$= -14.4 – -15.7‰ PDB). Trace elements abundance in calcite is relatively lower than the abundance measured in both clinopyroxene phenocrysts and bulk rocks (LREE≤100 chondrite).

Textural and mineral chemistry data indicate, unambiguously, that calcite in the CA lava flows has crystallized from a carbonate-bearing melt in a magmatic environment. Although, carbon isotopic

composition could-suggests a mantle origin for the carbonate-bearing melt, oxygen isotopic composition and trace element abundance suggest a different origin. We propone an origin of calcites in CA lava flows from the ^{18}O-rich, ^{13}C-poor fluids that typically originate in skarn environment and/or during sin-eruptive carbonate assimilation [Freda et al., 2011].

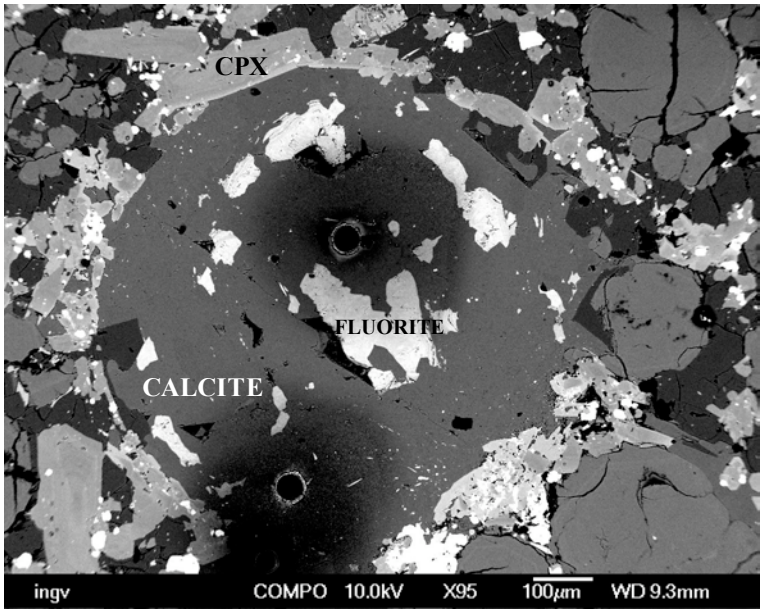

Figure 2. Spherical "ocellus" filling of calcite and fluorite and with tangentially arranged crystals of clinopyroxene; holes were produced by LAM measurements.

References

Gaeta, M., Di Rocco, T., Freda, C. (2009). *Carbonate assimilation in open magmatic systems: the role of melt-bearing skarns and cumulate-forming processes*. Journal of Petrology 50, 361-385.

Freda, C., Gaeta, M., Giaccio, B., Marra, F., Palladino, D.M., Scarlato, P., Sottili, G. (2011). *CO_2-driven large mafic explosive eruptions: a case study from the Colli Albani (Central Italy).* Bulletin of Volcanology 73, 241-256.

Numerical modeling of shock tube experiments for two-phase flow

Giuseppe La Spina[1], Mattia de' Michieli Vitturi[2]

[1]*Istituto Nazionale di Geofisica e Vulcanologia, Sezione di Pisa, Italy*
[2]*Università di Pisa, Dipartimento di Matematica, Pisa, Italy*

Volcanoes erupt when magma, a combination of liquid melted rock, volatile phases, and solid crystals and clasts, migrates and escapes at the surface. Volcanoes exhibit a wide range of eruption styles. Relatively slow effusive eruptions generate lava flows (low viscosity magma) and lava domes (high viscosity magma) and tend to evolve over days to decades. Alternatively, explosive eruptions can inject very large volumes of fragmented magma and volcanic gas high into the atmosphere over shorter periods (minutes to weeks to months). Because of the significantly different hazards associated with various eruptive phenomena, understanding and quantifying factors that control transitions in eruption style and scale is a central theme in Volcanology [2,3,5,13]. The lack of direct observations of sub-surface magma ascent and the limited resolution of indirect methods (such as ground deformation, seismic, and petrologic studies) suggest that a mathematical approach is appropriate. However, the complexity of the gas-magma-solid system is reflected also in the complexity of a corresponding mathematical model [1,6,8,9]; the set of non-linear hyperbolic partial differential and constitutive equations, which describe the physical system, are challenging.

The standard approach to deriving governing equations for two-phase flow is based on averaging procedures, which leads to a system of governing equations in the form of mass, momentum and energy balance laws for each phase coupled with algebraic and differential source terms which represent phase interaction. For this work, we applied a different approach based on the theory of thermodynamically compatible systems [11,14], in order to formulate the governing equations for two-phase compressible flow in the form of a hyperbolic system of partial differential equation in conservative from. The system of equations obtained, not being based on an assumption of dilute regime, can describe both the bubbly flow region below fragmentation level and the gas-particle flow above fragmentation [7]. Furthermore, the particular form of the equations allows overcoming the difficulties of the use of classical upwind schemes, requesting the evaluation of the Jacobian of the flux and its characteristic decomposition. On the contrary, the adoption of high-resolution versions of central schemes [12], not being tied up in the specific eigenstructure of the problem, makes the numerical solution of the two-phase model easier and faster. We present numerical results of some test problems obtained by applying the presented two-phase model to a shock-tube system for a gas-particle mixture, simulating some of the processes that characterize the initial stages of explosive volcanic events inside the conduit. Furthermore, we compare the results with previous studies employing different models for the gas-particle mixture assuming a dilute regime [4,10].

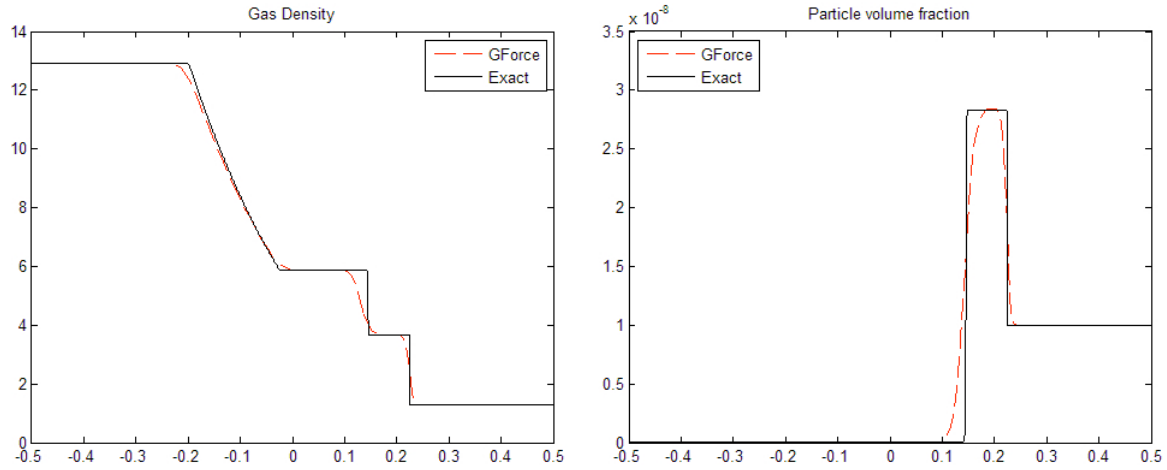

Figure 1. Comparison of the exact (solid line) and the approximate (dashed line) solutions of a simulation of a shock-tube experiment with a model for dilute dusty flow. The approximation is evaluated with a finite volume centered scheme on a 200 cells grid.

References

[1] de' Michieli Vitturi, M.; Clarke, A.; Neri, A. and Voight, B. (2010). *Transient effects of magma ascent dynamics along a geometrically variable dome-feeding conduit*. Earth and Planetary Science Letters 295(3-4), 541 - 553.

[2] Gonnermann, H. M. and Manga, M. (2007). *The fluid mechanics inside a volcano.* Annual Reviews of Fluid Mechanics 39, 321--356.

[3] Jaupart, C. and Allègre, C. J. (1991). *Gas content, eruption rate and instabilities of eruption regime in silicic volcanoes.* Earth and Planetary Science Letters 102, 413--429.

[4] Ling, Y.; Haselbacher, A. and Balachandar, S. (2009). *Transient phenomena in one-dimensional compressible gas–particle flows.* Shock Waves 19(1), 67--81.

[5] Mason, R. M.; Starostin, A. B.; Melnik, O. E. and Sparks, R. S. J. (2006). *From Vulcanian explosions to sustained explosive eruptions: the role of diffusive mass transfer in conduit flow dynamics.* Journal of Volcanology and Geothermal Research 153, 148--165.

[6] Melnik, O. and Sparks, R. S. J. (1999). *Nonlinear dynamics of lava dome extrusion.* Nature 402, 37--41.

[7] Melnik, O. E. (2000). *Dynamics of two-phase conduit flow of high-viscosity gas-saturated magma: Large variations of Sustained Explosive eruption intensity.* Bulletin of Volcanology 62, 153--170.

[8] Melnik, O.; Barmin, A. A. and Sparks, R. S. J. (2005). *Dynamics of magma flow inside volcanic conduits with bubble overpressure buildup and gas loss through permeable magma.* Journal of Volcanology and Geothermal Research 143, 53--68.

[9] Papale, P. (2001). *Dynamics of magma flow in volcanic conduits with variable fragmentation efficiency and nonequilibrium pumice degassing.* Journal of Geophysical Research 106(B6), 11043--11065.

[10] Pelanti, M. and LeVeque, R. J. (2006). *High-Resolution Finite Volume Methods for Dusty Gas Jets and Plumes.* SIAM Journal on Scientific Computing 28, 1335.

[11] Romenski, E.; Drikakis, D. and Toro, E. (2010). *Conservative Models and Numerical Methods for Compressible Two-Phase Flow.* Journal of Scientific Computing 42(1), 68--95.

[12] Toro, E. and Titarev, V. (2006). *MUSTA fluxes for systems of conservation laws.* Journal of Computational Physics 216(2), 403 - 429.

[13] Woods, A. W. and Koyaguchi, T. (1994). *Transitions between explosive and effusive eruptions of silicic magmas.* Nature 370, 641- 644.

[14] Zeidan, D. (2011). *Numerical resolution for a compressible two-phase flow model based on the theory of thermodynamically compatible systems.* Applied Mathematics and Computation 217(11), 5023 - 5040.

Pre-Eruptive Conditions of La Sommata Basalt (Vulcano, Aeolian Islands): Constraints from Experimental Petrology

Giovanni Lanzo

Università degli Studi di Palermo, Dipartimento di Scienze della Terra e del Mare, Palermo, Italy

One of the most primitive magma of Aeolian Arc is the basalt erupted (about 50 ka B.P.) by the La Sommata scoria cone at Vulcano; this is a silica-undersaturated (ne-normative) low-phyric (10-20 wt. %), Ca-rich (CaO = 13 wt. %) shoshonitic basalt (K_2O = 2.28 wt.%) in which olivine phenocrysts host melt inclusions more primitive than whole rock composition and with an ultra-calcic character: $CaO/Al_2O_3 > 1.4$ [Métrich and Clocchiatti, 1996; Gioncada et al., 1998; Schiano et al., 2000]. Phenocrysts mainly include olivines (Fo_{92}) and clinopyroxenes (Fs_5). Plagioclase microlites (from An_{79} to An_{67}) are the most abundant groundmass phase (45 wt. %), together with clinopyroxene (Fs_{11}) and olivine (Fo_{85}). Moreover, the groundmass is dotted by Fe-Ti oxides and rare Cr-spinel is included into olivine phenocrysts.

This experimental petrology study was focused on the following main objectives: (1) to constrain the pressure-temperature-fluid activity during the ascent paths of La Sommata primitive magma, (2) to experimentally investigate the influence of H_2O in this magma and the effects on phase equilibria, (3) to depict a petrological model and constrain the pre-eruptive conditions of this very peculiar eruption.

Experiments were realized with an IHPV housed at Centre National de la Recherche Scientifique - Institut des Sciences de la Terre d'Orléans (CNRS-ISTO, France). In order to simulate the pre-eruptive conditions (P, T, aH_2O) experienced by La Sommata magma all the experiments were run loading H_2O+CO_2 together with the chosen starting material, at different XH_2O and carried out in the pressure range of 150 - 50 MPa and temperature of 1180-1050 °C, under two main guidelines: (i) a well characterized isobaric section at 150 MPa, the inferred maximum pressure of magma storage region (suggested by H_2O-CO_2 contents in MIs from Gioncada et al. [1998]; (ii) an isothermal section at 1150 °C (suggested by the homogenization temperature of MIs from Gioncada et al. [1998]) in the pressure range 150 - 50 MPa, in order to simulate the ascent path.

The liquidus phase at T = 1150 °C and P = 150 MPa is Mg-Cr-spinel followed by clinopyroxene, olivine and finally plagioclase. The cpx+ol assemblage is characterized by a broad stability field. Plagioclase is stable only at H_2O-poor conditions. Comparison among the natural and experimental phase abundance and compositions allows a first estimation of the La Sommata magma pre-eruptive conditions. The natural phase assemblage (clinopyroxene, olivine, plagioclase and oxide) is reproduced by the following conditions: T = 1120 °C, P = 100 - 150 MPa, H_2O_{melt} = 2.55 - 2.84 wt.% with a crystallinity in the range 15 - 25 wt.%, matching the natural rock crystallinity. Given that our experimental data clearly show that plagioclase saturation occurs at very low pressure, the crystallization of plagioclase requires a strong reduction of initial water by depressurization-exsolution.

Previous works on La Sommata olivine-hosted melt inclusions [Gioncada et al., 1998] suggests a water content between 2.1 and 3.8 wt.% (mean 3 wt.%; CO_2 < detection limit) and a homogenization temperature of 1200 °C. These inferred temperatures for the given water content results overestimated since, according to our data, at this conditions (and P = 150 MPa) the Som-1 composition is in the near-liquidus region. Moreover, melt inclusions study of Gioncada et al. [1998] is based on olivine-hosted MI, but our phase relationships clearly show that olivine is not the liquidus phase (Fe-Ti oxides and clinopyroxene instead).

Due to the positive slope of the mineral saturations curves in the P-H_2O phase diagram, an adiabatic ascent of La Sommata magma is supposed not to crystallize until water saturation is reached. The negative slope of plagioclase-in curve, on the contrary, implies that plagioclase crystallization increases upon decompression.

La Sommata magma ascent may be summarized by two discrete crystallization levels: (i) a first stage occurred in a high level crustal reservoir (100-150 MPa, 1120 °C and H_2O_{melt}=2.6-2.8 wt.%) consisting in the crystallization of a Fs_{4-9} clinopyroxene first and a Fo_{90-92} olivine later for a crystal content of about 10 wt. %; (ii) a second stage of crystallization at low pressure (50 MPa) that involves a significant amount of water exsolution allowing thus (microlitic) plagioclase precipitation.

The compositions of the experimental liquids allows to depict an evolutionary path to be compared with Vulcano rocks that cover the same compositional range. Magmas erupted at Vulcano, vary greatly in

both potassium (from HKCA to SHO-KS) and silica (from basalts to rhyolites). The highest K_2O content of the experimental melts (5.4 wt.% at T = 1080 °C, P = 150 MPa and H_2O_{melt} = 1.4 wt. %) is at a rather high crystallinity (55 wt. %), that would make hardly eruptable such crystal-loaded magma. Nevertheless, an important point of our experiments is that strong K_2O enrichments crossing the HKCA-SHO suite limits and pointing toward potassic suite, can be achieved by simple equilibrium crystallization, crystallizing clinopyroxene + olivine + plagioclase. If squeezed out from its crystal-mush, this K-rich melt might represent one end-member composition potentially involved in magma mixing process.

The data obtained in our experiments at the explored conditions suggest that a Sommata type magma can produce liquids similar to latite/shoshonitic magmas at Vulcano, e.g. Saraceno lava, Molineddo pyroclasts and Vulcanello scoriae if more than 45 % of crystals are fractionated.

References

Gioncada, A., Clocchiatti, R., Sbrana, A., Bottazzi, P., Massare, D. and Ottolini, L., (1998). *A study of melt inclusions at Vulcano (Aeolian Islands, Italy): insights on the primitive magmas and on the volcanic feedings system*. Bull. Volcanol. 60, 286-306.

Métrich, N. and Clocchiatti, R., (1996). *Sulfur abundance and its speciation in oxidized alkaline melts*. Geochim. Cosmochim. Acta 60, 4151-4160.

Schiano, P., Eiler, J.M., Hutcheon, I.D. and Stolper E.M., (2000). *Primitive CaO-rich, silica-undersaturated melts in island arcs: Evidence for the involvement of clinopyroxene-rich lithologies in the petrogenesis of arc magmas*. Geochem. Geophys. Geosyst., 1 (5). 1999GC000032. ISSN 1525-2027.

A New Technique for the Characterization of Volcanic Particle Shape by CAMSIZER and Cluster Algorithms

Maria D. Lo Castro[1], Daniele Andronico[1], Carmelo Cassisi[2], Placido Montalto[1], Michele Prestifilippo[1], Gert Beckmann[3], Kai Dueffels[3], Joerg Westermann[3]

[1]*Istituto Nazionale di Geofisica e Vulcanologia, Sezione di Catania - Osservatorio Etneo, Italy*
[2]*Università degli Studi di Catania, Dipartimento di Matematica e Informatica, Catania, Italy*
[3]*Retsch Technology GmbH, Rheinische Str. 43, 42781 Haan, Germany*

Volcanic explosive eruptions generate various pyroclastic products differing in shape and dimensions from bombs to fine ash. Volcanic ash particles have different components, namely juveniles (tachylite and sideromelane) lithics and crystals characterized by peculiar surface textures and morphologies [Heiken and Wohletz, 1985].

The shapes of volcanic particles are controlled by magma fragmentation processes and consequent modifications occurring during transport and deposition. For this reason, classifying the shape of volcanic particles is very important to understand the style of a given eruption and all those information concerning magma physical properties (viscosity, volatile content, degree of interaction with external water etc.)

Moreover, data on particle shape are considered crucial input parameters for the application of numerical models simulating both plume and tephra dispersal, because particle shape affects the terminal settling velocity of volcanic particles and therefore how far the particle will be transported by the wind. Even though the shape variable is relevant, analysis on the shape of volcanic particles are rather scarce in literature and models have to assume the particles to be spherical, despite their irregular shapes [Dellino and La Volpe,1996; Riley et al., 2003; Scollo et al., 2008].

The measurement and quantification of particle shape are hard challenges, especially when the number of the particles to analyse is high and their size is small (i.e. sub-millimetric), as in the case of volcanic ash.

The methods for quantitative measurements of particle shape currently used in volcanology are based on image processing, mainly achieved by manual outputs (e.g. investigations under microscope). These techniques are usually time consuming and meticulous permitting to analyse only a limited number of particles.

Here we present preliminary results of a new procedure for the characterization of the shape of pyroclastic particles funding on results obtained from CAMSIZER, a compact laboratory instrument, developed by Retsch Technology, for the simultaneous measurement of particle size distribution and particle shape of incoherent materials in the range of 30 µm to 30 mm (Fig. 1). CAMSIZER is based on digital image processing and permits to obtain measurements of shape parameters of a high number of particles.

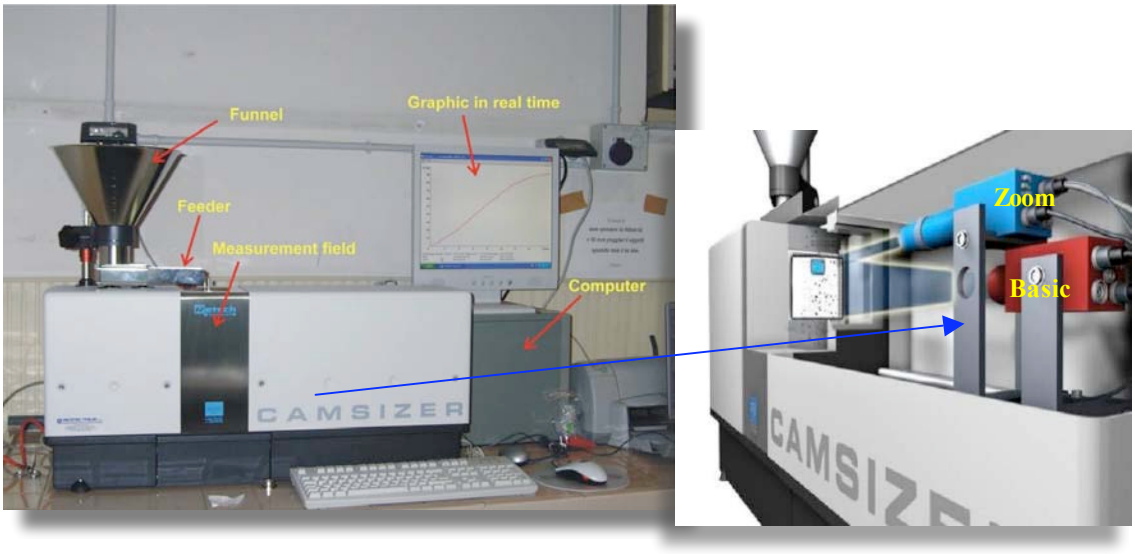

Figure 1. Main components of CAMSIZER.

Our procedure firstly consisted on measurements of a set of samples (both volcanic and non-volcanic) by CAMSIZER in order to obtain the conventional shape descriptors (features or particle shape parameters). Successively, these parameters were used as input data in density-based cluster and classification algorithms in order to identify clusters grouping particles according to their morphologic characteristics (Fig. 2).

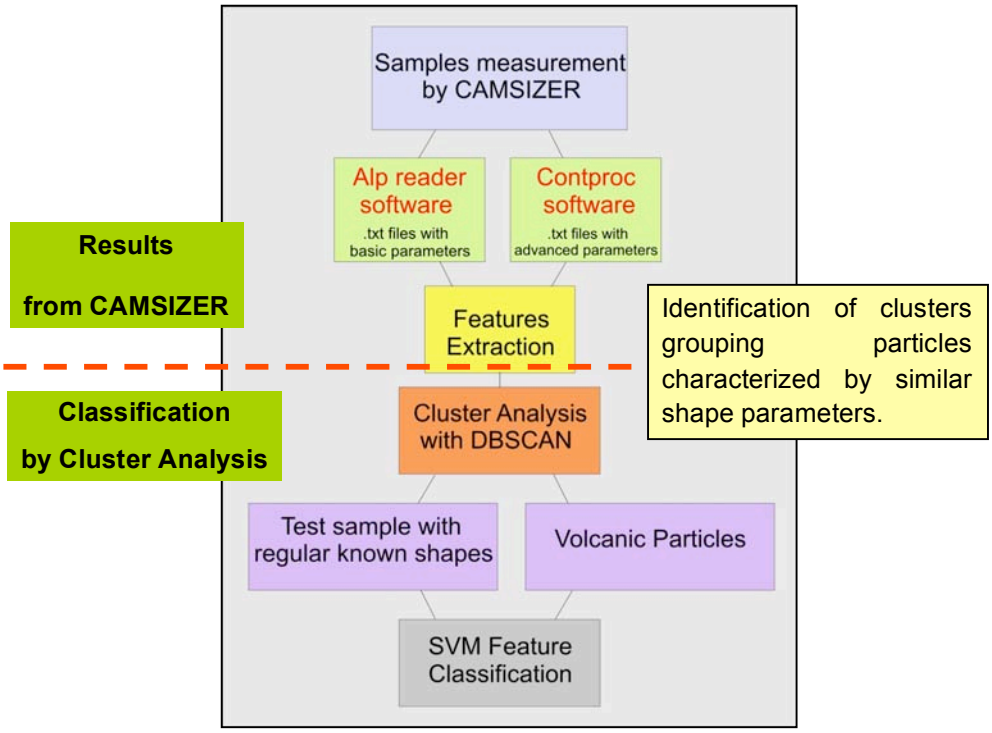

Figure 2. Scheme of the proposed procedure.

The potential of such a combined methodology is mainly a better, faster and reliable characterization of the ash erupted from diverse eruptions eventually leading to infer on peculiar explosive styles. Future applications of this procedure seem to be promising for the improvement of plume dispersion models and for the rapid actions to be performed during the routine monitoring survey of active volcanoes.

References

Dellino, P. and La Volpe, L., (1996). *Image processing analysis in reconstructing fragmentation and transportation mechanisms of pyroclastic deposits. The case of Monte Pilato-Rocche Rosse eruptions, Lipari (Aeolian islands, Italy).* Journal of Volcanology and Geothermal Research. vol. 71 pp. 13-29.

Heiken, G. and Wohletz, K., (1985). *Volcanic Ash*. University of California Press, Berkeley.

Riley, C. M., Rose, W. I., Gregg, J. S. and Bluth, G. J. S., (2003). *Quantitative shape measurements of distal volcanic ash.* Journal of Geophysical Research, vol. 108, no. b10, 2504, doi:10.1029/2001jb000818.

Scollo, S., Folch, A. and Costa, A., (2008). *A parametric and comparative study of different tephra fallout models.* Journal of Volcanology and Geothermal Research 176, 199–211.

Relative Location of Hybrid Events at Stromboli Volcano, Italy

Mariantonietta Longobardi

Istituto Nazionale di Geofisica e Vulcanologia, Sezione di Napoli - Osservatorio Vesuviano, Italy

In this work we analyzed distinctive seismic events known as hybrid events. They were observed at Stromboli volcano, during the 2007 eruption. Hybrid events have intermediate characteristics between volcano-tectonic and long period events. Three main swarms of hybrid events occurred during March 2007 on days between 6-8, 20 and 22. The total number of hybrid events observed during this period was about 4000. Different procedures were used for the analysis: first the clustering of waveforms, then the absolute and relative location of these events. The waveform clustering (using Self-Organizing\Maps neural networks) has shown that most of the events belong to three main families. These clusters have persisted for a long period of time (more than 20 days). This suggests that the source has not undergone significant changes over this period. During the three most intense swarms we recorded also other waveforms belonging to different families. For each family we performed waveform stacking, to improve the signal/noise ratio. Then, using a manual procedure, we obtained a preliminary absolute location for each family. Relative waveform shift for each family have been computed using the cross-spectrum method. These data have been used to perform a relative hypocenter location of each family using a double-difference approach. We observe that almost all the hypocenters falls at very shallow depth. This observation suggests that their source is linked to processes occurring very close to the volcano surface. In the period from March 6 to 8 the formation of a macroscopic fracture system was observed at the summit of the volcano. We infer a causal link between these structures and the source of the hybrid events located on the same position.

Experimental Insights into the Origin of Crystal-Poor Phonolitic Magmas

Matteo Masotta[1], Carmela Freda[2], Mario Gaeta[1,2]

[1]*Università degli Studi La Sapienza, Dipartimento di Scienze della Terra, Rome, Italy*
[2]*Istituto Nazionale di Geofisica e Vulcanologia, Sezione Sismologia e Tettonofisica, Italy*

Crystal-poor phonolitic magmas have been commonly erupted during the quaternary explosive volcanism of Central Italy. The origin of crystal-poor magmas represents a complex issue of igneous petrology and since the first studies on crystal fractionation by settling, many alternative mechanisms of crystal-melt separation have been proposed [see Bachmann and Bergantz, 2004 and references therein]: i) convective fractionation in a crystallizing boundary layer; ii) gas-driven filter press; iii) thermal gradient responsible for mass transport (thermal migration) resulting in segregation of melt from the mushy, boundary zone of magma chambers; iv) melt migration induced by crystal compaction; v) instability of "solidification front". In the frame of the highly explosive volcanism of Central Italy, that was fed by differentiated and thermally zoned pre-eruptive systems, not all of the abovementioned mechanisms would operate efficiently. Moreover, these mechanisms are mainly based on theoretical models and natural evidences, but poorly constrained by experiments.

In this work, in order to shed light on the origin of large volumes of highly differentiated, crystal-poor magmas in thermally zoned systems, we have experimentally investigated crystallization, differentiation, and crystal-melt separation in the presence of a thermal gradient. Melt differentiation has been investigated under isothermal conditions (i.e. phase equilibria experiments) as well. As a case study, we have used the Sabatini Volcanic District, one of the main volcanic districts of the Roman Province characterized by several explosive eruptions producing large volumes of crystal-poor phonolitic magma [Masotta et al. 2010]. Phase equilibria experiments constrained the liquid line of descent leading to phonolitic magmas but gave no insights into the origin of crystal-poor textures. On the contrary, thermal gradient experiments produced structures clearly showing crystal-rich textures overlaid by crystal-poor batches of differentiated melt (Figure 1). The structures pictured at the cool top of the charges remind the so-called solidification front [Marsh, 1996].

Thermal gradient experiments, being performed under controlled conditions, allowed us to determine parameters necessary to model the processes responsible for the formation of these batches of differentiated, crystal-poor melt. We advocate that these experiments represent an important tool to model crystal-melt separation in thermally zoned natural systems as well.

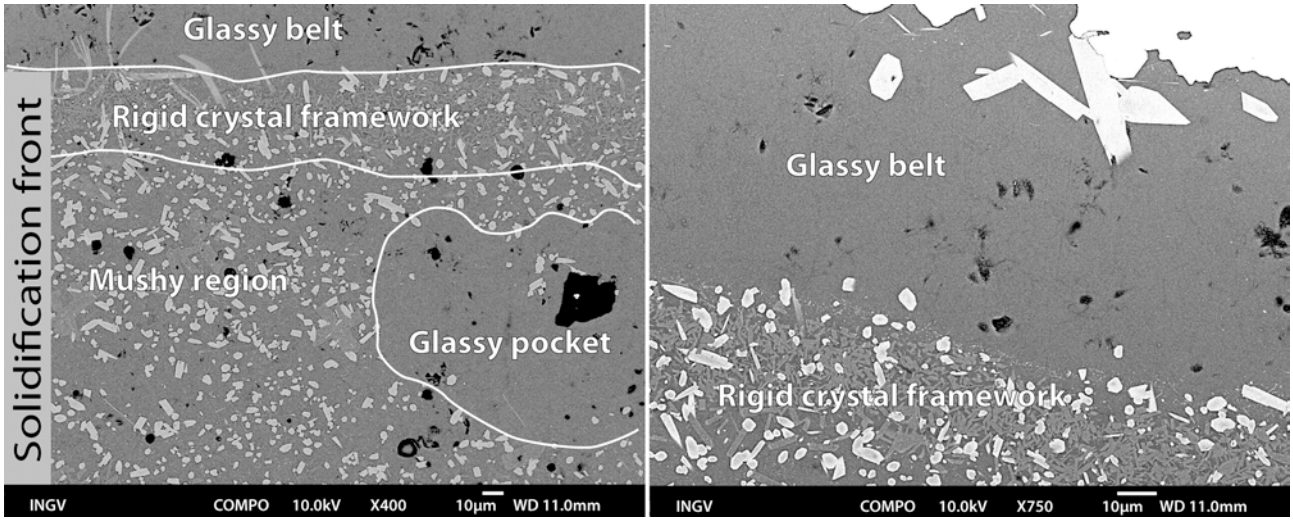

Figure 1. Backscattered images of the top cool zone of thermal gradient charge showing glassy belts and pockets overlaying a clinopyroxene+feldspar touching framework (rigid crystal framework) and a crystal-rich region (mushy region). This heterogeneously crystallized zone is the experimental analogue of the theoretical "solidification front" proposed by Marsh [1996].

References

Bachmann, O., Bergantz, G.W., (2004) *On the origin of crystal-poor rhyolites: extracted from batholithic crystal mushes*. Journal of Petrology, 45, 1565–1582.

Marsh, B.D., (1996). *Solidification Fronts and Magmatic Evolution*. Mineralogical Magazine, 60, 5–40.

Masotta, M., Gaeta, M., Gozzi, F., Marra, F., Palladino, D.M., Sottili, G., (2010). *H_2O- and temperature-zoning in magma chambers: the example of the Tufo Giallo della Via Tiberina eruptions (Sabatini Volcanic District, central Italy)*. Lithos, 118, 119–130.

Cooling History of a Dike as revealed by Mineral Chemistry: A Case Study from Mt. Etna Volcano

Silvio Mollo[1], Gabriele Lanzafame[2], Matteo Masotta[3], Gianluca Iezzi[4], Carmelo Ferlito[2], Guido Ventura[1], Piergiorgio Scarlato[1]

[1]*Istituto Nazionale di Geofisica e Vulcanologia, Sezione Sismologia e Tettonofisica, Italy*
[2]*Università di Catania, Dipartimento di Scienze Geologiche, Catania, Italy*
[3]*Università degli Studi La Sapienza, Dipartimento di Scienze della Terra, Rome, Italy*
[4]*Università G. d'Annunzio, Dipartimento DIGAT, Chieti-Pescara, Italy*

A dike outcropping at Mount Etna volcano and intruded during the Ellittico magmatic activity was investigated collecting seven samples from innermost to the outermost portion. Whole rock and chemical analyses on crystals have been performed using XRF and SEM, respectively, on all samples. Whole rock analyses indicates that the dike have an homogeneous composition along its width; the averaged compositions led to classify the rock as a trachybasalt. Despite an unvarying composition of the samples, crystal analyses results show textural and compositional variations due to the relative position of the samples, and therefore as function of the increasing cooling rates. The dike chilled margin is characterized by dendritic and anhedral crystals of plagioclase, clinopyroxene and titanomagnetite, whereas euhedral crystals with well defined edges are found at the dike core. Plagioclase is progressively enriched in An from innermost to the outermost part of the dike. Similarly, clinopyroxene components En + CaTs + CaFeTs increase, whereas Di + Hd decrease. The Usp content in titanomagnetite also systematically decrease from dike core-to-rim. Such compositional variations are due to the nucleation and growth of the crystals under variable dynamic conditions [Zhou et al., 2000; Faure and Schiano, 2004; Chistyakova and Latypov, 2009; Baginski et al., 2009]. Partition coefficients and thermometers based on the crystal-liquid exchange reaction [Putirka et al. 1996; 2003; Putirka, 2008] indicate that, due to faster cooling rates at the dike outer portions, early-formed crystal nuclei do not re-equilibrate with the melt; as a consequence, mineral compositions are shifted towards those of high-temperature formation. We used the clinopyroxene compositional variations measured from dike core-to rim to determine the cooling rates experienced by the crystals. Thermal gradient profiles at 1 and 50 hours show that this crystallization temperature is reached over two different cooling rates of 50 and 1 °C/h for the dike rim and core, respectively. These cooling rates are comparable with those of 67.8 and 1.2 °C/h determined through the model of Mollo et al. [2010] based on clinopyroxene compositional variations.

This case study allows a better understanding of the compositional variations of minerals formed during magma intrusion. Results are also useful to check the reliability of thermodynamic models based on the crystal-liquid exchange reaction, such as hygrometers, thermometers, and barometers.

References

Baginski, B., Dzierzanowski, P., Macdonald, R., and Upton, B.G.J., (2009). *Complex relationships among coexisting pyroxenes: the Paleogene Eskdalemuir dyke*. Scotland Mineralogical Magazine, 73, 929–942.

Chistyakova, S., Latypov, R., (2009). *On the development of internal chemical zonation in small mafic dykes*. Geological Magazine 147, 1–12.

Faure, F., Schiano, P., (2004). *Crystal morphologies in pillow basalts: implications for midocean ridge processes*. Earth Planetary Science Letters, 220, 331–344.

Mollo, S., Del Gaudio, P., Ventura, G., Iezzi, G., and Scarlato, P., (2010). *Dependence of clinopyroxene composition on cooling rate in basaltic magmas: Implications for thermobarometry*. Lithos 118, 302–312.

Putirka, K.D., (2008). *Thermometers and barometers for volcanic systems*. In: Putirka, K.D., Tepley, F. (Eds.), Minerals, Inclusions, and Volcanic Processes: Rev. in Mineral. Geochem. 69, 61–120.

Putirka, K., Johnson, M., Kinzler, R., and Walker, D., (1996). *Thermobarometry of mafic igneous rocks based on clinopyroxene–liquid equilibria, 0–30 kbar*. Contribution Mineralogy and Petrology. 123, 92–108.

Putirka, K., Ryerson, F.J., and Mikaelian, H., (2003). *New igneous thermobarometers for mafic and evolved lava compositions, based on clinopyroxene+liquid equilibria*. Amer. Mineral. 88, 1542–1554.

Zhou, W., Van der Voo, R., Peacor, D.R., and -Zhang, Y. (2000). *Variable Ti-content and grain size of titanomagnetite as a function of cooling rate in very young MORB*. Earth Planetary Science Letters, 179, 9-20.

Stratigraphy of a Slightly Peralkaline, Rheomorphic Welded Ignimbrite: The Monte Ulmus Unit (SW Sardinia)

Maurizio Mulas[1], Raffaello Cioni[1,2], Filippo Mundula[1]

[1]*Università di Cagliari, Dipartimento Scienze Terra, Cagliari, Italy*
[2]*Istituto Nazionale di Geofisica e Vulcanologia, Sezione di Pisa, Italy*

The Monte Ulmus ignimbrite (15,5 ± 0,5 Ma [Morra et al. 1994]) represents one of the last eruptive events of the Oligocene-Miocene volcanic activity in the south-western sector of Sardinia [Cioni et al. 2001]. These volcanic products are referred to the activity of a magmatic arc active between 32.4 and 13.8 Ma [Lecca et al.1997], the results of NNW subduction of oceanic lithosphere [Savelli et al. 2002, and reference therein]. Monte Ulmus unit is a low-aspect-ratio rhyolite to comenditic, high-grade welded ignimbrite with thickness between 8 to 98 m, locally rheomorphic, spread over an area of 300 km^2 (Fig 1a). About 41 stratigraphic sections, sited in San Pietro, Sant'Antioco and Sulcis-Iglesiente areas, were studied and described. The Monte Ulmus unit drapes a commenditic ignimbrite (Ventrischio Unit) in all its outcroups, while in the northern sector of San Pietro island, it directly rests on some comenditic lava flow units (Nasca and Vinagra units). The Monte Ulmus is overlain by the final products of the Sardinia late Miocene activity, represented by the Paringianu and Serra di Paringianu ignimbrite units and by the last comenditic lava flow event (Monte Tortorisio unit). The Monte Ulmus unit is divided into four main subunits: a basal fall-out deposit followed by three welded pyroclastic flow deposits (named A, B1 and B2) (Fig 1b).

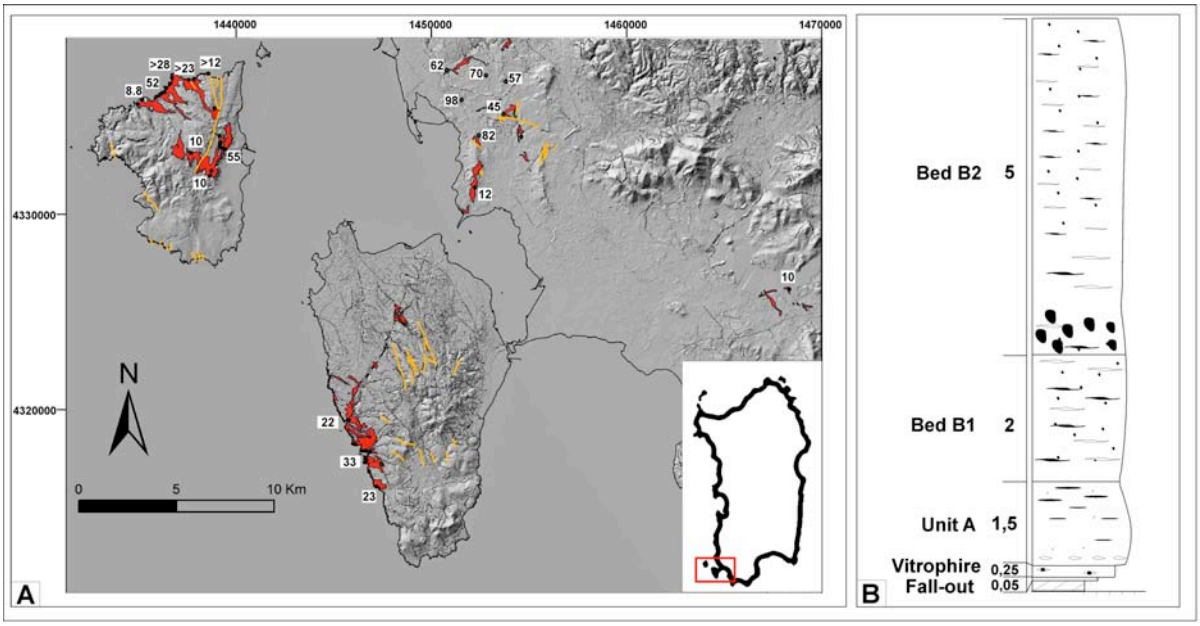

Figure 1. a) Total thickness of Monte Ulmus Unit; b) section type sites in the northern sector of San Pietro island.

The absence of erosional surfaces and the unique set of columnar jointing which cross-cuts all the subunits of the ignimbrite, suggest a single cooling unit associated to multiple flow units. The coarse, massive, totally argillified ash fall deposit ranges in thickness between 20cm and 2 cm. Upon the fall deposit there is a basal vitrophire,30 cm thick, often strongly argillified. In Sant'Antioco areas the basal vitrophire, presents oblate eutaxitic white fiammae (10%) with average size of 3 cm and aspect ratio (ratio between mayor and minor axes) (A/R) 2:1-3:1. Quartz and alkali feldspar crystals (lower than 5 vol %) have 2 mm maximum size, while size of the rare rounded lithics clasts is lower than 3 cm. The core of sub-unit "A" is a 2 to 32m thick, reddish, fine grained, high-grade welded, rheomorphic ignimbrite that crops out mainly in Sant'Antioco island. Two different types of fiammae are present: blackish (10-15 %), obsidian-like,

parataxitic fiammae with A/R variable from 15:1 to 30:1, and whitish (6-7%), highly compacted, sub-rounded to oblate fiammae (A/R from 2:1 to 5:1). Quartz and alkali feldspar crystals (1-2 vol%) have maximum size of 3 mm and lithics (1-2 vol %) are sub-angular. The sub-unit A, where thicker than 10 meters, shows a gradual vertical change in welding and rheomorphic facies. A lower massive densely welded zone is overlain by a flow-banded densely welded core with rotational structure and by a strongly rheomorphic zone. Folds smaller than 0.5 m, prolate vesicles, sheet-joints, ramps and breccias are localized at the base of the rheomorphic zone, while, at top of the sub-unit, where the ignimbrite is lava-like, folds bigger than 1-meter, diapiric structures and decametric-wide blisters occur. Sub-unit B crops out mainly in San Pietro island and Sulcis area. It is a 3 to 52 m thick, poorly porphyritic with Quartz (Qtz) and Sanidine (Sd), high grade welded ignimbrite composed by two beds (B1 and B2) divided by a sharp contact. This sub-unit is locally rheomorphic and it is characterized by a high concentration of different, randomly oriented, juvenile pyroclasts, that were deposited in different physical conditions. Bed B1, 2 to 24m thick, is a reddish, fine grained, matrix-rich welded tuff with three types of juvenile clasts: blackish, highly porphyritic (Sd-bearing) dense fiammae; reddish, low porphyritic, fine grained fiammae; and whitish, vesicular fiammae. The blackish fiammae are deformed in contact with lithics clast, while the white fiammae bend the matrix. Lithic fragments are mainly represented by fragments of old ignimbrite units, and present angular to partially rounded shapes. Bed B1 shows rheomorphic facies in Sant'Antioco, where it covers the thicker crop out of sub-unit A, and in San Pietro island, in the correspondence of thickest outcrops. Bed B2, 5 to 28 thick, is a light-gray, moderately welded tuff. Fragments decrease in size (from dm-size to mm-size) and percentage upwards. At the base, juvenile clasts range in size between 5 and 60 cm and they are randomly oriented with a roughly parataxitic structure. Juvenile fragments are represented by blackish, glassy, dense, highly porphyritic (Sd-bearing) eutaxitic, dm-sized fiammae and by whitish, eutaxitic, vesicular, dm-sized fiammae. Lithic fragments are mainly rounded, reddish, highly porphyritic welded tuffs, and reach a maximum size of 70cm in San Pietro Island. The basal portion of bed B2 is highly rheomorphic with >1m folds while at top it pass, laterally gradually and vertically with a sharp contact, to a blackish, vitrophyre. The eruptive centre is hard to locate but trends of flow lineations (NW-SE in Sulcis area and NE-SW in San Pietro island), the occurrence of coarse lithic boulders in the northern sector of San Pietro island, and the shape of the isopach curves of the fall deposit suggest that the source was possibly located north-northeast of the San Pietro Island. While generally deposited in a sub-aerial environment, some deposits features observed both on Sant'Antioco and San Pietro islands suggest deposition in shallow water.

Acknowledgements

This work is supported by the operating program of Regione Sardegna (European Social Fund 2007–2013), L.R.7/2007, "Promotion of scientific research and technological innovation in Sardinia" to MM.

References

Cioni, R., Salaro, L., and Pioli, L., (2001). *The Cenozoic volcanism of San Pietro Island (Sardinia, Italy).* Rendiconti Seminario Facoltà Scienze Università Cagliari, 71, (2) 149-163.

Lecca, L., Lonis, R., Luxoro, S., Melis, E., Secchi F., and Brotzu, P., (1997). *Oligo-Miocene volcanic sequences and rifting stages in Sardinia: a review.* Periodico Mineralogia, 66, 7-61.

Morra, V., Secchi, F.A., Assorgia, A., (1994). *Petrogenetic significance of peralkaline rocks from Caenozoic calcalkaline volcanism from SW Sardinia.* Chemical. Geology, 118, 109-142.

Savelli, C., (2002). *Time–space distribution of magmatic activity in the western Mediterranean and peripheral orogens during the past 30 Ma (a stimulus to geodynamic considerations)*. J. Geodynamics, 34, 99–126.

Diapiric and Blister Structures in Welded Ignimbrites: the Example of the "Serra di Paringianu" Ignimbrite (SW Sardinia, Italy)

Filippo Mundula[1], Raffaello Cioni[1,2], Maurizio Mulas[1]

[1]*Università di Cagliari, Dipartimento Scienze Terra, Cagliari, Italy*
[2]*Istituto Nazionale di Geofisica e Vulcanologia, Sezione di Pisa, Italy*

Diapiric structures (DS) have been observed in many different geological context e.g.: salt-sediment intrusions, plutonism and texturally stratified obsidian lavas [e.g. Fink, 1983]. In all these cases DS are generated by an unstable gravitational density stratification (Rayleigh-Taylor instability) which forced the intrusion and the buoyant rise of lower lighter material into the denser upper cover. These structures are uncommon in welded ignimbrite deposits where they have been described only in few cases [e.g. Leat and Schmincke, 1993].

In welded ignimbrites, the time scale of the cooling process below the glass transition temperature represents the upper limit for the duration of the process of plastic deformation. The knowledge of the density contrast between the DS and the host rocks, together with the style of deformation and the knowledge of the cooling time scale allow to constrain the rheological behavior of the system.

The Serra di Paringianu rhyolitic ignimbrite (SEP) represents the youngest major ignimbrite of the Cenozoic volcanism of SW Sardinia. It widely crops out on San Pietro and Sant'Antioco islands, while scattered outcrops are present in the Sulcis mainland. At "La Punta", north of San Pietro Island, SEP is constituted by a single cooling unit, subdivided into four eruptive units: 1) a lower unit (U1), comprising basal, dm thick, argillified fall and surge deposits, overlain by a 1.4 m thick, black ignimbrite (vitrophyre) and by a 10-12 m thick, densely welded (ρ = 2200 kg m^{-3}), red ignimbrite with parataxitic texture; 2) an intermediate lower unit (U2), comprising a 10 m thick, lithic rich, white to pink to red, partially welded ignimbrite (ρ = 1600 kg m^{-3}); 3) an intermediate upper unit (U3), represented by a 5- 6 m thick, red to pink, densely welded ignimbrite (ρ = 2200 kg m^{-3}) with eutaxitic texture 4) an uppermost 4 m thick, grey-violet, partially welded ignimbrite unit (U4).

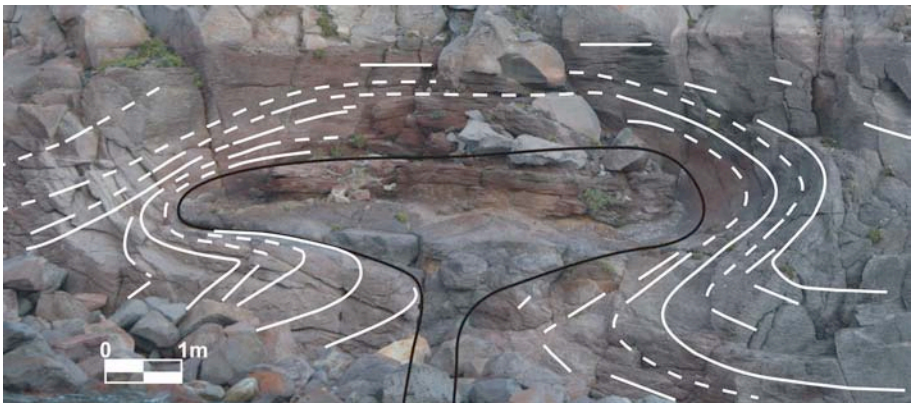

Figure 1. Vertical cross-section of a diapiric structure.

At the same locality, tens meters-sized mushroom-shaped diapiric structures (DS) and metric to decametric lens-shaped voids, named blisters, have been observed within SEP. DS are constituted by the partially welded intermediate unit (U2) intruding the upper densely welded cover (U3). DS are generally connected with their source region and their roots, characterized by vertical re-orientation of flattened purple scoriae, are placed about 8-10 m below the roof, within the U2. In plane-view, stem region is generally elongated and characterized by sub-vertical dip of the foliation planes. Cup region presents horizontal cross-sectional shape, varying from circular to elliptical. Within the cup, foliation shows an approximately concentrical distribution, with dip increasing from the margins trough the center. Eutaxitic structures as well as flow banding, foliations and contact-transition between the different eruptive units are mainly sub-

horizontal at "La Punta". These structures deviate from their planar-horizontal character close to the contact with blister and inside and outside DS. Below the cup region of DS, the host-rock (U3) is folded, with axial plane gently dipping outward the diapir axis. In correspondence of the maximum diameter of the cup, at about 2 m out of the margins, the host rock shows undisturbed horizontal dip, which rapidly changes to vertical close to the margin. Close to the roof of the cup region, host-rock shows upward convex arrangement of foliation, grading into planar-horizontal at about 1 m above the cup.

At least 30 blister are present within U3 in about 1 km^2 wide area. Blisters have horizontal, circular to elliptical, cross-sectional shape and vertical, lens to cupola cross-sectional shape. Horizontal vs. vertical dimensions ratio ranges between 3 and 4. Foliation seems to envelope completely the blisters, reproducing their shape close to the contact with them (first 20-40 cm from the wall). Within the host-rock the vertical strike of foliation, close to the blister wall, changes progressively to horizontal at 1.3-2.5 m from the wall.

In order to simulate the ascent of the DS in a reliable conditions and to estimate the cooling and compaction history of SEP, we performed several numerical simulations (using a trial and error approach) with the AshPac software [Riehle et al., 1995]. The simulated cooling history shows that U2, emplaced at 625 °C, heated up during the first year, due to the thermal equilibration with of the lower and overlaying hottest units, approaching its glass transition temperature (Tg, 650° C) 54 days after its emplacement. At the same time, a cooling front moved downwards the upper surface of the deposit and after 5 months, U3, emplaced at 750°C, cooled its upper portion below Tg. The density gradient at the interface between U2 and U3 increased during the firsts days, approaching a maximum at 42 days and then decreasing asymptotically.

We estimated the viscosity of the melt through the model of Giordano et al. [2008]. Melt viscosity corrected for the crystal content ranges between 10^{12} and $10^{9.8}$ Pa s at temperature between 650 and 760°C.

The ascent velocity of a diapir with a Newtonian rheology ascending through a rock having Newtonian rheology can be calculated using the Stokes equation [Burov et al., 2003]. We simulated the ascent of a 10 m wide DS, with a stepwise process (1 m each step) assuming that temperature of DS and host rocks varied according to the variation in temperature and density reproduced by the simulated cooling-compaction history.

The model of development of DS can be schematized in three steps:

1. During the first phase of post-emplacement cooling-compaction, density contrast between U2 and U3 increased, while the difference in the emplacement temperature favored the U2 heating up above Tg.
2. After about 50 days plume ascent is triggered by the formation of a Rayleigh-Taylor instability at the interface between U2 and U3, driven by the maximum density gradient.
3. The plume rose up with a velocity in the order of 10^{-7} m s^{-1} until it approached the ductile-fragile transition level of the host rock, where it slowed down and stopped starting a lateral intrusion for the continuous feeding from the source region. The degassing marginal parts of the plume head decreased its density, and possibly contributed to feed blisters formation.

The blisters and the diapirs are strictly associated in a small area of about 1 km^2. They occur inside the same unit deforming the foliation planes and so suggesting a contemporaneous development. We state that blisters represent degassing structures in which volatiles of SEP converge during compaction in many cases favored by the presence of the DS, which could represent preferential degassing channels. A detailed geochemical work (in prep.) could solve the uncertainty in interpreting blisters structures and their genetic relationships with DS.

References

Burov E., Jaupart C. & Guillou-Frottier L. (2003). *Ascent and emplacement of buoyant magma bodies in brittle-ductile upper crust.* J. Geophys. Res., 108, 2177.

Fink J.H. (1983). Structure and emplacement of a rhyolitic obsidian flow: Little Glass Mountain, Medicine Lake Highland, northern California. Geol. Soc. Am. Bull. 94, 362-380.

Giordano D., Russell J. K., Dingwell D. B. (2008). *Viscosity of magmatic liquids: A model.* Earth Plan. Sci. Lett., 271, 123–134.

Leat P. T. and Schmincke H.U. (1993). Large-scale rheomorphic shear deformation in Miocene peralkaline ignimbrite E, Gran Canaria. Bull. Volcanol. 55, 155-165.

Riehle J.R., Miller T.F. & Bailey R.A. (1995). *Cooling, degassing, and compaction of rhyolitic ash flow tuffs: a computational model*. Bull. Volcanol., 57, 319–336.

New Discovery of a Small-Size Eruptive Center in the Volcano-Stratigraphic Succession of Val Calanna (Mt. Etna, Italy)

Eugenio Nicotra, Carmelo Ferlito, Marco Viccaro, Renato Cristofolini

Università di Catania, Dipartimento di Scienze Geologiche, Catania, Italy

Since the beginning of its activity about 500 ka ago, Mt. Etna was characterized by the growth and destruction of several eruptive centers. From the earliest researches into Mt. Etna geology, the steep and friable walls of Valle del Bove, carved on the eastern flank of the volcano, offered an opportunity to expand our knowledge on the most ancient eruptive centers.

Figure 1. View of the Val Calanna area.

The understanding of the long-term evolution of magmas can also lead to a more global view of Mt. Etna in terms of volcanological and geochemical evolution. In this frame, the multidisciplinary study on a past eruptive center provides new insights for interpreting the current volcanic activity, also suggesting general models of magma evolution and eruptive behavior. An integrated geological-petrographic-geochemical study of the Val Calanna area, which is located at the south-eastern end of the Valle del Bove, was therefore carried out. The volcanic succession of Val Calanna is of particular importance in the study of the evolution of Mt. Etna given that the remains of several eruptive centers attributed to the first stages of alkaline activity outcrop on its flanks [cf. Ferlito and Nicotra, 2010]. The new geological survey of the Val Calanna area, along with petrographic and geochemical data, highlighted some differences in the volcanic succession with respect to that previously reported by literature.

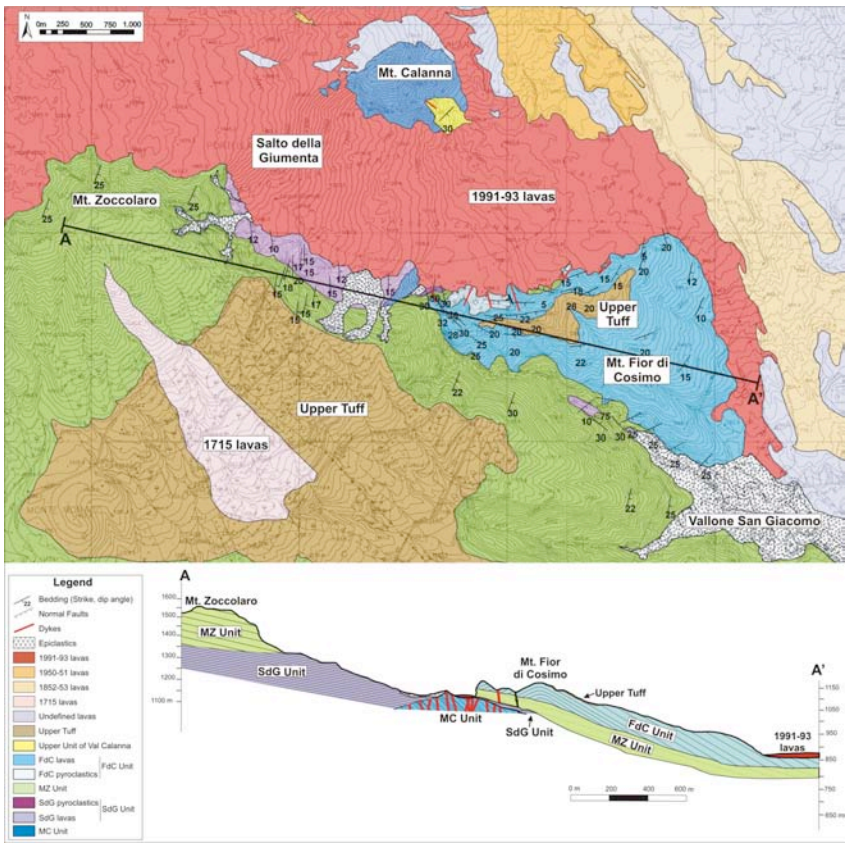

Figure 2. Geological map and volcano-stratigraphic section of the Val Calanna area.

Our study confirms that the most ancient volcano-stratigraphic Unit of the VdB crops out at Mt. Calanna, recently interpreted as a dyke swarm [Ferlito and Nicotra, 2010]. The Mt. Calanna Unit is

overlain by the 80-m-thick lava succession of the Salto della Giumenta Unit, one of the Ancient Alkaline Centers (220 - 100 ka; Romano, 1982). Above this, volcanics of the Mt. Zoccolaro Unit constitute the frame of the present-day homonymous ridge. Mt. Zoccolaro lavas are benmoreites characterized by amphibole megacrysts, showing features similar to those of the Trifoglietto phase (80-60 ka). The eastern portion of the Mt. Zoccolaro edifice is overlain by the volcanic succession of a newly recognized small-sized eruptive Center: the Fior di Cosimo (FdC).

The FdC Unit is constituted by a sequence of alternating lavas and pyroclastic deposits which dip radially away from an inferred vent hypothetically located in the middle of Val Calanna. Relationships between major oxides of FdC lavas and their stratigraphic position show an increasing degree of differentiation through time, from basalt to benmoreite. Furthermore, lava flows at the top of the Fior di Cosimo succession show the presence of amphibole, a mineral phase uncommon for Mt. Etna: this suggest an increase of volatile pressure in the system during the last stage of "life" of the eruptive center. Simulations of crystal fractionation by MELTS revealed that the most evolved FdC lavas can be derived by subtraction of 54% of solid phases (An_{66-82} plagioclase, augitic clinopyroxene, Fo_{68-72} olivine, Ti-magnetite and traces of apatite) from a basaltic composition. The proposed model for the FdC magmatic evolution is therefore the intrusion of a slightly differentiated magma at shallow crustal levels. Magma supply should have then ceased forming a reservoir that allowed differentiation by crystal fractionation, gradually leading to an increase of the volatile pressure of the system. This favored amphibole crystallization, as observed in the last-emitted products.

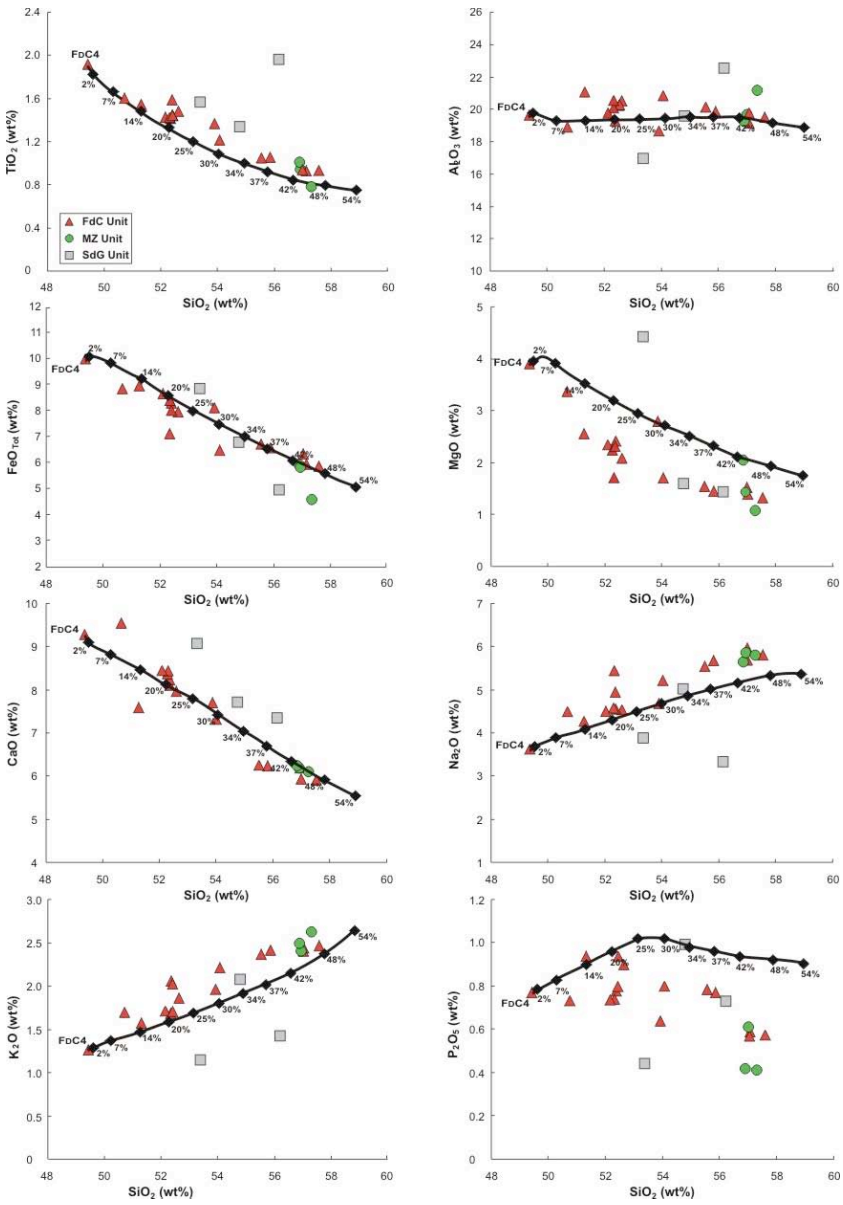

Figure 3. SiO_2 vs. major elements diagrams of Val Calanna volcanic rocks. The crystal fractionation trend obtained by MELTS starts from the most basic sample of Mt. Fior di Cosimo Center, which is at the bottom of the succession. Simulation was performed between 1100°C and 980°C, at 100 MPa of pressure, at the QFM buffer and with an initial H_2O content of 2.3 wt%.

The available data suggest that FdC can be attributed to a pre-Ellittico eruptive phase.

References

Ferlito, C. and Nicotra, E., (2010). *The dyke swarm of Mount Calanna (Etna, Italy): an example of the uppermost portion of a volcanic plumbing system.* Bulletin of Volcanology, 72, 1191-1207.

Romano, R., (1982). *Succession of the volcanic activity in the Etnean area*. Memorie della Società Geologica Italiana, 23, 27-48.

The Source Characteristics of Mt. Etna Magmas Erupted During the Last 60 ka

Eugenio Nicotra[1], Marco Viccaro[1], Sandro Conticelli[2], Renato Cristofolini[1], Carmelo Ferlito[1], Ian L. Millar[3]

[1]*Università di Catania, Dipartimento di Scienze Geologiche, Catania, Italy*
[2]*Università di Firenze, Dipartimento di Scienze della Terra, Florence, Italy*
[3]*British Geological Survey, NERC Isotope Geosciences Labs, Kingsley Dunham Centre, Keyworth, NG12 5GG, Nottingham, England*

During the last decades, Mt. Etna volcano attracted the attention of the scientific community due to its odd geodynamic location and geochemical signature of the erupted lavas. Indeed, they have OIB-like compositions although the edifice is placed above the front of a compressive regional tectonic setting. During the 500 ka of life, Mt. Etna has shown a complex geochemical variability, with sub-alkaline products erupted during the first stage of activity followed since ~220 ka by an alkaline stage. The various phases of the alkaline stage exhibit long-term geochemical variations, which chiefly derive from the superimposition of several evolutionary processes that magma underwent at various levels of the plumbing system during ascent to the surface. However, Mt. Etna lavas also display short-term changes in specific eruptive periods. Since the 1971 eruption, as an example, an increase in some LILEs and volatiles coupled with marked changes in Sr-Nd-Pb-Hf isotope ratios was observed [e.g., Clocchiatti et al., 1988; Michaud, 1995; Métrich et al., 2004; Viccaro and Cristofolini, 2008; Viccaro et al., 2011]. The evolution of a volcano studied in terms of long vs. short-term geochemical variations is one of the best ways to get important responses on: 1) the geodynamic significance; 2) the mechanism of partial melting; 3) the processes able to modify the pristine compositions of magmas and their eventual repetition through time; 4) the link with possible changes of the eruptive behavior.

Although Mount Etna can certainly be regarded as one among the most studied volcanoes on Earth, the main characteristics of the mantle source and of partial melting processes are still debated. This is primarily due to the lack of mantle xenoliths brought to the surface by magmas, which are efficiently fractionated in the deepest levels of the plumbing system. Only indirect information can be therefore obtained from the compositions of the erupted volcanics. In order to achieve these goals, we have focused the attention on some Ellittico and Recent Mongibello lavas (RM).

The behavior of incompatible trace elements for mantle-equilibrated magma compositions of the Ellittico and RM, and in particular of their Enrichment ratio [Ei, as defined by Class and Goldstein (1997)] reveal that the Etnean magmas are produced by a variable, low degrees of partial melting. Furthermore, the Ei provides information on the mantle mineralogy of the Etnean source: magmas can be produced from a classic garnet peridotite (i.e., constituted by various proportions of olivine, orthopyroxene, clinopyroxene and garnet) enriched by metasomatic mineral phases such as amphibole and/or phlogopite (Fig.1). The enriched signature of the Etnean mantle source is confirmed by the Zr/Nb vs. Ce/Y and Ba/Th vs. Lu/Hf diagrams (Fig. 2a-b), which are sensitive of the partial melting degree. The Zr/Nb vs. Ce/Y diagram shows that the contribution of metasomatic phases increased through time from the Ellittico to present-day magmas. The Ba/Th vs. Lu/Hf diagram, which is a blow-up for some pre-1971 and post-1971 magmas, shows the short-term coupled increase of the

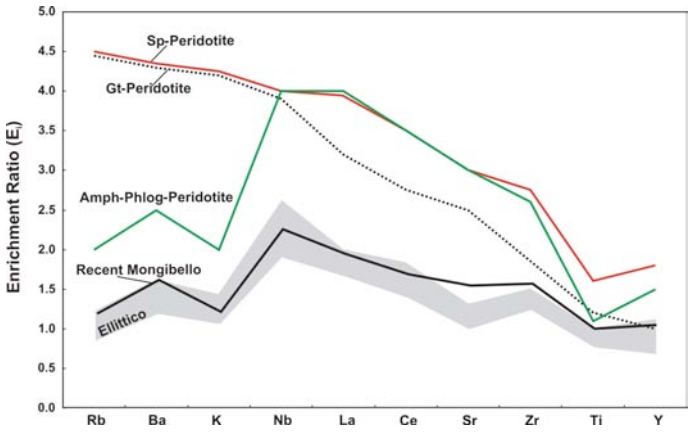

Figure 1. Enrichment ratio (Ei) patterns calculated by partial melting of spinel (sp), garnet (grt) and hydrous-phase bearing peridotites (amphibole and phlogopite). Best fit for Etna volcanic rocks is obtained by melting of ahydrous-phase-bearing peridotite.

contribution by metasomatic agents and partial melting degree.

Several authors also debated on the mantle components involved in the process of partial melting generating the Etnean magmas. The integration of Sr-Nd-Pb-Hf isotopic ratios suggested that FOZO [FOcus ZOne; cf. Stracke et al. 2005] is the dominant component in the Etnean source [cf. Cadoux et al., 2007; Viccaro et al., 2011]. The origin of the FOZO mantle source has been attributed to recycling of oceanic lithosphere little affected by sub-arc alteration, with composition and age different than the recycled crust producing the HIMU signature. The sole FOZO component is, however, not enough to explain the observed isotopic variations from the Ellittico to RM. The involvement of an enriched material should be therefore considered. The isotopic compositions of the Ellittico and RM magmas can be justified by addition of variable proportions (up to 10%) of an EM1-type component to a dominant FOZO source. The origin of the EM-1 component in literature has been ascribed to the presence of: 1) pelagic sediments; 2) recycled lower continental crust or 3) sub-continental lithosphere metasomatized by fluids and/or melts. The coupled analysis of Sm/Hf and Th/Hf ratios, along with Hf isotope compositions, provided evidence that the enriched component in the Etnean source could be metasomatizing silicate melts. Long- vs. short-term compositional variations of Mt. Etna magmas could be therefore related to partial melting of a recycled, altered oceanic lithosphere, infiltrated by metasomatizing silicate melts. Variable amounts of the enriched component participating to partial melting are able to affect its degree and the geochemical signature of the produced magmas.

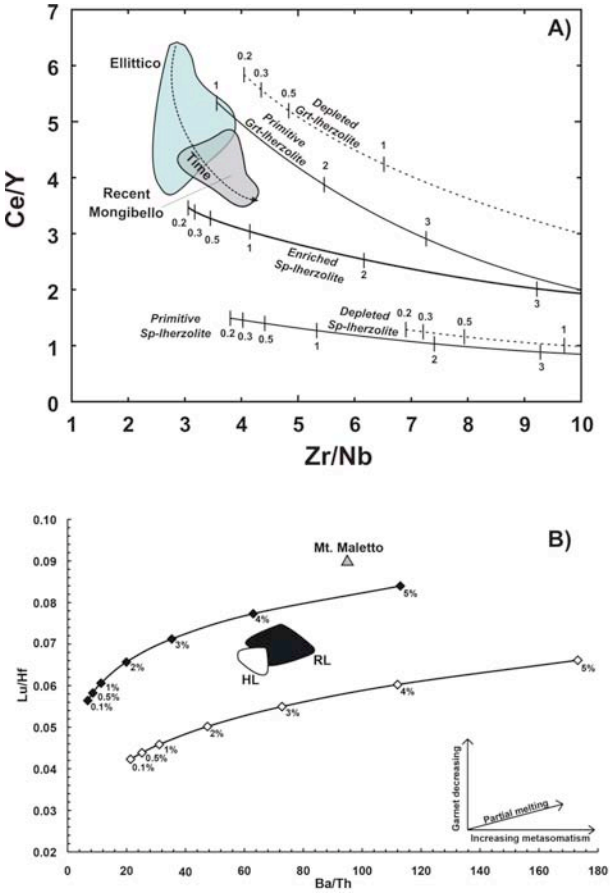

Figure 2. A) Zr/Nb vs. Ce/Y diagram for some mantle-equilibrated Etna volcanic rocks. Dashed arrow indicates the evolution with time for Etnean products. B) Ba/Th vs. Lu/Hf ratios resulting from modal fractional melting modelling of two different mantle sources: white diamonds are calculations for a peridotite source with a FOZO isotopic signature, black diamonds for a source resulting by mixing FOZO composition with 10% of an EM-1 source.

References

Cadoux, A., Blichert-Toft, J., Pinti, D.L., Albarède, F., (2007). *An unique lower mantle source for Southern Italy volcanics*. Earth and Planetary Science Letters, 259, 227-238.

Class, C. and Goldstein, S.L., (1997). *Plume-litoshpere interactions in the oceanic basins: constraints from the source mineralogy*. Earth and Planetary Science Letters, 150, 245-260.

Clocchiatti, R., Joron, J.L., Treuil M., (1988). *The role of selective alkali contamination in the evolution of recent historic lavas of Mt. Etna*. Journal of Volcanology and Geothermal Research 34, 241-249.

Mètrich, N., Allard, P., Spilliaert, N., Andronico, D., Burton, M., (2004). *2001 flank eruption of the alkali- and volatile-rich primitive basalt responsible for Mount Etna's evolution in the last three decades.* Earth and Planetary Science Letters, 228, 1-17.

Michaud, V., (1995). *Crustal xenoliths in recent hawaiites from Mount Etna, Italy – evidence for alkali exchanges during magma-wall rock interaction*. Chemical Geology, 122, 21-42.

Stracke, A., Hofmann, A.W., Hart, S.R., (2005). *FOZO, HIMU, and the rest of the mantle zoo*. Geochemistry Geophysics Geosystems 6, Q05007.

Viccaro, M. and Cristofolini, R., (2008). *Nature of mantle heterogeneity and its role in the short-term evolution of Mt. Etna (Italy)*. Lithos, 105, 272-288.

Viccaro, M., Nicotra, E., Cristofolini, R., Millar, I.L., (2011). *The magma source at Mount Etna volcano: Perspectives from the Hf isotope composition of historic and recent lavas*. Chemical Geology, 281, 343-351.

Multiphase Flow Dynamics of Pyroclastic Density Currents

Simone Orsucci[1,2], Tomaso Esposti Ongaro[2], Fulvio Cornolti[1], Augusto Neri[2]

[1]*Università di Pisa, Dipartimento di Fisica, Pisa, Italy*
[2]*Istituto Nazionale di Geofisica e Vulcanologia, Sezione di Pisa, Italy*

During explosive volcanic eruptions a mixture of gas, droplets and solid particles (ash, pumices and crystallized magma) is released into the atmosphere at high velocity, pressure and temperature. Due to rapid expansion and turbulent mixing, the eruptive mixture is rapidly diluted with atmospheric air and can be conveyed vertically, forming a convective column, or collapse to the ground forming pyroclastic density currents. Pyroclastic density currents can propagate along the volcanic slopes at high velocity, originating complex depositional sequences and causing a widespread damage in reason of their high energy and temperature. The analysis of pyroclastic flow structure and dynamics presents many non-trivial problems for physical models and numerical techniques, some of which will be addressed in this study.

This work starts from the present state-of-the-art and in particular from the PDAC (Pyroclastic Dispersal Analysis Code) model developed at INGV – Pisa [Esposti Ongaro et al., 2007]. This model is based on the multiphase transport teory [Gidaspow, 1994; Neri et al, 2003], describing the full set of transport equations for a polydisperse mixture of (N+1) phases, namely one gaseous and N pyroclastic particles, treated as continua, in the eruptive mixture. The numerical code solves, for every phase, the transport equations of mass, momentum and enthalpy, closed by the appropriate set of consitutive equations (the equation of state, solid and fluid stress tensors, interphase exchange terms and a Large-Eddy closure for turbulence).

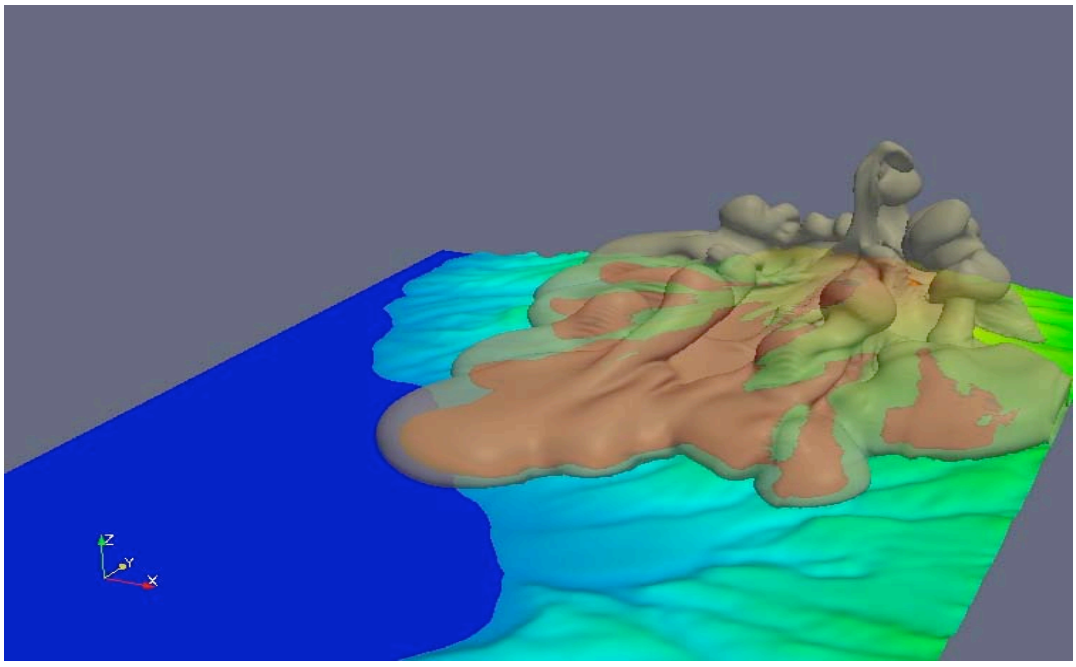

Figure 1. South-East wiew of Mt.Pelée. Two different temperature isosurfaces (70°C and 800°C), 85 seconds after the dome explosion with initial volume V = 12 x 10^6 m^3 and temperature T = 950°C. In this work we have used three particulate phases with different diameter (50μm, 500μm and 5mm).

Due to some approximations in the formulation of the viscous stress tensor for particles, the model is presently not suited to describe flow regimes where the volumetric fraction of a granular phase exceeds about 5%. Moreover there are several terms in the equations, often derived from semi-empirical models, which pose some difficult questions (what is the meaning of "pressure" and "viscosity" for a particulate

phase?). A better understanding of the physics of granular materials in explosive eruptions could be gained by using some techniques of statistical mechanics and kinetic theory of gases. Following this methodology, derived from the study of dense gases, the present model formulation is estended to dense flow regimes and coarser particles, improving its applicability to a wider range of eruptive conditions and the reliability of pyroclastic density current scenario simulations.

The model can be applied to the 3D simulation of explosive eruptions on a realistic topography and, in particular, has been recently exploited for the simulation of a dome explosion scenario at Mt. Pelée (Martinique), to investigate the dynamics and impact of the famous catastrophic eruption that destroyed Saint-Pierre in 1902 [Boudon et al., 2005]. During such kind of events, the sudden collapse of the summit dome caused the rapid depressurization of a shallow magma body, which expanded laterally forming a fast and lethal pyroclastic density current. Such dynamics had been previously modelled by Esposti Ongaro et al. [2008] for the volcanic blast at Soufrière Hills volcano (Montserrat, UK), a similar volcano of the Caribbean arc. The preliminary simulation at Mt. Pelée (Figure 1), constrained by the available geologic data, well reproduces the timing and impact of the flow, but cannot describe the dense, basal part of the current. To better describe the hazard associated to such events and to make a further step towards the description of the emplacement properties of pyroclastic density currents, a new formulation of the multiphase flow dynamics in the dense, collisional regime, seems thus necessary.

References

Boudon, G., Le Friant, A., Villemant, B., and Viode, J.P., (2005). *Martinique*. In: J.M. Lindsay, R.E.A. Robertson, J.B. Shepherd & S. Ali (Eds), Volcanic Atlas of the Lesser Antilles, Seismic Research Unit, The University of the West Indies, Trinidad and Tobago, WI, 65-102.

Gidaspow, D., (1994). *Multiphase Flow and Fluidization: Continuum and Kinetic Theory Descriptions*, Academic Press.

Neri, A., Esposti Ongaro, T., Macedonio, G., Gidaspow, D., (2003). *Multiparticle simulation of collapsing volcanic columns and pyroclastic flows*, J. Geophys. Res.

Esposti Ongaro, T., Cavazzoni, C., Erbacci, G., Neri, A., Salvetti, M.V., (2007). *A parallel multiphase flow code for the 3D simulation of explosive volcanic eruptions*, J. Geophys. Res.

Esposti Ongaro, T., Clarke, A.B., Neri, A., Voight, B., and Widiwidjayanti, C., 2008, *Fluid dynamics of the 1997 Boxing Day volcanic blast on Montserrat,* W.I: Journal of Geophysical Research, v. 113, p. B03211, doi:10.1029/2006JB004898.

Interaction Between Strombolian and Phreatomagmatic Eruptions in the Monogenetic Volcanic Fields of the Iberian Peninsula and Lanzarote Island

Dario Pedrazzi, Joan Martí

Institute of Earth Sciences "Jaume Almera", CSIC, Lluís Solé i Sabarís s/n, 08028 Barcelona, Spain

Monogenetic volcanoes can develop under very different geodynamic, structural and environmental conditions with a large diversity of eruptive styles, morphologies and deposits [e.g. Houghton et al., 1999; Valentine and Gregg, 2008]. The controlling factors such as magma flux, ascent rate together with regional and local tectonics and the presence of water are responsible for the eruption style, volcanic facies of deposits and morphology of the edifices. A detailed examination of the type of deposits, stratigraphic variations in grain size characteristics (including median sorting values) and component analysis provide a way to characterize the eruptive behaviour of monogenetic volcanoes. Similarities and differences among different monogenetic volcanic fields may be outlined with a detailed reconstruction of the corresponding successions of deposits. Differences in the eruptive behaviour of monogenetic volcanoes are usually explained by changes in magma composition or in the geological substract.

The main goal of this research is to study different monogenetic volcanic areas of the Iberian Peninsula and the Canary Islands in order to define the relation between the existing volcanic landforms and the external variables that may have influenced the eruptions and depositional styles of the different monogenetic centers.The selected areas have been chosen as they represent different environments and geological settings under which the volcanism has developed. We will pay particular attention to the phreatomagmatic episodes that characterize each one of these areas. In particular the Catalan Volcanic Zone (CVZ) and the Campo de Calatrava Volcanic Field (CCVF) are monogenetic volcanic fields which have been developed in a continental environment, showing different degrees of phreatomagmatism, whilst the monogenetic volcanoes of El Cuchillo and El Golfo situated on Lanzarote Island (Canarian Archipelago) are good examples of littoral cones formed by shallow sea water-magma interaction. The Catalan Volcanic Zone (CVZ), at the NE of the Iberian peninsula (Gerona Province), is one of the quaternary alkaline volcanic provinces of the European rifts system. The CVZ has been active during the last 12 Ma and is mostly unknown compared to the contemporaneous alkaline volcanism in other parts of Western and Central Europe [Martí et al., 2011]. In this area the research has been focused on two main edifices: The Closa de Sant Dalmai and The Puig D'Adri. The former is a maar type volcano with a final strombolian phase [Martí et al., 1986; Pujadas et al., 2000] and the latter is a complex tuff ting type volcano hosting a scoria cone of smaller dimensions [Pujadas et al., 1997]. The Campo de Calatrava Volcanic Field (CCVF) is mainly located in the Ciudad Real Province of Central Spain. According to K–Ar and Ar–Ar ages from the lava [Ancochea, 1983; Bonadonna and Villa, 1984], there were at least two volcanic stages. The first stage in the center of the volcanic region ranges from 8.7 to 6.4 Ma. The second stage has its main activity phase between 4.7 and 1.75 Ma. Later, there was some volcanic activity in the early Pleistocene that greatly extended the period of volcanic activity in the region, between 1.3 Ma and 0.7 Ma [Gallardo-Millán and Pérez-González, 2000; Gallardo-Millán et al., 2002; Gallardo-Millán, 2004]. The geological evolution of Lanzarote Island according to Marinoni and Pasquarè [1994] can be divided in two principal stages of construction, separated by a main erosive event already identified by previous authors. These two stages are here called "Pre-erosional or Shield stage" and "Post-erosional or Differentiate stage". The emergent part of the island is essentially formed of volcanic rocks dating from about 19 Ma [Abdel-Monem et al., 1971] to the present [Marinoni and Pasquarè, 1994]. At Lanzarote Island two edifices have been considered as good examples of magma-shallow marine water interaction: El Cuchillo and El Golfo. The former is a tuff ring with a succession mainly made of wet base surge deposits and a final phase characterized by the evolution of a scoria cone inside the main crater. The latter is a tuff cone which only consists of base surge deposits and some associated hydromagmatic fall deposits and ballistic bombs [Martí and Colombo, 1990].

These monogenetic hydrovolcanic edifices show a complex eruptive behaviour that could depend on the stratigraphic, structural and hydrogeological characteristics of the substrate above which the volcanoes were emplaced representing good case studies of hazardous phenomena that could be considered not so unpredictable.

References

Abdel-Monem, A., Watkins, N.D., Gast, P.W., (1971). *K-Ar ages, volcanic stratigraphy and geomagnetic polarity history of the Canary Islands: Lanzarote, Fuerteventura, Gran Canaria and La Gomera.* Am. J. Sci., 271, 490-521.

Ancochea, E., (1983). *Evolución espacial y temporal del volcanismo reciente de España Central*. Tesis Doctoral, Univ. Complutense, Madrid.

Bonadonna, F.P. and Villa, J.M., (1984). *Estudio geocronológico del vulcanismo de las Higueruelas.* I Reunión Estratigrafía Regional Castilla-La Mancha (Albacete), vol. 3, Espacio y Sociedad, 249–253.

Gallardo-Millán, J.L., (2004). *Evolución geodinámica de las cuencas neógenas del Campo de Calatrava (Ciudad Real) y su relación con el volcanismo reciente.* PhD. thesis. Complutense University.

Gallardo-Millán, J.L., Ancochea, E., Pérez-González, A., (2002). *Secuencia magnetoestratigráfica y edad de los materiales volcánicos y sedimentarios de Poblete (Ciudad Real).* Geogaceta, 32, 35–38.

Gallardo-Millán, J.L. and Pérez-González, A., (2000). *Magnetoestratigrafía del relleno neógeno en las cuencas del Campo de Calatrava (Ciudad Real)*. Geotemas, 1, 101–104.

Houghton, B.F., Wilson, C.J.N., Smith, I.E.M., (1999). *Shallow-seated controls on styles of explosive basaltic volcanism: a case study from New Zealand.* Journal of Volcanology and Geothermal Research, 91, 97–120.

Marinoni, L.B. and Pasquarè, G., (1994). *Tectonic evolution of the emergent part of a volcanic ocean island: Lanzarote, Canary Islands*. Tectonophysics, 239, 111-135.

Martí, J. and Colombo, F., (1990). *Estratigrafía, sedimentología y mecanismos eruptivos del edificio hidromagmático de El Golfo (Lanzarote).* Boletín Geológico y Minero, Jul-Ago 101 (4), 560-579.

Martí, J., Ortiz, R., Claudin, F., Mallarach, J.M., (1986). *Mecanismos eruptivos del volcán de la Closa de Sant Dalmai (Prov. Gerona).* Anales de Física, Vol. esp. serie B, 82, 143–153.

Martí, J.; Planagumà, L.; Geyer, A.; Canal, E.; Pedrazzi, D., (2011). *Complex interaction between strombolian and phreatomagmatic eruptions in the Quaternary monogenetic volcanism of the Catalan Volcanic Zone (NE of Spain).* Journal of Volcanology and Geothermal Research, 201 (1-4), 178-193.

Pujadas, A.; Pallí, L.; Brusi, D. ; Roqué, C., (1997). *El vulcanisme de la Vall de Llémena.* Colecció Dialogant amb les Pedres 5, Ed. Universitat de Girona, 67 pp.

Pujadas, A.; Pallí, L.; Brusi, D. ; Roqué, C., (2000). *El vulcanisme de la Selva*. Colecció Dialogant amb les Pedres 8, Ed. Universitat de Girona, 63 pp.

Valentine, G.A. and Gregg, T.K.P., (2008*). Continental basaltic volcanism—processs and problems.* Journal of Volcanology and Geothermal Research, 177, 857–873.

Etna Flank Eruption History (1610-2006) as a Constraint on Lava Flow Hazard

Cristina Proietti, Emanuela De Beni, Mauro Coltelli, Stefano Branca

Istituto Nazionale di Geofisica e Vulcanologia, Sezione di Catania - Osservatorio Etneo, Italy

Volcanic threat is the combination of hazards (the dangerous or destructive natural phenomena produced by a volcano) and exposure (the people and property at risk from the volcanic phenomena). Volcanic hazard is the probability that given areas will be affected by potentially destructive volcanic processes [Fournier, 1979] and its evaluation is generally based on the past eruptive behavior assuming that previous activity is representative of that in the future [Guest and Murray, 1979; Behncke et al. 2005]. Hazard evaluation can be supported by the use of computer simulation codes that are becoming valuable tools for better understanding and forecasting lava flow emplacement [Vicari et al. 2006].

Mount Etna is a basaltic composite stratovolcano formed along the Ionian cost of eastern Sicily as a consequence of a complex eruptive history during the last 500 ka [Branca et al. 2008]. Since Etna volcano is located in a densely inhabited area, the assessing of the hazard posed by its eruptions is particularly important and should be based on the long record of its activity. Eruptions of Etna consist of quasi-continuous activity at summit craters and quite frequent events along fissures on its flanks [Branca and Del Carlo, 2005], though summit activity poses relatively minor problems to inhabited areas than flank eruptions [Duncan et al. 1981; Wadge et al. 1994; Behncke et al. 2005].

Data of Etna flank eruptions of the last 400 years was extracted from the new geological map (NGM), updated to 2007 [Branca et al. 2011], and the previous ones produced by Waltershausen [1845-59] and Romano et al. [1979] as regard to the geometrical parameters and vent positions. Moreover the recent revisions of the catalogue of the historical eruptions of Etna [Branca and Del Carlo, 2004; Branca and Del Carlo, 2005] furnished information on the eruption durations and volumes. All the collected data (e.g. eruption year and flow name, eruption style, duration, area, geological map from which the limits were traced, outcropping area, volume, outcropping fracture length, main vent location) were stored in a geodatabase implemented with the ArcGis software (www.esri.com).

Sixty-seven effusive events relative to the period 1610-2006 are reported in the historical catalogues and they were firstly distinguished on the basis of their present outcrop with respect to their original shape. The partially or widely hidden lava fields on the NGM were retrieved from older geological maps. After the analysis of all the available data sources the parameter defining the flow outcrop was updated showing that two hidden-flows were retrieved and that the definition of the planar expansion of the lava flows was improved. As a matter of fact, the percentage of partially, widely or totally hidden flows decreased from 52% to 17%.

A second analysis consisted on studying the distributions of the duration, volume and elevation of the main vent. Ten events were excluded from this analysis because some of these parameters were unknown. Nine eruptions were also excluded because they represent exceptional events of Etna flank history of the last 400 years, due to their extraordinarily brief (1869, 1908 and 1942) or long duration (1651-54 and 1614-24) as well as extremely low (1883, 1968, and December 1985) or high volume (1651-54 and 1669). Forty-eight flank eruptions are therefore available for the analysis. The distribution of eruption durations and lava volumes allowed evidencing that the threshold values can be set at 45 days as well as 35 and 100 x 106 m^3, respectively. A global analysis was performed, on the whole volcano, to evaluate the recurrence of the classes and estimate, for each class the range, average values and standard deviations of duration, volume and elevation of the main vent. The same analysis was repeated by subdividing the volcano into three sectors, defined on the basis of the distribution of all the eruptive fissures of the last 15 ka. The classes resulted as having a different recurrence in the various sectors and different distribution of the volumes, durations and elevations of the main vent.

Finally, a resurfacing map was evaluated considering all the flows emplaced during the last 400 years. The resurfacing map counts how many times each pixel of the DEM was covered during the investigated period, while the normalized resurfacing map allows to evaluate, in a probabilistic way, the areas mostly invaded by lava flows.

References

Behncke, B., Neri, M. and Nagay, A., (2005). *Lava flow hazard at Mount Etna (Italy): New data from a GIS-based study*. Geological Society of America, 396, 189-208.

Branca, S. and Del Carlo, P., (2004). *Eruptions of Mt Etna during the past 3,200 Years: a revised compilation integrating the historical and stratigraphic records, in Mount Etna volcano laboratory*. (A. Bonaccorso, S. Calvari, M. Coltelli, C. Del Negro and S. Falsaperla, Ed.), pp. 1-27. Geophysical monograph series, 143, AGU, Washington.

Branca, S. and Del Carlo, P., (2005). *Types of eruptions of Etna volcano AD 1670–2003: implications for short-term eruptive behavior*. Bull. Volcanol., 67, 732-742.

Branca, S., Coltelli, M., De Beni, E. and Wijbrans J., (2008). *Geological evolution of Mount Etna volcano (Italy) from earliest products until the first central volcanism (between 500 and 100 ka ago) inferred from geochronological and stratigraphic data.* Int. J Earth Sci. (Geol Rundsch), 97, 135–152.

Branca, S., Coltelli M., Groppelli G. and Lentini F., (2011). *Geological map of Etna volcano, 1:50,000 scale.* It. J. Geosci., in press.

Fournier, E.M., (1979). *Objectives of volcanic monitoring and prediction.* J. Geol. Soc. London, 136, 321–326.

Guest, J.E. and Murray J.B., (1979). *An analysis of hazard from Mount Etna volcano.* Journal of the Geological Society, 136, 347-354.

Romano, R. Lentini, F., Sturiale, C. et alii, (1979). *Carta geologica del Monte Etna, scala 1:50.000*. Progetto Finalizzato Geodinamica, Istituto Internazionale di Vulcanologia-C.N.R (Catania).

Vicari, A., Herault, A., Del Negro, C., Coltelli, M., Marsella, M. and Proietti C., (2006). *Modeling of the 2001 lava flow at Etna Volcano by a Cellular Automata approach.* Environ. Model. Softw., doi:10.1016/j.envsoft.2006.10.005.

Wadge, G., Young, P.A.V. and McKendrick, I.J., (1994). *Mapping lava flow hazards using computer simulation.* J. Geoph. Res., 99, 489-504.

Waltershausen, W.S., (1845-59). *Atlas des Aetna.* Berlin, Göttingen, Weimar.

Lesser Antilles Subduction Zone Investigation by Using a Combined On-/Offshore Network

Rosario Raffaele[1], Alfred Hirn[2], Sebastiano Imposa[1] and Luciano Scarfì[3]

[1]*Università degli Studi di Catania, Dipartimento di Scienze Geologiche, Catania, Italy*
[2]*Departement of Seismology, Institut de Physique du Globe de Paris, Paris, France*
[3]*Istituto Nazionale di Geofisica e Vulcanologia, Sezione di Catania - Osservatorio Etneo, Italy*

Earthquakes associated to subduction zones represent the largest part of seismic activity worldwide. In this study we present some results of the investigation programme SISMANTILLES I, conducted from November 1999 to January 2002, on the Lesser Antilles Arc. The latter forms the eastern boundary of the Caribbean plate beneath which the Atlantic crust is subducted at a rate now known to be 2 cm/yr (Fig. 1) [DeMets et al., 2000].

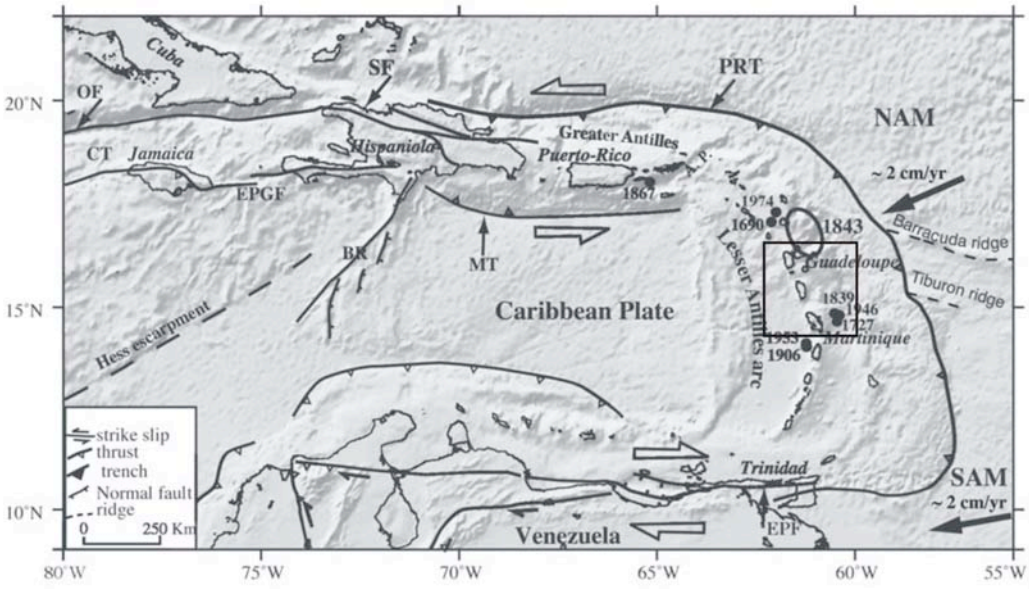

Figure 1. Geodynamic context of Lesser Antilles Arc. Subduction rates from DeMets et al. [2000]. CT: Cayman Trough, OF: OrienteFault zone, EPGF: Enriquillo-Plantain Garden fault zone; BR: Beata Ridge; MT: Muertos trough, PRT:Puerto Rico trench, EPF: El Pilar Fault zone. Black circles: major historical earthquakes (M > 7) in the Lesser Antilles arc with dates. Black square: area under study. The patch ruptured by the 1843 earthquake is indicated. Modified from Feuillet et al. [2002].

We analyzed seismicity by using the data recorded by a combined on- and offshore network (fig. 2) that integrated the 39 seismic stations, mostly one-component, managed by "Observatoire Volcanologique de la Soufrière". The SISMANTILLES I landward network was composed by 43 three-component temporary stations. To improve azimuth coverage in earthquake location, it was complemented by 31 OBS.

A data-set of 155 well located earthquakes, with a total of 4054 and 2617 pickings for P- S-waves respectively, has been used to study the relationship between tectonic structures and seismicity. In particular, to obtain precise hypocenter locations, we applied the concept of minimum 1D model [Kissling et al. 1994], which incorporates the iterative simultaneous inversion of velocity and hypocenter parameters. To partly estimate the huge structural heterogeneity of the Lesser Antilles Subduction Zone, the minimum 1D model is complemented by station corrections which take into account near surface velocity heterogeneity and the geometry of the crust.

In this work, the use of S-wave readings was important to provide constraints on hypocenters because of their delay with respect to P-wave readings. Indeed if two waves emitted simultaneously from the source propagate with different velocities, the time delay is well resolved by each sensor and hypocentral location

receives an additional constraint.

Relocated hypocenters after the 1D inversion are showed in fig. 2. They improve our knowledge on the subduction zone because they have smaller uncertainties with respect to the locations of "Observatoire Volcanologique de la Soufrière". The vertical depth sections perpendicular to the arc define the slab structure and the pattern of the Wadati Benioff zone. For further studies, a P & S tomography local earthquake data will bring more constraints on the structure of Lesser Antilles Arc.

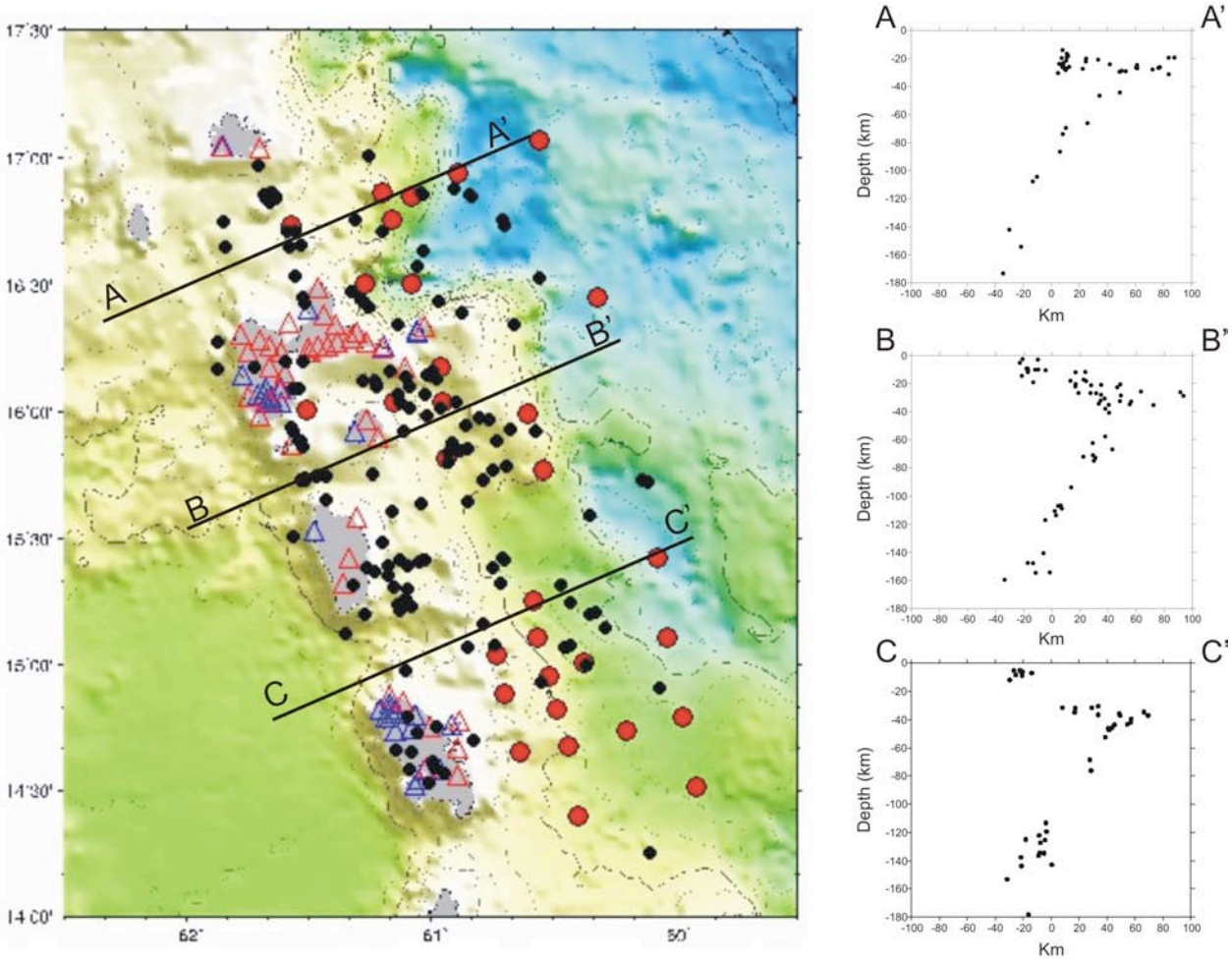

Figure 2. Accurate hypocenters (black circles) as determined by a1D inversion using a combined on-/offshore network. On the right: three vertical depth sections perpendicular to the arc show the hypocenter distribution. Blue triangles stations run by "Observatoire Volcanologique de la Soufrière". Red triangles: temporary landward stations. OBS are marked by red circles.

References

DeMets, C., Jansma, P. E., Mattioli, G. S., Dixon T. H., Farina, F., Bilham, R., Calais, E. and Mann, P., (2000). *GPS geodetic constraints on Caribbean-North America plate motion*. Geophysical Research Letters, 27, 437-440.

Feuillet, N., Manighetti, I., Tapponnier, P and Jacques, E., (2002). *Arc parallel extension and localization of volcani ccomplexes in Guadeloupe, Lesser Antilles*. Journal of Geophysical Research, 107, 2, 331-2, 360.

Kissling, E., Ellworth W.L., Eberhart-Phillips D. and Kradolfer U., (1994). *Initial reference models in local earthquake tomography*. Journal of Geophysical Research, 99, 19,635-19, 646.

Development of a System to Monitor SO_2 Flux Emitted by Volcanoes

Daniele A. Randazzo, Giuseppe G. Salerno, Tommaso Caltabiano, Mike Burton, Filippo Murè, Alessandro La Spina

Istituto Nazionale di Geofisica e Vulcanologia, Sezione di Catania - Osservatorio Etneo, Italy

Volcanoes have always been subject of studies aimed at understanding and predicting their activities. Their behaviour is reflected at the surface by a number of signals and parameters that allows the inspection of eruptive dynamic and style of activity. Since 80s, the modern volcanology approaches at active volcanoes using a multidisciplinary integration of data. This perspective has prompted the fast development of monitoring system that continuously and automatically allowed observation of geophysical and geochemical parameters. Volcanic gases are the principal engine of volcanoes, among the entire species sulphur dioxide (SO_2) represents a key species because it is the third species after H_2O and CO_2 and because it is a direct reflection of the amount of magma within the volcano at depths 3-4 km below the summit area. Moreover, due to its strong absorption in the ultraviolet region SO_2, it is easily detectable. Hence, SO_2 has been always a targeted gas species in volcanoes surveillance. The common method to perform SO_2 observation is the traverse method, which consist in crossing the volcanic plume with an ultraviolet spectrometer (e.g., COSPEC, MiniDOAS) mounted in a car, boat or helicopter. Measured SO_2 column amount is then multiplied by the wind-plume speed providing an estimate of the SO_2 flux emitted by the volcano. This technique is effective and still used, but it requires a physical and economic commitment, and it provides few samples of SO_2 flux per day. However, the switch to continuous monitoring has led to the development of an automatic measurement system (UV-Scanner) that allow the automatic, real time and high-frequency sampling of SO_2 flux. This novel system consists of a network of stationary measuring devices properly installed around the volcano. Since late 2004 a network of UV-Scanner was developed by the geochemical group of INGV Catania and installed at Stromboli, Etna and, recently, in Vulcano island. Each device consists of an ultraviolet spectrometer coupled with a rotating optics which measures the UV spectra on different angles to scan the sky above the instrument providing SO_2 flux observation with time resolution of ~ 6 minute. However, the automation required for monitoring and the large flow of data produced every day, has opened up challenges in the development of the system which allowed to reach a reliable robotic performance of mechanical, electronic, software and data transmission; nevertheless when the sequence of these applications is performed without abnormal interruptions, a minimum computational and communication resource is required whereas if this sequence crashes the restore of the system might require considerable computational resources. Therefore, in order to overcome this problem UV-Scanner was designed to be fully operational in stand-alone mode by the development of custom and dedicated software that continuously check the activity of each sub-application in order to keep always working the entire system. This represents a fundamental feature for the efficiency and reliability of the network. The combination of electronics and applications has provided a robust device which allowed the continuous detection of SO_2 flux at Mt Etna, providing a fundamental tool for volcano surveillance.

Characterization for a Therapeutic Purpose of the Thermal Water and Mud of the Lazio Region, Italy

Marco Redolfi

Università degli Studi Roma Tre, Dipartimento di Scienze Geologiche, Rome, Italy

The aim of this work is the characterization of the thermal water and mud of the Lazio region for the identification of therapeutic proprieties and a better optimization of the natural resource present in the thermal districts of the region with the development of a GIS database for the collection of the data and for a rapid and simple distribution to the competent regional office.

The first two step of this work is the collection of literature data and a deep review of this after the regional decrease of the water table in underground aquifer in the Lazio region in the last years. The third step, now in progress with the first two is the collection of water and mud samples in the area with recent activity and with a temperature of the spring above the medium annual temperature of the area.

The development of a analysis protocol of the water and the mud based on [Summa and Tateo 1998] and [Ferrand and Yvon 1990] is expected followed by the introduction of the data inside the GIS database. The classifications of the water and mud are base on the work of [Bettero et Al. 1999]

We also developed a collaboration with the Medicine Faculty in order to understand the different medical proprieties of the water and mud based on their composition having like starting point the work of [Carretero 2002]. From a experimental point of view we plan also to make an artificial thermal mud from every studied spring following the procedure reported in [Sanchez et Al. 2001]. We will also develop an analysis of the potential of the studied spring.

References

Bettero, A., Marcazzan, M., and Semenzato, A., (1990). *Aspetti reologici e tensiometrici di matrici fangose di impiego termale e cosmetico. Proposta di un protocollo per la loro qualificazione.* Mineralogica et Petrographica Acta, XXLII, 277-286

Carretero, M.I., (2002). *Clay minerals and their beneficial effects upon human health.* Applied Clay Science, 21, 155-163.

Ferrand, T., Yvon, J., (1991). *Thermal proprieties of clay pastes for pelotherapy.* Applied Clay Science, 6, 21-38.

Sanchez, C.J., Parras, J., and Carretero, M.I., (2001). *The effect of maturation upon the mineralogical and physicochemical properties of illlic-smectitic clays for pelotheraphy*. Clay minerals 37, 457-463

Summa, V., Tateo, F., (1998). *The use of pelitic raw material in thermal centres: Mineralogy, geochemistry, grain size and leaching tests. Example from Lucania area (Southern Italy)*. Applied Clay Science, 12, 403-417.

Phreato – magmatic Activity of Berican Mountain (Vicenza, Italy): Volcanology Analysis and Petrographic Data of Diatremic Complexes and Environmental Reconstruction: the "Diatrema of Lumignano" Study Case

Sabrina Russo, Elena Marrocchino, Carmela Vaccaro

Università degli Studi di Ferrara, Dipartimento di Scienze della Terra, Ferrara, Italy

The Berici Hills are a part of the-Southalpine domain only marginally affected by Alpine deformation events. [Castellarin et al., 2006; Dal Piaz, 2001]. The Berican Magmatism is part of the Veneto Volcanic Province, the main volcanic event of the Southern Alps foreland during the Alpine Orogenesis [Coltorti et al, 2000; Macera et al, 2003; Lustrino et al, 2007]. The area is characterized by a volcano-sedimentary succession (Maastrichtian – Langhian age), consisting by platform limestones, marls of basinal sedimentation to passersby, with, Late Paleocene to Late Oligocene in age intercalations of lava flows and volcanoclastic deposits issued by diatremic conduits [Bassi, 2005]. The field data indicates in the Late Eocene a prevalent effusive activity in Lessinian Mountains, an intense explosive activity which are associated to a numerous volcanic craters in Berican Mountain and submarine lava emission (Hyaloclastite and pillow lava products) in Euganean Hills. The environmental condition typical of a lagoon is deduced by paleo - bathymetric data [Bassi, 2005]. These conditions have favoured phenomena of magma-water interactions testify by abundant phreatomagmatic eruptions. Two conjugate faults systems have allowed the formation of several eruptive centres [De Vecchi et al., 1995]. The Berici Hills Diatremes are characterised by elliptical and sub-circular shapes and by a depressed morphology. Three lava groups with distinctive geochemical and petrographical feature and different serial affinity were identified: basanites (Bn), alkaline basalts (AB), olivine basalts (OB), hawaiites (Hw), latibasalts (Lb), andesine basalts (AnB). This composition feature is in agreement with the monogenic and polygenic nature of eruptive centers.

The groundmass is mainly composed by prevalent glass in some cases affected of palagonite alteration, with extremely variable devitrification glass/magma mesostasis ratio [Tamas et al., 2003]. It is possible to observe a direct correlation between textural features and distance from the emission crater: in fact, in areas outside the conduit most prevalent are tefra products, while closer to the ducts are observed breccias. The breccias fragments are composed of volcanic bombs and fragments of the volcanic conduit.

The distribution and types of volcanic products allow to distinguish three different areas in the Berici Hills:

1) a north-west area, in geological continuity with the South Mountains Lessini, characterised by fissural activities with massive lava flows, mainly constituted by subaerieal activity and tuffs beds resulting from explosive volcanic events from surrounding areas;
2) Mid-South area (Val Liona) dominated by basic submarine magmatism (Hyaloclastic product) due to fissural magmatic activity with intercalations of pyroclastic product from adjacent diatremes;
3) an eastern and central north portion, characterised by many caldera and diatremes where the "Diatreme of Lumignano" is located.

On "Diatreme of Lumignano" (diameter of about 300 m) a detailed investigation was carried out that includes: a) the stratigraphic analysis of Eocene formations intruded by the diatreme; b) the study of filling breccia, including tessiturale analysis of the matrix; c) the petrology survey of basaltic breccia and paleontological study of carbonate included. All these volcanic products are typical intra plate magmatism and are similar to magmatism in the Lessinian Mountains to the early basaltic undifferentiated magma of Euganean area [De Vecchi & See, 1995].

References

Bassi D., (2005). *Larger foraminiferal and coralline algal facies in an Upper Eocene storm influenced shallow-water carbonate platfonn (Colli Berici, north-eastern, Italy)*. Paleogeography Paleoclimatology Paleoecology 226 pp. 17-35.

Castellarin A., Nicolich R., Fantoni R., Cantelli L., Sella M., Selli L., (2006). *Structure of the litosfere beneath the Eastern Alps (southern sector of the TRANSALP transect.* Tectophysics 414 pp 259-282.

Coltorti M., Beccaluva L., Bonadiman C., Salvini L., Siena F., (2000). *Glasses in mantle xenoliths as geochimical indicators of metasomatic agents*. Earth and Planetary Science Letters 183 pp. 303-320.

Dal Piaz G.V., (2001). *History of tectonic interpretation of the Alps*. Journal of Geodynamics 32 pp. 99-114.

De Vecchi G., Sedea R., (1995). *The Paleogene basalts of the Veneto Region (NE Italy)*. Mem. Sci. Geol. 47 pp. 253-274.

Lustrino M., Wilson M., (2007). *The circum-Mediterranea anorogenic Cenozoic igneous province*. Earth-Science Reviews 81 pp. 1-65.

Macera P., Gasperini D., Piromallo C., Blichert-Toft J., Bosch D., Del Moro A., Martin S., (2003). *Geodynamic implication of deep mantle upwelling in the source of Tertiary volcanics from the Veneto region (South-Eastern Alps)*. Journal of Geodynamics 36 pp. 563-590.

Tamas C.G., Milesì J.P., (2003). *Hydrotermal breccias pipe structures – General features and genetic criteria – II Phreatic Breccias*. Studia Universitatis Babes – Bolyai, Geologia XLVIII pp 55-66.

Analysis of Historical Etna Flank Eruptions for Hazard Evaluation and Planning of Mitigation Action

Silvia Scifoni[1], Mauro Coltelli[2], Maria Marsella[1], Cristina Proietti[2]

[1]*Università degli Studi La Sapienza, Dipartimento di Ingegneria Civile Edile e Ambientale, Rome, Italy*
[2]*Istituto Nazionale di Geofisica e Vulcanologia, Sezione di Catania - Osservatorio Etneo, Italy*

Since eruptions from Etna volcano threaten the densely inhabited areas on its lower slopes, hazard assessment can also be based on the analysis of past destructive or potentially destructive eruptions. More specifically the reconstruction of the spatial and temporal evolutions of historical flank lava flows represent an useful contribution for planning mitigation measures to reduce the impact of future eruptions by protecting sensitive areas. After the well-known 1669 eruption, only recently in 1928, 1971 and 1981 lava flows [Fig. 1] have reached and destroyed inhabited areas. In particular, the 1928 eruption completely destroyed the town of Mascali.

In our research we quantitatively reconstruct the spatial and temporal evolutions of the lava fields emplaced during the 1928, 1981 and 2001 Etna eruptions and we estimated the trend of the time average discharge rate. To obtain such estimation we applied the volumetric approach, i.e. the measure of flow volume change in a known time span. Final volumes were measured by comparing pre and post-eruption Digital Elevation Models (DEM) extracted using digital photogrammetric techniques for processing aerial historical images and validated by GPS surveys. Lava volume growth was estimated by locating flow front positions from literature data, for the 1928 [Friedlaender, 1928; Imbò, 1933] and the 1981 [Cosentino et al., 1981; Villari, 1983; Romano and Vaccaro, 1986; Guest et al., 1987] eruptions, and from helicopter photos for the 2001 eruption. All the data were incorporated and processed in a GIS system.

The 1928 eruption began the 2 November at 4:30 p.m. from NE crater with highly explosive activity. A fissure opened at 6:05 p.m. in Valle del Leone and was characterized by explosive and effusive activity until midnight of the same day. A second fissure opened the 3 November at 3:30 a.m. to the northeast of the central crater between 2200 m and 1550 m. A lava flow fed from this fissure covered the "Cerrita" and "Cubania" forests, and it flowed towards the town of Sant'Alfio without causing damage to the town. On the night of 4 November, a third fissure opened between 1400 and 1200 m feeding a lava flow that cut the "Circumetnea" and the "Catania-Messina" railways and completely destroyed the town of Mascali on 6 November. The eruption ended on 20 November and emitted a total lava volume of 65 x 10^6 m^3 as evaluated from the comparison of the pre and post-eruption DEMs extracted from cartography (1877 – 1938) and aerial photos (1967) [D'Aranno, 2011].

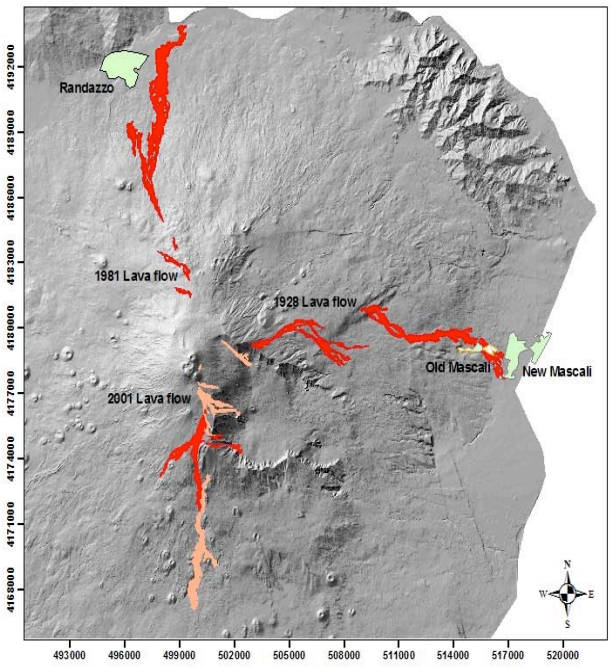

Figure 1. Lava flow fields of the 1928, 1981 and 2001 Etna eruptions overlapped to Etna shaded relief. The towns endangered or destroyed by these flows are also delimited. The red flows are those for which the discharge rate trends have been reconstructed.

The 1981 Etna eruption started on 16 March and in a few hours its main flow overpassed the "Circumetnea" railway, the main road "S.S. 120", the railway "FF.SS Taormina – Randazzo" and the main road "S.P. Randazzo – Mojo". The lava destroyed many houses and farmland areas whilst the front of the main flow reached the bed of the Alcantara River, situated about 10 km away from the vent, 40 hours after

the beginning of the eruption. The 1981 main flow had a final volume of 20.6 x 10^6 m^3, as evaluated from the comparison of the DEM extracted from the 1978 and 2004 aerial surveys [Coltelli et al., in preparation].

During the 2001 eruption, lava flows emitted by seven vents propagated mainly on the southern flank of Etna [Coltelli et al., 2007]. In particular, the lava emitted from the 2700 and 2550 m a.s.l. vents, on 26-31 July and 18-27 July 2001 respectively, threatened the tourist facilities on the Rifugio Sapienza area. The flows from the 2700 and 2550 m vents had a final volume of 3.18 x 10^6 m^3 and 4.15 x 10^6 m^3, respectively that were evaluated from the comparison of the pre-eruption DEM obtained from a 1:10.000 vector map and the post eruption DEM extracted from an aerial survey performed in 2001 [Scifoni et al. 2010].

The 1928 and 1981 eruptions are peculiar mainly for two reasons, the presence of vents located at a low altitude and the high effusion rate. The reconstruction of the time average effusion rate provided very high peak effusion rates (over 600 m^3/s). During the 1928 and 1981 eruptions no mitigation measures to slow down the lava flows were applied. As a matter of fact during the 1928 the only intervention consisted on evacuating the population from Mascali that was completely destroyed. During the 1981 eruption the mitigation measures were not considered because most of the areas invaded by the main flow were farmlands, even if it destroyed a few houses. On the contrary during the 2001 eruption, thirteen earth barriers were built up during the eruption to protect the tourist facilities of the Rifugio Sapienza area, succeeding firstly in delaying the advance of the flows and then in diverting it toward SE, away from the aforementioned facilities. In particular, the first five upper barriers were almost totally buried by lava, whereas the four barriers closest to Rifugio Sapienza were successful partially thanks to the decreasing effusion rate [Barberi and Carapezza, 2004].

The reconstruction of the emplacement history and the temporal evolution of the average discharge rate of the 2001 lava flows allowed evaluating the feasibility of a barrier system. The derived simulation tests of the lava propagation highlighted the contribution of numerical simulations for enhancing the efficiency of barrier building [Vicari et al., 2007, Scifoni et al., 2010]. In the analysis the technical and operational characteristics of an optimal barrier system were defined. In order to improve the barrier design, and in particular to define its structural capacity to evaluate its resistance, a finite element model that simulates the behavior of the lava front estimating its pressure against the barrier was implemented.

References

Barberi, F. and Carapezza, M.L., (2004). *The control of lava flows at Mt. Etna*. In: Mount Etna volcano laboratory. A. Bonaccorso, S. Calvari, M. Coltelli, C. Del Negro and S. Falsaperla (Eds.), Geophysical Monograph Series, 143, pp. 357–369, AGU, Washington.

Coltelli, M., Proietti, C., Branca, S., Marsella, M., Andronico, D. and Lodato, L., (2007). *Analysis of the 2001 lava flow eruption of Mt. Etna from 3D mapping*. Journal of Geophysical Research 112, F02029.

Coltelli, M., Marsella, M., Proietti C. and Scifoni, S. (in preparation). *Understanding an unusually fast evolving Mount Etna effusive event: the 1981 eruption.*

Cosentino, M., Cristofolini, R., Ferri, M., Lombardo, G., Patanè, G., Romano, R., Viglianisi, A. and Villari, P., (1981). *L'eruzione dell'Etna del 17-23 Marzo 1981. Rapporto preliminare*. Rendiconti della Società Geologica Italiana, 4 (3), 249-252.

D'Aranno, P.J.V., (2011). *Analisi quantitative dell'evoluzione di una colata storica dell'Etna (Mascali, 1928) per la valutazione di scenari di mitigazione del danno*. Degree Thesis, Tutor: Prof.ssa Marsella, M., Sapienza University of Rome.

Guest, J.E., Kilburn, C.R.J., Pinkerton, H. and Duncan, A.M., (1987). *The evolution of lava flow fields: observations of the 1981 and 1983 eruptions of Mount Etna, Sicily*. Bulletin of Volcanology, 49, 527-540.

Imbò, G., (1933). *Osservazioni e ricerche in relazione all' eruzione etnea 2-20 Novembre 1928*. Bulletin Vocanologique, Series I, 120-176.

Romano, R. and Vaccaro, C., (1986). *The recent eruptive activity on Mt. Etna, Sicily: 1981-1985*. Periodico di Mineralogia, 55, 91-111.

Villari, L., (1983). *1981 Etna Report.* Open File Report, 2/83, I.I.V.-C.N.R., Catania, Italy.

Vicari, A., Herault, A., Del Negro, C., Coltelli, M., Marsella, M. and Proietti, C., (2007). *Modelling of the 2001 lava flow at Etna volcano by a cellular automata approach*. Environmental Modeling and Software 22, 1465-1471.

Scifoni, S., Coltelli, M., Marsella, M., Proietti, C., Napoleoni, Q., Vicari, A. and Del Negro, C., (2010). *Mitigation of lava flow invasion hazard through optimized barrier configuration aided by numerical simulation: the case of the 2001 Etna eruption*. Journal of Volcanology and Geothermal Research, 192, 16–26.

Modelling of North-East Crater Conduit and its Relation with the Feeding System of the 2008-2009 Eruption at Mt. Etna Inferred from Seismic and Infrasound Signals

Mariangela Sciotto[1], Andrea Cannata[2], Stefano Gresta[1], Eugenio Privitera[2], Laura Spina[1]

[1]*Università di Catania, Dipartimento di Scienze Geologiche, Catania, Italy*
[2]*Istituto Nazionale di Geofisica e Vulcanologia, Sezione di Catania - Osservatorio Etneo, Italy*

On 13 May 2008 an eruption took place on Mt. Etna from an eruptive fissure located on the upper eastern flank of the volcano. The early phase of the eruption was characterized by strong seismic energy release and marked ground deformation in the summit area as well as changes in low frequency seismic signals (volcanic tremor and long period events) [Di Grazia et al., 2009]. Low frequency signals, due to their strict relationship with the dynamics of volcanic fluid, help to obtain information about variations in magmatic system conditions. In recent studies infrasound signal analyses turn out to be useful in conjunction with seismic and volcanic monitoring to understand the style of an eruption and the processes inside the conduit.

In this work we focused the analyses on infrasonic and seismic signals recorded a couple of days before the eruption beginning. Since 12 May until the onset of the eruption 157 infrasound events were extracted by STA/LTA algorithm. Such infrasound events lasted 10-15 s and were characterized by an impulsive and energetic first pulse and sinusoidal oscillations. Time evolution of the spectral content is visualized by means of pseudo-spectrogram (Fig. 1a). It shows the presence of two spectral peaks, that exhibit changing values in the frequency bands 0.4-0.7 Hz and 1.5-2.0 Hz. Peak frequencies and amplitudes were therefore calculated separately into two frequency bands: 0.2-1 and 1-5 Hz (the lower frequency band had never been observed in Mt. Etna infrasound events before this episode). In particular, we noted increasing trends of both peak frequencies and amplitudes over the time preceding the eruption onset.

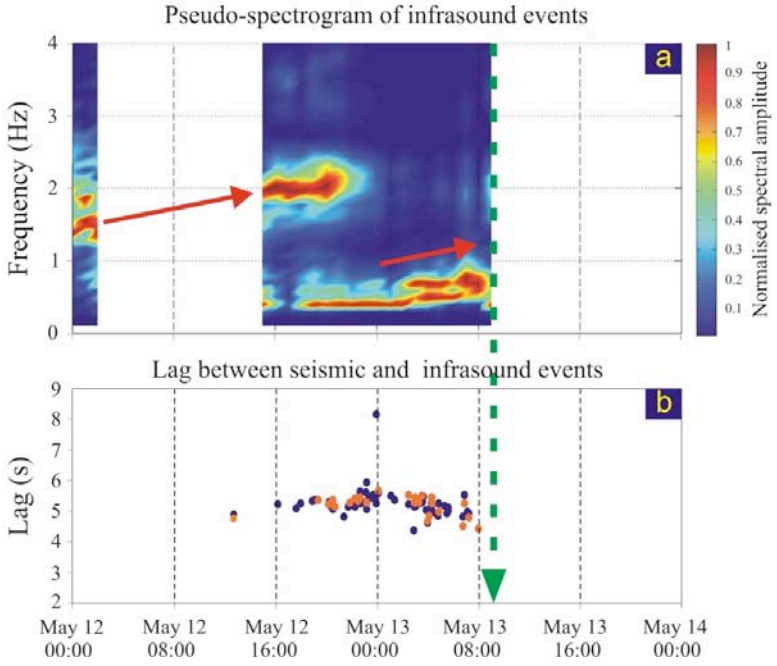

Figure 1. (a) Pseudo-spectrogram of infrasound events, made up of 48 spectra, each of which was obtained averaging the spectra of the events occurring during 1 hour-long time span. White rectangles indicate periods when the pseudo-spectrograms could not be calculated because of the small number of triggered infrasound events. Red arrows point out the time evolution of the spectral content during the hours preceding the eruption onset (green dashed arrow). (b) Lag between each infrasound event and the associated seismic event, evaluated by means of visual inspection (orange dots) and cross-correlation function (blue dots).

A peculiar feature of such infrasound events is the occurrence of associated long-period seismic events. Both infrasound and seismic events were separately localized below the North-East Crater (NEC), where no ash emission or strombolian activity were observed. Infrasound and the related seismic events show marked similarity in waveforms and spectral content. This fact, together with locations, led us to hypothesize a model in which infrasound and seismic events were excited by the same source process. Under this assumption we evaluated the temporal variation of the lag between each infrasound event and the associated seismic event at a reference station (Fig. 1b). Results show decreasing trend in the lag a few hours before the onset of the eruption at the fissure. Variations of lag over time can give information about changes in source depth and/or wave propagation medium properties.

Spectral and waveform characteristics of infrasound events led us to attribute their source mechanism to resonance phenomena of fluid inside the conduit of NEC, similarly to other volcanoes [e.g. Kilauea, Fee et al., 2010; Garces and McNutt, 1997]. We modelled the portion of NEC conduit above the fragmentation level (Fig. 2a), filled with a gas-mixture, with a pipe resonator producing the higher frequency peak (1.5-2.0 Hz). Then, taking into account a frequency value of 2 Hz and a range of sound speed of 400-750 m/s, we obtained a range of conduit length of 100-200 m. Further, we imagined a narrowing in the upper part of the conduit (Fig. 2a) which acts as a neck of an Helmholtz resonator generating the lower frequency peak (0.4-0.7 Hz). The Helmholtz resonance model allowed us to constrain the NEC conduit radius at 25-45 m.

Spectral features of low frequency infrasound and seismic events depend on physical and geometrical properties of the radiating source. Therefore, according with resonance model, changes in frequency content of the infrasound events, occurring a few hours before the eruption onset at the eruptive fissure, are indications that sound speed in the gas-mixture inside the NEC conduit increased and/or fragmentation level became shallower. The decrease of the seismo-infrasound lag, observed at the same time as the spectral changes, supports the latter hypothesis. On the basis of geological and geophysical data Bonaccorso et al. [2011] inferred a northward intrusion of a dyke from below the summit craters during the early phase of the eruption. Such an intrusion could have intersected the NEC conduit causing a variation of the fragmentation depth (Fig. 2b).

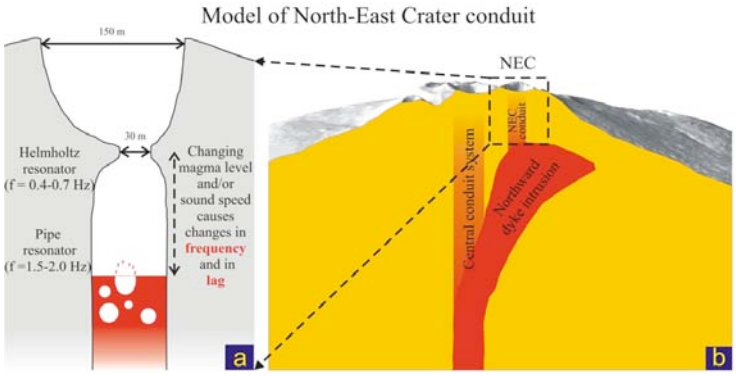

Figure 2. (a) Sketch representing the NEC conduit. According to the model proposed the conduit portion above the fragmentation level behaves as a pipe resonator. The narrowing on the upper part of the conduit generates Helmholtz resonance. (b) Cartoon of the northward dike intrusion during the early phase 13 May eruption and the hypothesized intersection with the NEC conduit generating changes in seismo-infrasound events.

References

Bonaccorso, A., Bonforte, A., Calvari, S., Del Negro, C., Di Grazia, G., Ganci, G., Neri, M., Vicari, A. and Boschi, E., (2011). *The initial phases of the 2008-2009 Mount Etna eruption: A multidisciplinary approach for hazard assessment.* Journal of Geophysical Research, 116, doi:10.1029/2010JB007906.

Di Grazia, G., Cannata, A., Montalto, P., Patanè, D., Privitera, E., Zuccarello, L. and Boschi, E., (2009). *A multiparameter approach to volcano monitoring based on 4D analyses of seismo-volcanic and acoustic signals: the 2008 Mt. Etna eruption*. Geophysical Research Letters, 36, L18307.

Fee, D., Garces, M., Patrick, M., Chouet, B., Dawson, P. and Swanson, D., (2010). *Infrasonic harmonic tremor and degassing bursts from Halema'uma'u Crater, Kilauea Volcano, Hawaii*. Journal of Geophysical Research, 115, B11316, doi:10.1029/2010JB007642.

Garces, M.A. and McNutt, S.R., (1997). *Theory of the airborne sound field generated in a resonant magma conduit*. Journal of Volcanology and Geothermal Research, 78, 155-178.

Seismic Unrest at Mt. Etna Volcano Leading to the 2001 Eruption

Simona Sicali[1], Graziella Barberi[2], Ornella Cocina[2], Domenico Patanè[2]

[1]*Università di Catania, Dipartimento di Scienze Geologiche, Catania, Italy*
[2]*Istituto Nazionale di Geofisica e Vulcanologia, Sezione di Catania - Osservatorio Etneo, Italy*

We analysed the seismicity occurred from November 2000 to July 11, 2001, before the intense seismic swarm (July 12-17, 2001) which heralded the 2001 Mt Etna lateral eruption, one of the most important in the last decade.

During the study period the level of seismic activity was at low levels until October 2000 when an increase in the earthquakes occurrence rate and strain release was observed. Then, a strong seismic swarm occurred on April, 20 2001 in the south-western sector of the volcano and, interpreted by some authors [Bonaccorso et al., 2004; Mattia et al., 2007] as the response of the etnean crust to the magma intrusion along the southern rift, feeding this eruption.

683 earthquakes have been firstly located by means of 1D velocity model derived from Hirn et alii, 1991 using the software HypoEllipse [Lahr, 1989]. Then, a selection of 522 earthquakes has been obtained according to the following parameters: gap ≤ 200, Erh < 1.5, Erz < 2, RMS ≤ 0.5, and a minimum number of S phases equal to 2.

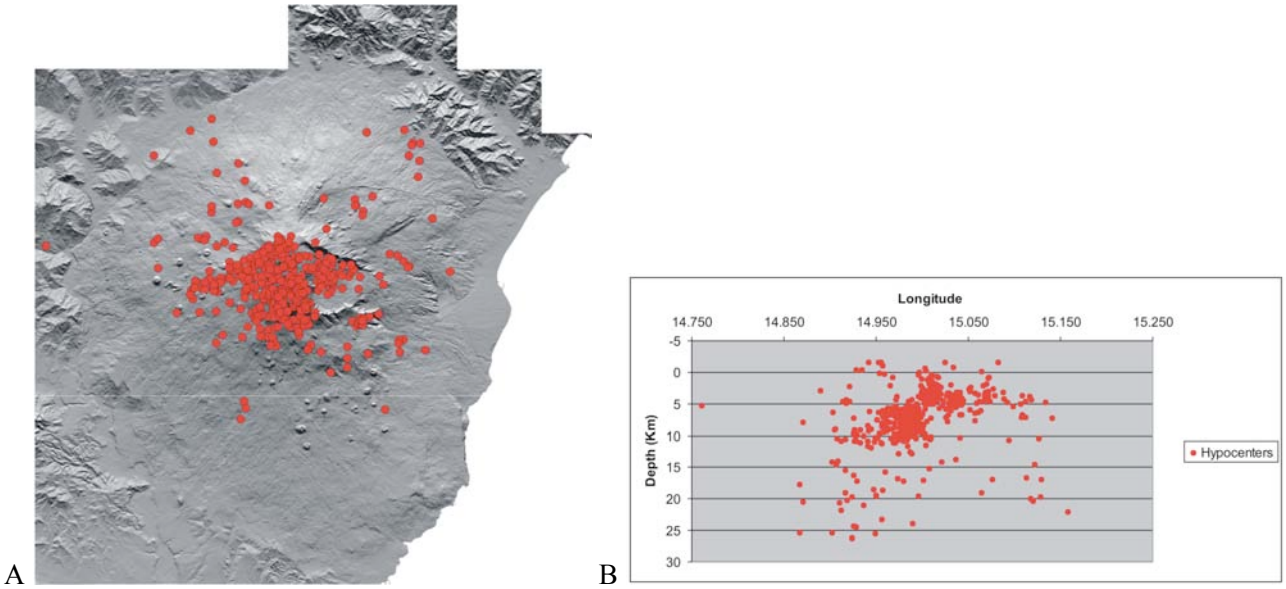

Figure 1. (A) Epicentral map of the 522 Etnean selected earthquakes, located with the software HypoEllipse and the relative hypocentral distribution (B).

TomoDD code [Zhang and Thurber, 2003] and a 3D velocity model have been used to relocate the selected earthquakes, allowing to improve earthquake locations due to the usage of differential times obtained from catalogue picks and/or waveform cross-correlation techniques. Moreover, the study of the space-time distribution of the seismicity has been performed.

The results show that the seismicity is mainly located in the western sector of the volcano in a depth interval 1.6 Km a.s.l. and 28 Km b.s.l. Moreover, two main cluster have been clear identified, the first located between 0 and 5 Km of depth and the second one between 5 and 10 Km b.s.l..

3D locations allow us to calculate more accurate earthquake fault plane solutions (FPS) by using the software FPFIT [Reasenberg and Oppenheimer, 1985] and, on the basis of restricted selection criteria (Npol ≥ ; focal plane uncertainties ≤ 20°; number of FPS solutions < 2; number of discrepancies ≤ 15%) we finally obtained a dataset composed by 100 FPSs. Similarly to other inter-eruptive periods, the analysis of P axes distribution show a radial compression respect to a unique pressure source, located at South of the Central Craters, suggesting that, at Mt Etna a new recharging phase began during the study period.

References

Bonaccorso, A., D'Amico, S., Mattia, M. and Patanè, D., (2004). *Intrusive Mechanism at Mt Etna Forerunning the July-August 2001 Eruption from Seismic and Ground Deformation Data*. Pure and Applied Physics, 161, 1469-1487.

Lahr, J. C., (1989). *HYPOELLIPSE/VERSION 2.0*: A Computer Program for Determining Local Earthquake Hypocentral Parameters, Magnitude, and First-motion Pattern*. U. S. Geol. Survey, Open-File Report 89/116, 81 pp.

Mattia, M., Patanè, D., Aloisi, M. and Amore, M., (2007). *Faulting on the western flank of Mt. Etna and magma intrusions in the shallow crust*. Terra Nova, 91, 89-94.

Reasenberg, P. and Oppenheimer, D., (1985). *FPFIT, FPPLOT, and FPPAGE: FORTRAN Computer Programs for Calculating and Displaying Fault Plane Solutions*. U.S. Geological Survey Open File Rep. 85/739, 109 pp.

Zhang, H. and Thurber, C.H., (2003). *Double-difference tomography: the method and its application to the Hayward fault California*. Bulletin of the Seismological Society of America, 93, 1875-1889.

Mt. Etna Seismicity Characterization by Analyzing the Interevent Time Distribution

Simona Sicali[1], Salvatore D'Amico[2], Maria Serafina Barbano[1]

[1]*Università di Catania, Dipartimento di Scienze Geologiche, Catania, Italy*
[2]*Istituto Nazionale di Geofisica e Vulcanologia, Sezione di Catania - Osservatorio Etneo, Italy*

Several authors have modeled empirical histograms to describe the waiting times distribution between two consecutive earthquakes using a gamma law. This is the case of a single-peaked distribution, typical for global or national catalog, and it is clearly different from the shape of the interevent time distribution for regional or local catalog which has generally a bimodal shape originated from the mixing of the contribution of both correlated aftershocks (which have short interevent time) and independent events (which tend to be separated by longer time slot) [Nayolor et al., 2010]. Therefore, for smaller region, the bimodal shape of interevent time distribution is strongly influenced by the high percentage of correlated event (aftershocks).

The space-time interevent time distribution of Mt. Etna's seismicity has been analyzed, in order to find out the periodicity or stationary features of Etna's earthquakes and comprehending their meaning.

The analyzed dataset consists of an earthquake catalogue of 8.520 events, occurred between January 1988 and December 2010 and recorded by IIV-CNR, POSEIDON and INGV seismic networks [Calvari et al., 2004; Alparone et al., 2010; Gruppo Analisi Dati Sismici, 2010]. The completeness data analysis showed that the completeness magnitude, M_c, for the whole seismic catalogue gradually decreased thanks to the seismic network equipment upgrade, moving from Md = 2.5 in the 1988 to Md = 1.5 at the end of '90s, reaching the actual value of about Md = 1.0. So, the earthquake analysis was performed using two different thresholds of magnitude: 1) Md > 2.5 for the whole available period (1988-2010); and 2) Md > 1.5 for the more recent period (1995-2010).

As the Etna area is subjected to seismicity connected both to volcano's dynamic and to regional stress field, the interevent time distribution of Etna's earthquakes has also been compared (Fig. 1) with the one of a larger area corresponding to the whole national territory, using the CSI catalogue 1.1 [Castello et al., 2006].

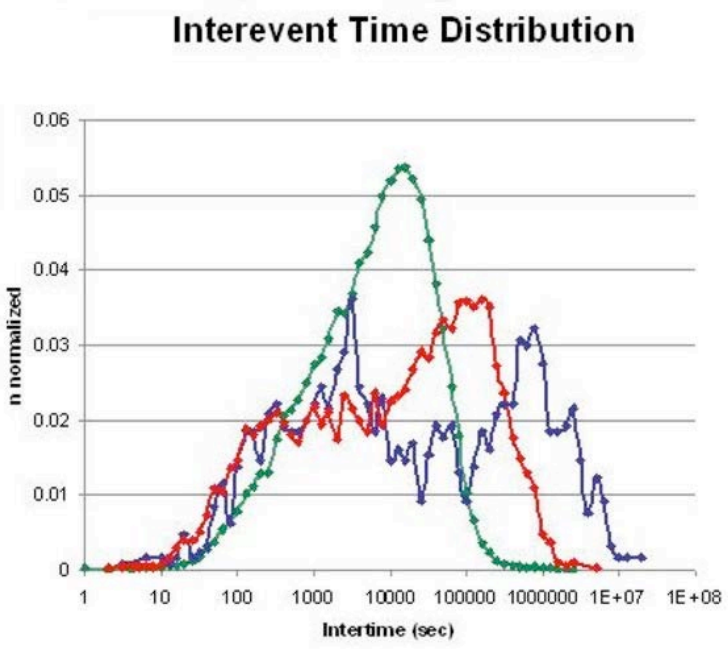

Figure 1. Interevent time histogram for Italian territory (in green) compared with the interevent time calculated only for Etna's earthquakes since 1988 to 2010 (in blue) and since 1995 to 2010 (in red). Datasets are filtered by the respective completeness magnitudes.

The interevent time distribution, obtained from the time interval between subsequent events occurring in the whole Italian peninsula, is well modeled by a gamma distribution. Such a distribution is similar to the one observed at worldwide scale and its distinctive pattern is typical in areas with prevalent tectonic behavior, where the interevent time of uncorrelated earthquakes (events that are not part of the same seismic sequence or swarm) are numerically larger than the correlated ones (aftershocks) [Touati et al., 2009].

The comparison between the interevent distribution of Etna earthquakes and the ones occurring on the whole Italian peninsula, highlights very different results. In fact, the Etna seismic catalogue contains a lot of earthquakes with very short interevent time, generating a bimodal curve. This feature is more evident in the dataset 1988-2010, that is, the one with Md > 2.5, with respect to the dataset 1995-2010 (with Md > 1.5).

Plotting the interevent time with

respect to the time, it appears evident that there are independent seismic event that occur constantly, with waiting times of about 9 days (100.000 – 1.000.000 sec), and they are not linked to specific phases of the volcano. Moreover, it is possible to see interevent time classes (with a mean value of about one hour) well represented only during specific phases of volcano, mainly during periods of strong seismic activity before the eruption. These events create a sudden growth of the seismic rate, seen also the high number of correlated events (aftershocks), generally caused by the strictly volcanic activity that increase and vary the state of the stress fields acting on the Etna crustal volume. So, the two peaks (or modes), which appear to be into the Etna interevent time distribution, can be associated in this context to: (i) the background stationary seismic activity, (ii) the contribution of the seismic swarms that occasionally interrupt the normal seismicity of Mt. Etna.

A bimodal interevent time distribution has been recently observed at Kilauea [Bell and Kilburn, 2008] for the rift zone. This distribution has a strong deviation from the one obtained for the south flank of the volcano, region with mostly tectonic features, and the authors claim that different seismogenic areas can be characterized by different patterns of the interevent time.

A preliminary analysis has been performed considering earthquake subdatasets of different Mt. Etna sectors (the eastern flank, the western flank and the crater area), and evaluating for each sector the interevent time distribution in different span time.

The eastern sector, the most seismically active, shows an interevent time distribution shape similar to the one observed for both the whole Italian peninsula and the southern flank of Kilauea, highlighting a strong component of uncorrelated events.

In the craters' zone, strongly influenced by the volcanic activity, the interevent time distribution is characterized mainly by short interevent time, typical of the seismic swarms. Conversely, the uncorrelated events are less evident. This behaviour is more evident in the dataset with $M > 2.5$.

The western sector of Mt. Etna has a more complex behavior and further deeper analysis is need.

Additional analysis and result validation will be developed in the near future to better understand, through the space-time analysis of the interevent time, how the seismicity of the different crustal Etna sectors are mostly influenced by the volcano dynamic and/or by the regional tectonic.

References

Alparone, S., D'Amico, S., Maiolino, V. and Ursino, A., (2010). *Sismicità all'Etna dal 1989 al 2010: evidenze sull'evoluzione spazio-temporale della attività sismica*, 29° Convegno Nazionale GNGTS, Prato, 28-28 Ottobre 2010, riassunti estesi delle comunicazioni.

Bell, A. and Kilburn, C., (2008). *Patterns of accelerating rates of volcano-tectonic seismicity preceding basaltic flank eruptions*. EGU General Assembly 2008, Geophysical Research Abstracts, Vol. 10, EGU2008-A-03752.

Calvari, S., Coltelli, M., Bonaccorso, S., Del Negro, C. and Falsaperla, S., (2004). In: Mount Etna volcano laboratory. A. Bonaccorso, S. Calvari, M. Coltelli, C. Del Negro and S. Falsaperla (Eds.), Geophysical Monograph Series, 143, pp. 147-165, AGU, Washington.

Castello, B., Selvaggi, G., Chiarabba, C. and Amato, A., (2006). *CSI Catalogo della sismicità italiana 1981-2002*, versione 1.1. INGV-CNT, Roma http://csi.rm.ingv.it/

Gruppo Analisi Dati Sismici (2010). *Terremoti recenti localizzati con la rete sismica della Sicilia Orientale.* INGV, Catania, available from http://www.ct.ingv.it/Sismologia/analisti

Nayolor, M., Touati, S., Main, I. and Bell., A., (2010). *Earthquake interevent time distributions reflect the proportion of dependent and independent events pairs and are therefore not universal*. EGU General Assembly 2010, Geophysical Research Abstracts, Vol. 12, EGU2010-8699.

Touati, S., Naylor, M. and Main, I. G., (2009). *Origin and Nonuniversality of the Earthquake Interevent Time Distribution*. Physical Review Letters, 102, 168501.

Slope Stability Analysis by Multi-temporal DEMs and 3D Modelling: The 2002 and 2007 Stromboli Landslide Events

Alberico Sonnessa[1], Maria Marsella[1], Paolo Tommasi[2]

[1]*Università degli Studi La Sapienza, Dipartimento di Ingegneria Civile Edile e Ambientale, Rome, Italy*
[2]*Consiglio Nazionale delle Ricerche, IGAG, Rome, Italy*

Natural hazard related to the volcanic activity represents a potential risk factor, particularly in the vicinity of human settlements. Besides to the risk related to the explosive and effusive activity, the instability of volcanic edifices may develop into large landslides often catastrophically destructive, as shown by the collapse of the northern flank of Mount St. Helens in 1980.

A combined approach was applied to analyse slope failures that occurred at Stromboli volcano. SdF slope stability was evaluated by using high-resolution multi-temporal DTMMs and performing limit equilibrium stability analyses.

High-resolution topographical data collected with remote sensing techniques and three-dimensional slope stability analysis play a key role in understanding instability mechanism and the related risks.

Analyses carried out on the 2002–2003 and 2007 Stromboli eruptions, starting from high-resolution data acquired through airborne remote sensing surveys, permitted the estimation of the lava volumes emplaced on the SdF slope and contributed to the investigation of the link between magma emission and slope instabilities.

Limit Equilibrium analyses were performed on the 2001 and 2007 3D models, in order to simulate the slope behavior before 2002-2003 landslide event and after the 2007 eruption. Stability analyses were conducted to understand the mechanisms that controlled the slope deformations which occurred shortly after the 2007 eruption onset, involving the upper part of slope. Limit equilibrium analyses applied to both cases yielded results which are congruent with observations and monitoring data.

The results presented in this work undoubtedly indicate that hazard assessment for the island of Stromboli should take into account the fact that a new magma intrusion could lead to further destabilisation of the slope, which may be more significant than the one recently observed because it will affect an already disarranged deposit and fractured and loosened crater area.

The two-pronged approach based on the analysis of 3D multi-temporal mapping datasets and on the application of LE methods contributed to better understanding volcano flank behaviour and to be prepared to undertake actions aimed at risk mitigation.

References

Andronico, D., Cristaldi, A. and Taddeucci, J., (2007). *Eruzione Stromboli 2007. L'evento parossistico del 15 marzo,* http://www.ct.ingv.it/Report/RPTVSTRCEN20070315.pdf.

Apuani, T., Corazzato, C., Cancelli A. and Tibaldi A., (2004). *Stability of a collapsing volcano (Stromboli, Italy): Limit equilibrium analysis and numerical modelling*. Journal of Volcanology and Geothermal Research, 144, 1-4, doi: 10.1016/j.jvolgeores.2004.11.028.

Baldi, P., Bonvalot, S., Briole, P. and Marsella, M., (2000). *Digital photogrammetry and kinematic GPS applied to the monitoring of Vulcano Island, Aeolian Arc, Italy*. Geophysical Journal International, 142, 801-811.

Baldi, P., Bonvalot, S., Briole, P., Coltelli, M., Gwinner, K., Marsella, M., Puglisi, G. and Remy, D., (2002). *Validation and comparison of different techniques for the derivation of digital elevation models and volcanic monitoring (Vulcano Island, Italy).* International Journal of Remote Sensing, 22, 4783-4800.

Baldi, P., Fabris, M., Marsella, M. and Monticelli R., (2005). *Monitoring the morphological evolution of the Sciara del Fuoco during the 2002-2003 Stromboli eruption using multi-temporal photogrammetry, ISPRS* Journal of Photogrammetry and Remote Sensing, 59, 4, 199-211.

Baldi, P., Coltelli, M., Fabris, M., Marsella, M. and Tommasi P., (2008a). *High precision photogrammetry for monitoring the evolution of the NW flank of Stromboli volcano during and after the 2002-2003 eruption*. Bulletin of Volcanology, 70 (6), 703–715, doi:10.1007/s00445-007-0162-1.

Baldi, P., Bosman, A., Chiocci, F.L., Marsella, M., Romagnoli, C. and Sonnessa, A., (2008b). *Integrated Subaerial–Submarine Evolution of the Sciara del Fuoco After the 2002 Landslide*. In: The Stromboli Volcano: An Integrated Study of the 2002–2003 Eruption S. Calvari, S. Inguaggiato, G. Puglisi, M. Ripepe, M. Rosi (Eds), Geophysical Monograph Series, vol. 182, AGU Washington, 171–182.

Bevivino, C. (2005). *Fenomeni di instabilità di fianchi di edifici vulcanici. Il caso di Vulcano*. Degree Thesis, University of Rome La Sapienza (in Italian).

Boldini, D., Wang, F.W., Sassa, K., Tommasi, P., (2005). *Mechanism of landslide causing the December 2002 tsunami at Stromboli volcano (Italy)*. In: Landslide: Risk Analysis and Sustainable Disaster Management, 173-180, Sassa K., Fukuoka H., Wang F.W., Wang G. (Eds), Springer, Berlin.

Boldini, D., Wang, F.W., Sassa, K., Tommasi, P., (2009). *Application of large-scale ring-shear tests to the analysis of tsunamogenic landslides at Stromboli*. Landslides, 6, 231–240, doi:10.1007/s10346-009-0155-6.

Bonaccorso, A., Calvari, S., Garfì, G., Lodato, L. and Patanè D., (2003). *Dynamics of the December 2002 flank failure and tsunami at Stromboli volcano inferred by volcanological and geophysical observations*. Geophysical Research Letters, 30, 18, 1941, doi:10.1029/2003GL017702.

Calvari, S., Spampinato, L., Lodato, L., Harris, A.J.L., Patrick, M.R., Dehn, J., Burton, M.R. and Andronico, D., (2005). *Chronology and complex volcanic processes during the 2002-2003 flank eruption at Stromboli volcano (Italy) reconstructed from direct observations and surveys with an handheld thermal camera*. Journal of Geophysical Research, 110, B02201, doi:10.1029/2004JB003129.

Chiocci, F.L., Romagnoli, C., Tommasi, P., Bosman A., (2004). *The December 2002 submarine landslide at Stromboli Volcano: morphologic definition, tsunamogenic potential and scar evolution*. 32th Geological Congress, Florence 20–28 August 2004.

Investigating the Mt. Etna Shallow Plumbing System by Means of Infrasonic Signals

Laura Spina[1], Andrea Cannata[2], Eugenio Privitera[2], Sylvie Vergniolle[3], Carmelo Ferlito[1], Stefano Gresta[1], Placido Montalto[2], Mariangela Sciotto[1]

[1]*Università di Catania, Dipartimento di Scienze Geologiche, Catania, Italy*
[2]*Istituto Nazionale di Geofisica e Vulcanologia, Sezione di Catania - Osservatorio Etneo, Italy*
[3]*Institut de Physique du Globe de Paris, Institut de recherche associé CNRS et Université de Paris, France*

We investigated the link between different active crater vents on Mt. Etna volcano and the dynamics of magma inside the conduit, by means of infrasonic signals. Infrasonic signals, continuously recorded by the permanent infrasound network managed by the Istituto Nazionale di Geofisica e Vulcanologia (Osservatorio Etneo-Catania section), were analyzed during a period spanning from August 2007 to December 2009. Such a period was characterized by several volcanic phenomena comprising quiet degassing, ash emission, strombolian activity, lava fountains and effusive activity from a fracture.

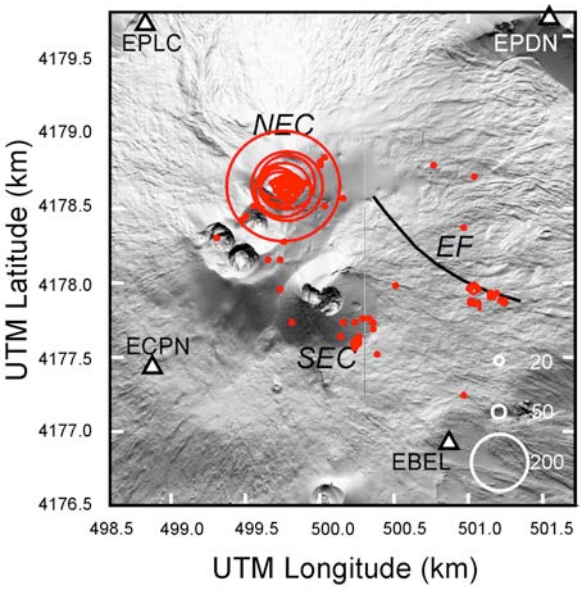

Figure 1. Digital elevation model of Mt. Etna summit with the source locations of the infrasound events, indicated by red circles, occurring during September 2007 – December 2008. The radii of the circles are proportional to the number of the locations in each grid node (see white circles and numbers reported in the lower right corner of the map). The sites of the four summit infrasonic sensors are indicated with triangles.

We performed two different spectral analyses on ~40000 infrasonic events: FFT and Sompi analyses [Kumazawa et al., 1990]. We also localized those events, characterized by good signal to noise ratio at least at three stations, applying the semblance algorithm [Neidell and Taner, 1971]. Three main active sources have been recognized (Fig. 1): North East Crater (NEC), South East Crater (SEC) and Eruptive Fissure (EF). Infrasonic signals radiated from NEC (NEC events) are characterized by frequency content generally lower than 2.5 Hz and a duration greater than 10 seconds. Furthermore, these events have their energy mainly concentrated in two frequency bands: the first one lower than 0.5 Hz, and the second, sometimes with integer harmonics, comprised between 0.8-2.5 Hz. The former was recorded only from November 2009, after the replacement of Monacor sensor (cut-off frequency 1 Hz) with a Grass broad-band microphone (cut-off frequency 0.3 Hz), except for a brief episode preceding the start of 2008-2009 eruption [Di Grazia et al., 2009]. Events from SEC and EF (SEC and EF events) are very similar in waveforms: SEC events are short infrasonic transients (1-2 seconds) with dominant frequency higher than 2.5 Hz and higher peak to peak amplitude than NEC events, while EF events have dominant frequency mainly comprised in 2-4 Hz band, and show the shortest duration and the highest peak to peak amplitude at all. Furthermore, NEC events were radiated continuously during the whole period. Indeed, they are numerically dominant in respect to SEC and EF events, whose radiation is strictly related to periods characterized by explosive activity. We highlight that infrasonic activity at NEC is related to eruptive activity occurring at SEC-EF, revealing the existence of a link among those vents. Indeed, we observed that the dominant frequency value in the upper frequency band of NEC events systematically decreased after the eruptive activity at SEC-EF, and later in times it gradually went back to its previous value (Fig. 2). It is noteworthy that quality factor of NEC events in most cases increased and their amplitude slightly decreased after those eruptive activities. We investigated the change in the spectral features focusing on three main periods, containing important eruptive episodes such as lava fountains

occurring on 4 September and 23 November 2007 from SEC, and the increase of strombolian activity that took place from 8 to 21 June 2008 from EF. As previously mentioned, NEC events showed two frequency bands: we suppose that the lower one is generated from an Helmholtz resonance, while the upper from the resonance of a portion of the conduit, comprised between the free magma surface and a constriction of the conduit section, conciding with the bottleneck of the Helmholtz resonator. The decrease of dominant frequency of NEC events can be interpreted in two ways. It can be caused by variations in geometrical characteristics of the resonating part of NEC conduit (e.g. a lengthening, caused by a drop in the level of free magma surface). Alternatively, it could be caused by a variation in acoustic velocity inside NEC conduit, induced from a change in composition of the fluid in which infrasonic waves propagate (e.g. increase in the ash content in a mixture with gas) just after the eruptions at SEC-EF. We found that a lengthening of the resonating part of the conduit is the most realistic hypothesis to explain these spectral variations. In other words, a deepening of the free magma surface inside NEC conduit, likely attributed to drainage caused by the eruptive activity at SEC-EF, could explain all the observed changes.

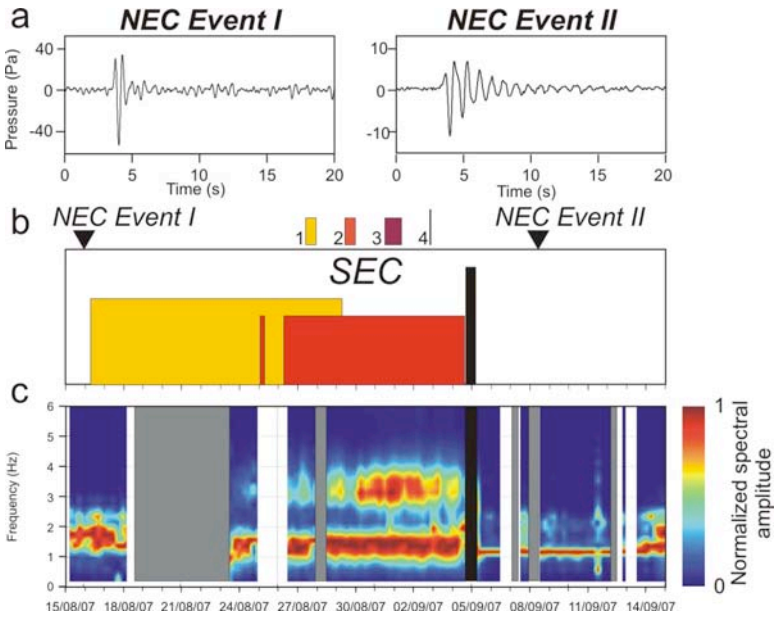

Figure 2. (a) Waveforms of two infrasonic events generated by NEC and recorded by EBEL station. (b) Scheme of the volcanic activity of Mt. Etna at SEC during 15 August – 15 September 2007 (1: ash emission; 2: strombolian activity; 3: effusive activity; 4: lava fountain). (c) Normalised pseudo-spectrogram, obtained averaging the spectra of all infrasonic events recorded by EBEL station in 6-hour-long time windows and displaying change in spectral amplitude as different colours. Grey and black rectangles in (c) represent periods of partial or complete lack of triggered events for bad weather conditions/station malfunctioning and infrasonic tremor, respectively. White rectangles indicate periods when the pseudo-spectrograms could not be calculated because of the small number of triggered events even in good signal to noise ratio conditions. Triangles at top of (b) indicate the time of occurrence of the events shown in (a).

References

Di Grazia, G., Cannata, A., Montalto, P., Patanè, D., Privitera, E., Zuccarello, L. and Boschi, E., (2009). *A new approach to volcano monitoring based on 4D analyses of seismo-volcanic and acoustic signals: the 2008 Mt. Etna eruption.* Geophysical Research Letters, 36, 18, doi:10.1029/2009GL039567.

Kumazawa, M., Imanishi, Y., Fukao. Y. and Yamamoto, A., (1990). *A theory of spectral analysis based on the characteristic property of a linear dynamic system*. Geophysical Journal International, 101, 613-630.

Neidell, N. and Taner, M. T., (1971). *Semblance and other coherency measures for multichannel data.* Geophysics, 36, 482-497.

Vulcamera: a User-Friendly Program for Measuring Volcanic SO_2 Flux and Strombolian Explosion with UV Cameras and its Application on Stromboli Volcano

Giancarlo Tamburello[1], Euripides P. Kantzas[2], Andrew J.S. McGonigle[2,3], Alessandro Aiuppa[1,3]

[1]*Università di Palermo, Dipartimento CFTA, Palermo, Italy*
[2]*Department of Geography, University of Sheffield, UK*
[3]*Istituto Nazionale di Geofisica e Vulcanologia, Sezione di Palermo, Italy*

Ultra-violet camera technology offers considerable promise in remote sensing of volcanic degassing phenomena, providing an high temporal resolutions of ~1 Hz and an high spatial resolution, particularly useful for exploring multiple-source SO_2 gas emissions [Bluth et al., 2007; Mori and Burton, 2006]. Here, we present Vulcamera [Tamburello et al., 2011a], a stand-alone user-friendly code for high temporal resolution volcanic SO_2 flux measurements. The code consists of two elements: Vulcamera and Vulcamera_post (Fig. 1), which manage image acquisition, and all elements of post-processing, respectively. Vulcamera will work with Apogee Instruments U260 and E6 units. The program is designed to operate with two cameras, simultaneously, with bandpass filters centred on 310 and 330 nm, respectively, to compensate for aerosol attenuation/backscattering. This approach minimises temporal mismatches associated with filter changes on a single camera [Kantzas et al. 2010]. Vulcamera has been extensively field tested at southern Italian volcanoes [Tamburello et al., 2011b], in particular on Stromboli, where we take advantage of the high spatial and time resolution (0.6-1 Hz) of this technique to obtain the first simultaneous characterisation of all the different forms of SO_2 release at Stromboli (including passive degassing, Strombolian eruptions and puffing). This work presents a first overview of the results.

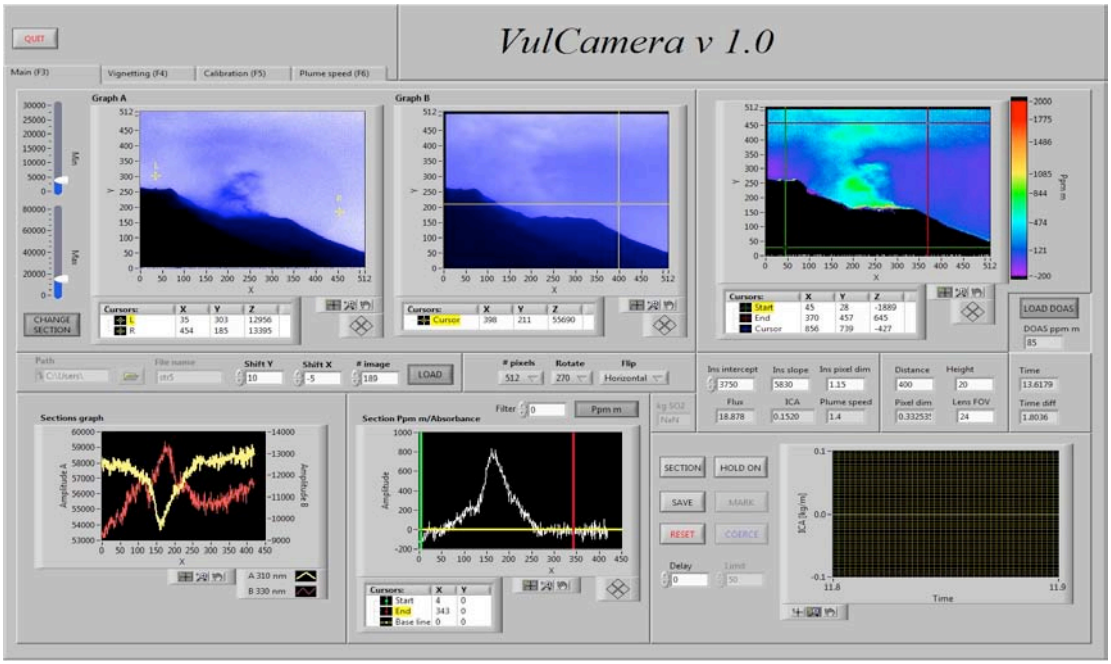

Figure 1. Screen shot of the main screen of Vulcamera_post in operation during post-processing volcanic degassing images from Stromboli. The plots Graph A and Graph B show the raw image files taken from the two cameras, with filters at 310 and 330 nm, respectively, showing the gas attenuation in the former case. A profile across the rising gas plume is identified in Graph A using the L and R cursors, the intensities across which are presented in the profiles in the Section graph. Calibration data, as obtained from the Calibration page are entered in appropriate fields to centre right of screen in order to generate the pseudo-colour graph of concentrations across the image shown top right, as well as the concentrations across the L-R profile in the Section ppm m/absorbance field. All of the above is then used to generate integrated column amount time series or explosive gas masses via the bottom right window.

References

Bluth, G.J.S., Shannon, J.M., Watson, I.M., Prata, A.J. and Realmuto, V.J., (2007). *Development of an ultra-violet digital camera for volcanic SO_2 imaging*. Journal of Volcanology and Geothermal Research, 161, 47-56, doi:10.1016/j.jvolgeores.2006.11.004.

Kantzas, E.P., McGonigle, A.J.S., Tamburello, G., Aiuppa A. and Bryant, R.G., (2010). *Protocols for UV camera volcanic SO_2 measurements*. Journal of Volcanology and Geothermal Research, 94, 55–60, doi:10.1016/j.jvolgeores.2010.05.003.

Mori, T. and M. Burton, (2006). *The SO_2 camera: A simple, fast and cheap method for ground-based imaging of SO_2 in volcanic plumes*. Geophysical Research Letters, 33, L24804, doi:10.1029/2006GL027916.

Tamburello, G., McGonigle, A.J.S., Kantzas, E.P. and Aiuppa A., (2011a). *Vulcamera: a program for measuring volcanic SO_2 with UV cameras*. Annals of Geophysics, accepted paper.

Tamburello, G., Kantzas, E.P., McGonigle, A.J.S., Aiuppa A. and Giudice, G. (2011b). *UV camera measurements of fumarole field degassing (La Fossa crater, Vulcano Island)*. Journal of Volcanology and Geothermal Research, 199, 47-52, doi: doi:10.1016/j.jvolgeores.2010.10.004.

Seismo-Volcanic Monitoring Techniques at Mt. Etna

Luciano Zuccarello[1,3], Marco Aliotta[1,2], Andrea Cannata[1], Carmelo Cassisi[2], Louis De Barros[3], Giuseppe Di Grazia[1], Placido Montalto[1], Domenico Patanè[1]

[1]*Istituto Nazionale di Geofisica e Vulcanologia, Sezione di Catania - Osservatorio Etneo, Italy*
[2]*Università degli Studi di Catania, Dipartimento di Informatica, Catania, Italy*
[3]*School of Geological Sciences, University College Dublin, Ireland*

According to Chouet [1996], in volcanic areas we can distinguish seismic signals belonging to two different groups: seismic events associated with shear failures in the volcanic edifice which are called volcano-tectonic (VT) or high-frequency earthquakes; the second class of events (hereafter referred to as seismo-volcanic signals), generated by processes originating in the fluid, includes long period (LP) events, very long period (VLP) events and volcanic tremor. Because of the peculiar characteristics of the seismo-volcanic signals, different from the tectonic and VT earthquakes in terms of both waveforms and source mechanisms, new techniques have been developed to investigate their features. Here we will show the most recent techniques applied to monitor and investigate the seismo-volcanic signals recorded at Mt. Etna together with some cases of study of such signals mainly regarding the 2008-2009 eruption.

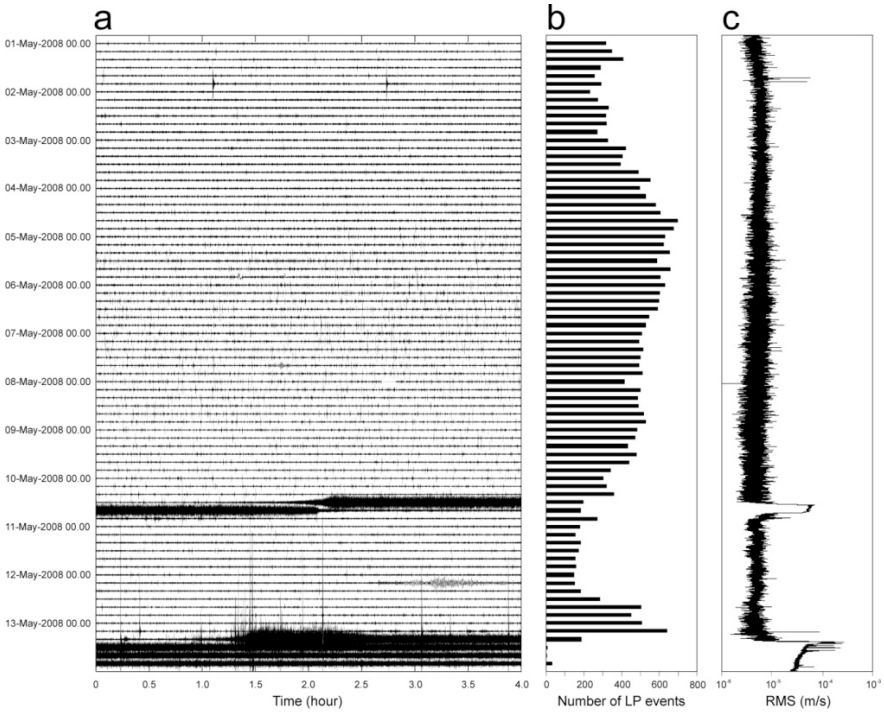

Figure 1. (a) Seismogram of the vertical component of ECPN station, (b) histogram of the number of LP events in 4-hour-long windows and (c) RMS time series.

First of all, to accomplish the task of extraction of seismic transients (LP, VLP events, etc…) from the continuous signal, a technique based on the percentile computation on RMS envelope was developed. For instance we observed an increase in LP activity (increases in both occurrence rate and amplitude of LP events) taking place a few days before the 10 May lava fountain and the following 13 May eruption onset during 2008. Such an energy increase of LP events can be interpreted as increasing overpressure inside the shallow part of the plumbing system. Moreover, since the frequency and damping of a resonant system is strongly influenced by the nature of liquid and gas content [Chouet, 1996], also the study of the spectral evolution of seismo-volcanic signals in volcanic areas provides very useful information for monitoring purposes. Therefore, to investigate the spectral changes of these signals, both parametric and non-parametric power spectrum estimation techniques are routinely applied. It was shown how at Mt. Etna eruptive activities are sometimes preceded and/or accompanied by changes in the spectral features and waveforms of LP, VLP events and volcanic tremor. Also the wavefield changes of the seismo-volcanic signals can provide information about internal variations of the plumbing system. The wavefield can be investigated by polarization analysis, that in earthquake seismology is able to provide important information about the wave types composing the wavefield and the seismic source location and mechanism. However, in volcano seismology polarization analysis cannot necessarily be used

for these objectives because of the heterogeneities and rough topography of volcanoes. On the other hand, this kind of analysis can be useful to detect even very small variations in location and/or source mechanism. At Mt. Etna several paroxysmal activities were preceded and/or accompanied by variations in the polarization parameters.

Finally, since the seismo-volcanic signals are generally related to dynamics of fluid inside the volcanic edifice, the location of their source is basic information for monitoring of volcanoes and also for identifying the elements of the plumbing system. Then, the tremor source locations are routinely retrieved by following the approach described by Patanè et al. [2008] and Di Grazia et al. [2009], inverting the spatial distribution of tremor amplitude and using a grid-search approach. We consider the RMS amplitudes of the 25th percentile instead of average values. This enables us to efficiently remove undesired transients in the signal and consider continuous recordings. Because of the wavefield features of the VLP events, radial semblance method [Kawakatsu et al., 2000] is routinely applied to constrain their source location. The source location of LP events is retrieved by following a new grid-search method based on the joint computation of two different functions: i) semblance, used to measure the similarity among signals recorded by two or more stations [e.g. Neidell and Taner, 1971]; and R^2 values, calculated on the basis of the spatial distribution of seismic amplitude [Patanè et al., 2008; Di Grazia et al., 2009]. Recently a new seismo-volcanic signals location approach have been performed by using of array geometries. Through the multichannel techniques, the propagation azimuths and apparent velocity of the incoming wavefronts are retrieved by inverting the inter-station delay times for the two cartesian components of the slowness vector, under a plane-wave approximation. All these methods were very effective to track the short migration (a few hundred meter) of the seismic source before and during the 2008-2009 eruption at Mt. Etna.

The high interest in the correct determination of source parameters for very long period (VLP) and long period (LP) events in volcanic areas, is mostly related to the fact that they may be directly generated by the dynamics of gas bubble and fluid transfers along the upper part of the conduit system. Thus VLP and LP could be candidates for volcanic activity parameters, or precursors of volcanic eruptions [Chouet, 1996]. In order to understand the low frequency events source mechanisms, we perform a moment tensor inversion in the frequency domain [De Barros et al., 2011]. The Green's Functions (GF) are calculated for a homogeneous velocity model with DEM Etna topography. Synthetic seismograms are generated by Discrete Elastic Lattice algorithm described by O'Brien and Bean [2004], based on discrete particle scheme.

All these techniques applied on seismo-volcanic signals provide very useful information that, together with other geophysical and geochemical parameters, constitute the fundamental knowledge for both eruptive precursors characterization and investigation of the magma dynamics.

References

Chouet, B. (1996). *Long-period volcano seismicity: Its source and use in eruption forecasting*. Nature, 380, 309-316.

Di Grazia, G., Cannata, A., Montalto, P., Patanè, D., Privitera, E., Zuccarello, L. and Boschi, E. (2009). *A new approach to volcano monitoring based on 4D analyzes of seismo-volcanic and acoustic signals: the 2008 Mt. Etna eruption*. Geophysical Research Letters, 36, L18307, doi:10.1029/2009GL039567.

De Barros, L., Lokmer, I., Bean, C.J., O'Brien, G.S., Saccorotti, G., Métaxian, J.-P., Zuccarello, L. and Patanè, D. (2011). *Source mechanism of long period events recorded by a high-density seismic network during the 2008 eruption on Mount Etna.* Journal of Geophysical Research, 116, B01304, doi:10.1029/2010JB007629.

Kawakatsu, H., Kaneshima, S., Matsubayashi, H., Ohminato, T., Sudo, Y., Tsutsui, T., Uhira, K., Yamasato, H., Ito, H. and Legrand, D. (2000). *Aso94: Aso seismic observation with broadband instruments.* Journal of Volcanology and Geothermal Research, 101, 129-154.

Neidell, N. and Taner, M.T. (1971). *Semblance and other coherency measures for multichannel data.* Geophysics, 36, 482-497.

O'Brien, G.S. and Bean, C.J. (2004). *A 3D discrete numerical elastic lattice method for seismic wave propagation in heterogeneous media with topography.* Geophysical Research Lettears, 31, L14608, doi:10.1029/2004GL020069.

Patanè, D., Di Grazia, G., Cannata, A., Montalto, P. and Boschi, E. (2008). *The shallow magma pathway geometry at Mt. Etna volcano*. Geochemistry Geophysics Geosystems, 9, Q12021, doi:10.1029/2008GC002131.

Coordinamento editoriale e impaginazione
Centro Editoriale Nazionale | INGV

Progetto grafico e redazionale
Daniela Riposati | Laboratorio Grafica e Immagini | INGV

Via di Vigna Murata, 605
00143 Roma
Tel. +39 06518601 Fax +39 065041181

http://www.ingv.it

Istituto Nazionale di Geofisica e Vulcanologia